NOVEL PEPTIDYLAMINOARYLMETHYL PHOSPHORAMIDE MUSTARDS FOR ACTIVATION BY PROSTATE-SPECIFIC ANTIGEN

by

XINGHUA WU

A Dissertation submitted to the

Graduate School-New Brunswick

Rutgers, The State University of New Jersey

in partial fulfillment of the requirements

for the degree of

Doctor of Philosophy

Graduate Program in Medicinal Chemistry

written under the direction of

Professor Longqin Hu

and approved by

_____

_____

_____

_____

New Brunswick, New Jersey

May, 2008

ABSTRACT OF THE DISSERTATION

NOVEL PEPTIDYLAMINOARYLMETHYL PHOSPHORAMIDE MUSTARDS

FOR ACTIVATION BY PROSTATE-SPECIFIC ANTIGEN

XINGHUA WU

Dissertation Director: Professor Longqin Hu

A series of nitroarylmethyl phosphoramide mustards was designed, synthesized and evaluated as nitroreductase-targeted prodrugs in gene-directed enzyme-prodrug therapy. Among them, fluorinated prodrugs showed improved bystander effect, cytotoxicity and selectivity. Based on the similar drug release mechanism via 1,6-elimination, a series of peptidylaminoarylmethyl phosphoramide mustards was designed, targeting prostate-specific antigen (PSA) as a prodrug-converting enzyme. By design, the prodrugs would only be activated after proteolytic cleavage of the PSA-specific peptide by PSA and then selectively release the highly cytotoxic phosphoramide mustard at the prostate tumor site. Among the synthesized prodrugs, the 2-fluorinated derivative had over 19-fold selectivity against PSA-secreting cancer cells with an IC_{50} of 5.3 μM according to *in vitro* antiproliferative cell assays.

To overcome the difficulty of synthesizing the designed peptidylaminoarylmethyl phosphoramide mustards, a novel selenocarboxylate/azide amidation methodology was

developed. This strategy not only played a crucial role in the success of this project but also provided an excellent solution to the acylation of highly electron-deficient amines. Selenocarboxylate/azide amidation has been successfully used to synthesize a series of amino acid-*p*NAs and amino acid-AMCs that are important synthons in the synthesis of chromogenic and fluorogenic protease substrates.

ACKNOWLEDGEMENTS

I also give my heartfelt thanks to Professor Joseph Rice for his help with my research. He never hesitated to answer my questions and always guided me in the right direction to solving problems. He also helped me to translate some important literatures written in German, which were definitely helpful to my research. It was a nice experience during my rotation in his lab.

I would like to thank Professor Spencer Knapp for attending my independent proposal and defense. It was a great moment to listen to his opinions and comments on my work. I also would like to thank Professor Lawrence J. Williams for his tremendous work on thio acid/azide amidation and discussions on selenocarboxylate/azide amidation that was part of my research. My thanks also goes to Professor Richard J. Knox for his help with *in vitro* antiproliferative cell culture assays on nitroreductase-targeted prodrugs.

I also would like to thank my former and current teammates, including but not limit to Yongying Jiang, Yiyu Ge and Yu Chen for their helpful discussions and suggestions. Particularly, my thanks goes to Prathima Surabhi for her help with preparation of some intermediates and her contribution to the selenocarboxylate/azide amidation project. I am also indebted to Daigo Inoyama for reading the draft of my proposal and thesis, and providing valuable comments that improved the contents of this dissertation.

I have to give my exceptional thanks to my parents for their endless support. Finally, I would like to express my deepest appreciation to my beautiful wife for her love, support and the greatest gift she gave to me – my little daughter.

DEDICATION

To my wife, my daughter and my parents

TABLE OF CONTENTS

LIST OF TABLES

LIST OF SCHEMES

ABBREVIATIONS

Ac   Acetyl

ACN   Acetonitrile

ADEPT   Antibody-directed enzyme prodrug therapy

12ADT   12-Aminododecanoyl-thapsigargin

Aib   α-Aminoisobutyrate

Ala   Alanine

AMC   7-Amino-4-methyl-coumarin

Arg   Arginine

Asp   Asparagin

Bn   Benzyl

Boc   *t*-Butoxycarbonyl

Bu   *t*-Butyl

Cbz   Benzoxycarbonyl

Chg   Cyclohexylglycine

CP   Cyclophosphoramide

CP450   Cytochrome P-450

Cys   Cysteine

dAcVIN   des-Acetyl-vinblastine

DCC   Dicyclohexylcarbodiimide

DEA   Diethylamine

DIBAL   Diisobutylaluminum hydride

DIEA   Diisopropylethylamine

DMAP	4-Dimethylaminopyridine
DMF	*N, N* - Dimethylformamide
DMSO	Dimethyl sulfoxide
Dox	Doxorubicin
EDA	Ethylenediamine
EMC	*ε*-Maleimidocaproic acid
EtOAc	Ethyl acetate
FBS	Fetal bovine serum
FCC	Flash column chromatography
Fm	9-Fluorenylmethyl
Fmoc	9-Fluorenylmethoxycarbonyl
FUDR	5-Fluoro-2´-deoxyuridine
GDEPT	Gene-directed enzyme prodrug therapy
Gln	Glutamine
Glu	Glutamic acid
Gly	Glycine
HSA	Human serum albumin
HBTU	2-(1H-benzotriazole-1-yl)-1,1,3,3-tetramethyluronium
His	Histidine
hk	Human glandular kallikrein
HOBt	1-Hydroxybenzotriazole
HOSu	*N*-Hydroxysuccinimide
HRPC	Hormone-refractory prostate cancer

Hyp	*trans*-4-Hydroxyproline
IGFBP	Insulin-like growth factor binding protein
Ile	Isoleucine
IP	Intraperitoneal
IPCF	Isopropyl chloroformate
Leu	Leucine
Lys	Lysine
Mab	Monoclonal antibody
Met	Methionine
MTD	Maximum tolerated dose
MTT	3-(4,5-Dimethylthiazol-2-yl)-2,5-diphenyltetrazolium bromide
Mu	Morpholinylcarbonyl
NAD(P)H	Nicotinamide adenine dinucleotide (phosphate), reduced form
NAC	*N*-Acetyl-cysteine
NBA	*N*-Boc-cysteine
NMP	*N*-Methylpyrolidone
NO	Nitric oxide
NTR	Nitroreductase
OPA	*o*-Phthaldialdehyde
PA	Proaerolysin
PABA	*para*-Aminobenzyl alcohol
Phe	Phenylalanine
pNA	*para*-Nitroaniline

PSA   Prostate-specific antigen

PSMA   Prostate-specific membrane antigen

Ser   Serine

SERCA   Sarcoplasmic/endoplasmic reticulum Ca^{2+}-dependent ATPase

suc   succinyl

TFA   Trifluoroacetyl

TG   Thapsigargin

THF   Tetrahydrofuran

Thr   Threonine

Trp   Tryptophan

Trt   Trityl

Tyr   Tyrosine

Val   Valine

VIN   Vinblastine

CHAPTER ONE

INTRODUCTION

I. Approaches for Treatment of Metastatic Prostate Cancer

Remarkably, 99.6% of normal prostate cells are neither proliferating nor dying; they, instead, are in a proliferatively quiescent state of Go.[1] The low proliferation rate is balanced with an equally low rate of cell death. Prostate cancer is a disease with high-grade prostatic intraepithelial neoplasia as the precursor for most peripheral-zone prostatic carcinomas.[2] In metastatic prostate cancer cells, the rate of cellular proliferation increases from 0.2% up to 3.1%, but there is no concomitant increase in the rate of cellular death.[3] This difference in survival is associated with an approximately 3-month doubling time, which is sufficient to cause death. Prostate cancer is now the third leading cause of cancer death in males following lung and colon/rectal cancer. Statistically, an American boy born today has a 16% chance of developing prostate cancer and about a 3% risk of dying from it. The American Cancer Society estimates that there will be about 218,890 cases of prostate cancer in the United States in 2007, with about 27,050 men dying from this disease.[4]

Prostatectomy and radiation are the major therapies for patients with localized prostate cancer, providing a nearly 100% 5-year survival rate. However, patients diagnosed at advanced stage of metastasis are not curable by these therapies, with only a 34% 5-year survival rate.[5] The traditional treatment paradigm for metastatic prostate cancer is using androgen ablation, which was first introduced by Charles Huggins in the 1940s.[6] Prostate cancer is initially quite responsive to androgen ablation therapy, resulting in initial

stabilization or regression of the disease. This treatment is not curative because it only affects cancer cells dependent upon androgen for growth and survival. Androgen-independent cells derived through genetic changes from hormonally dependent cells, however, remain able to proliferate. Unfortunately, most patients will develop incurable hormone-refractory prostate cancer (HRPC) within 2 years, leading to a median overall survival of 23–37 months from the time of initiation of androgen ablation therapy.[7]

Chemotherapy for HRPC was considered to be ineffective and primarily reserved for symptom palliation. Single-agent chemotherapeutic trials published between 1988 and 1991 in men with HRPC found an overall response rate of only 8.7%.[8] However, recent investigations demonstrated that giving docetaxel every 3 weeks plus low-dose prednisone improved the survival rate of HRPC and the quality of life as well. In 2004, FDA approved the combination of docetaxel and prednisone for the treatment of HPRC[9], giving new hope for improved survival and better quality of life to patients with advanced prostate cancer.

The absence of curative therapies for metastatic prostate cancer mandates development of novel and more efficient treatment regimens. Due to recent advances in basic and translational research, immunotherapy for advanced prostate cancer has steadily gained attention. Several prostate cancer vaccines, like Sipuleucel-T, DCVax$^@$-Prostate, GVAX$^@$, and PROSTVAC$^@$-VF, have been investigated in late-stage clinical trials and have shown evidence for clinical benefits.[10] The idea behind vaccine therapy is to produce systemic antitumor effects by stimulating immune responses such as the

secretion of nitric oxide and activation of T cells in tumor tissues. But questions remain as to how much prostrate cancer cells actually will be eliminated with vaccine therapy. Due to the presence of antigens in prostate cancer cells, such as prostate-specific antigen (PSA) and prostate-specific membrane antigen (PSMA), the monoclonal antibody (Mab)–based therapy is an attractive approach to the treatment of metastatic prostate cancer. A variety of Mab-based approaches are currently being developed. These include unconjugated antibodies that kill cancer cells by enhancing complement fixation, by initiating antibody-dependent cell-mediated cytotoxicity, or by inducing antitumor activity via modulating signaling pathways of cancer cells; and conjugated antibodies that carry with radioisotopes, cytotoxic agents or immunotoxins.[11,12]

Gene therapy for prostate cancer takes advantage of the fact that the normal and malignant prostate cells express unique genes encoding PSA, human glandular kallikrein 2 (hk2) and PSMA; and these genes have been cloned and their promoter/enhancer sequences have been identified. In one type of gene therapy, an adenovirus is prepared using prostate-specific promoters or enhancers. When taken up by non-prostatic cells, the virus is not transcribed. The virus is only transcribed in prostatic cells to induce a cytolytic response. CV706, a replication-competent, E3-deleted, cytolytic Ad5 adenovirus, has shown an associated decrease of PSA levels in patients with HRPC previously treated with radiation therapy.[13,14]

Prostate cancer-specific prodrug therapy is an exciting new strategy to selectively deliver antitumor agents to prostate cancer cells, allowing much higher drug doses and more

frequent treatments due to reduced toxicity. There are over-expressed prostate-specific proteases present within sites of prostate cancer, including serine proteases PSA, hk2 and the carboxypeptidase PSMA. They, therefore, provide ideal targets for prodrug design: if the non-cytotoxic prodrug form remains stable in blood and body fluids, the selective activation of prodrugs by these prostate-specific proteases on the site of prostate cancer can be achieved by proteolytic release of active anticancer agents. Some of the prodrugs targeting PSA, hk2 and PSMA have been reported and shown promising antitumor activity *in vitro*.[15-18]

In summary, although results from recent trials with systemic therapy for metastatic diseases have been encouraging, there is still an urgent need in the treatment of androgen-independent prostate cancer. On the basis of the knowledge in the molecular and biochemical mechanisms contributing to prostate cancer growth, there are several new approaches to prostate cancer-targeted therapies, including vaccine therapy, antibody-directed therapy, gene therapy and enzyme-targeted prodrug therapy. These types of approaches might provide the next generation of prostate cancer therapies.

II. PSA-Targeted Prodrug Therapy

A. Prostate-Specific Antigen

Prostate-specific antigen (PSA) was first identified in human seminal plasma in 1969.[19] PSA is a glycoprotein composed of a single polypeptide with a total mass of 33-34 kDa containing approximately 7% (*wt*/*wt*) of carbohydrate.[20] It belongs to the human kallikrein family of serine proteases with both antigenic and enzymatic activity.[21] The three members of this gene family include tissue kallikrein, human glandular kallikrein (hk), and PSA. Although PSA has approximately 70% sequence homology with tissue kallikrein and 80% with hk2, it has chymotrypsin-like activity while the other two proteins have trypsin-like activity.[22]

PSA is primarily produced by prostate ductal and acinar epithelium and is secreted into the lumen, where it cleaves semenogelin I and II in the seminal coagulum.[23] PSA activates urokinase-type plasminogen activator, which is believed to be involved in cancer invasion and metastasis.[24] It is also found that PSA could affect cancer spread by proteolytic modulation of cell adhesion receptors.[25] Furthermore, PSA is able to cleave insulin-like growth factor binding protein 3 (IGFBP-3) causing the release of active IGF-I, which in turn could enhance tumor growth.[26] However, other studies indicated that PSA may inhibit tumor growth by generating antiangiogenic angiostatin from plasminogen.[27,28]
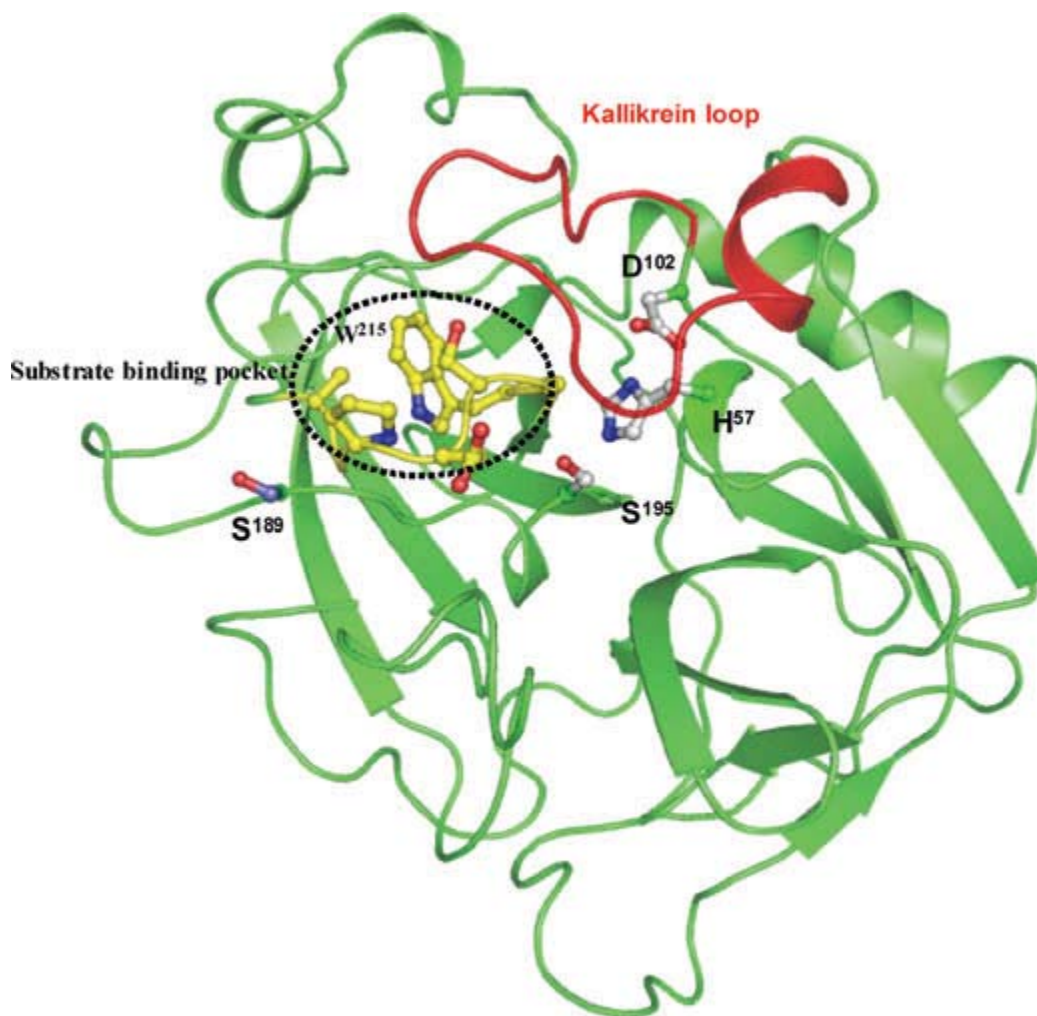
Figure 1. Homology Structure of Human Prostate-Specific Antigen

Catalytic triad His[57], Asp[102] and Ser[195] (silver ball and stick), Substrate-binding loop Trp[215]-Ala[220] (shown in yellow), Kallikrein loop (red) and Ser[189] (blue stick).

The crystal structure of human PSA is still not solved, presumably due to heterogeneity, autocatalysis, or other unknown reasons. Its three-dimensional structure was constructed using homology modeling based on human tissue kallikrein, stallion seminal plasma PSA, rat submaxillary gland serine protease, tonin, and mouse glandular kallikrein (Figure 1).[29] The homology model of human PSA suggested that PSA was composed of

two β-barrel domains, a kallikrein loop and a catalytic triad His[57], Asp[102], and Ser[195]. Structure of human PSA was quite similar to hk-1 and HPK-3. The substrate-binding pocket was predominated by hydrophobic and preferentially aromatic amino acid residues like Trp, which were determinants of substrate binding due to the presence of hydrophobic crevice between Tyr[99] and Trp[215].

The concentration of PSA in the prostate extracellular fluid is 1600-2100 nM (50-68 µg/mL) in normal prostate and primary prostate cancer, where 80-90% of PSA is enzymatically active.[30] However, intracellular PSA is enzymatically inactive due to the presence of high concentration of Zn^{2+} that forms an inactive complex with PSA. Remarkably, PSA is normally present in blood at very low level (<4.0 ng/mL). The increased serum PSA levels are often seen in prostate cancer patients, which are believed to be the result of cellular PSA leak caused by the absence of a basement membrane barrier that normally separates the prostate gland from surrounding stoma; and this lack of confinement is the hallmark of invasive prostate cancer.[31,32] There is evidence that serum PSA levels correlate well with the number of malignant prostate cells, and a high serum PSA level indicates a high risk of metastatic prostate cancer.[33] In 1994, FDA approved the PSA blood test to detect prostrate cancer for men. Most importantly, PSA present in bloodstream lacks enzymatic activity because it forms an inactive complex with protease inhibitors such as α_1-antichymotrpsin and α_2-macroglobulin.[22,34,35] Serum concentrations of these protease inhibitors are 10^5-10^6 fold higher than the serum PSA level and, therefore, are able to trap any active PSA present.[32,34] The loss of enzymatic activity of serum PSA, however, does not affect the use of PSA as a serological

biomarker because its immunoreactivity is not lost. Due to its remarkable characteristics, including specific production in the prostate tissue, enzymatically active form only in extracellular environment, enzymatically inactive form in serum and intracellular environment, and high concentrations of PSA in malignant prostate cancer cells, PSA is an excellent target to design prodrugs that rely on PSA's enzymatic activity for their activation, allowing site-specific release of anticancer drugs in the prostate tissue.

B. PSA-Targeted Prodrugs

Current research focuses on PSA-targeted prodrugs in which an anticancer agent is covalently linked to a PSA substrate peptide. By design, the anticancer agent would be released locally in the microenvironment around prostate cancer cells upon proteolytic cleavage of the prodrug by PSA. Ideally, the peptide-drug conjugate would remain inactive until it reaches the prostate due to either the absence of PSA or the inactive PSA-protease inhibitor complex in the systemic circulation. Therefore, the anticancer selectivity could be achieved through this site-specific activation mechanism.

The natural substrates of PSA are semenogelin I and II.[36] Several short peptide sequences were identified as excellent PSA substrates, including -Ser-Ala-Leu-**Leu-Ser**-Ser-Asp-Ile-, -Ala-Ala-Lys-**Phe-Glu**-Ser-Asn-Phe-, -Gln-Phe-Tyr-**Ser-Ser**-Asn-Lys-, -Ser-Ser-Phe-**Tyr-Ser**-Ser- and -Ser-Ser-Tyr-**Tyr-Ser**-Gly- (PSA cleavage site between amino acids is indicated in bold).[37-39] However, they were non-PSA specific and also could be cleaved by other serine proteases such as α-chymotrypsin. For peptide-drug conjugate

prodrugs, the ideal peptide should be specific to PSA and be stable upon exposure to other enzymes. Therefore, the activation of prodrugs would be localized in the prostate where 80-90% of PSA is enzymatically active. A few short peptides were synthesized and identified to be PSA specific via modification of the amino acid residues, including H-Ser-Lys-Leu-Gln-, H-His-Ser-Ser-Lys-Leu-Gln-, and Glutaryl-Hyp-Ala-Ser-Chg-Gln- that shared the same feature of having a Gln residue at P_1 site.[40,41] Peptide mapping showed that the most preferred cleavage occurred between Gln and Ser.[41,42]

Incorporation of peptides with various anticancer agents, including doxorubicin,[41,43] thapsigargin,[44,45] vinblastine,[46,47] 5-fluoro-2′-deoxyuridine,[48] diazeniumdiolate,[49] nitrogen mustard,[50] protoxin,[51] paclitaxel etc.,[52] led to prodrugs showing selective cytotoxicity against PSA-expressing cells.

i. Peptide-Doxorubicin Conjugates

Doxorubicin (**1**) is a topoisomerase II inhibitor with DNA intercalating cytotoxicity, which has been widely used for cancer treatment. As a single agent, doxorubicin has one of the best response rates against prostate cancer.[53,54] However, the anthracycline-associated cardiotoxicity and myelotoxicity limited its clinic use, especially in elderly patients. A properly designed doxorubicin prodrug could potentially minimize the side effects through the localized release of cytotoxic doxorubicin on the prostate tumor site. Incorporation of doxorubicin with a PSA-specific peptide is an apparent approach to increase the therapeutic index of doxorubicin.

Mu-His-Ser-Ser-Lys-Leu-Glu-Leu-Doxorubicin

The hexapeptide-doxorubicin conjugate **2**, Mu-His-Ser-Ser-Lys-Leu-Gln-Doxorubicin, was synthesized by coupling the peptide, Mu-His-Ser-Ser-Lys-Leu-Gln-OH, with doxorubicin via an amide bond linkage between the C-terminus of P_1-glutamine and the amino of daunosamine of doxorubicin (Figure 2). However, the PSA assay showed that the conjugate **2** was not cleavable by PSA due to the bulky doxorubicin moiety.[55] Insertion of a leucyl spacer between the P_1-glutamine residue and the amino of daunosamine of doxorubicin resulted in a heptapeptide-doxorubicin conjugate **3** (Figure 2), Mu-His-Ser-Ser-Lys-Leu-**Gln-Leu**-Doxorubicin, which was cleavable by PSA to release H-Leu-doxorubicin that was cytotoxic to prostate cancer cell lines with an IC_{50} of 50-100nM *in vitro* but had less cardiac toxicity than doxorubicin.[56-58] This conjugate **3** was >90% hydrolyzed to H-Leu-doxorubicin after 72-h exposure to PSA-producing LNCaP cells (human prostatic epithelial cells) with an IC_{50} of 70 ± 5 nM while the single agent, H-Leu-doxorubicin, had an IC_{50} of 50 ± 5 nM against LNCaP cells.

1 (Doxorubicin) R = H
2 R = Mu-His-Ser-Ser-Lys-Leu-**Gln-**
3 R = Mu-His-Ser-Ser-Lys-Leu-**Gln-Leu**-
4 R = Glutaryl-Hyp-Ala-Ser-Chg-**Gln-Ser**-Leu-
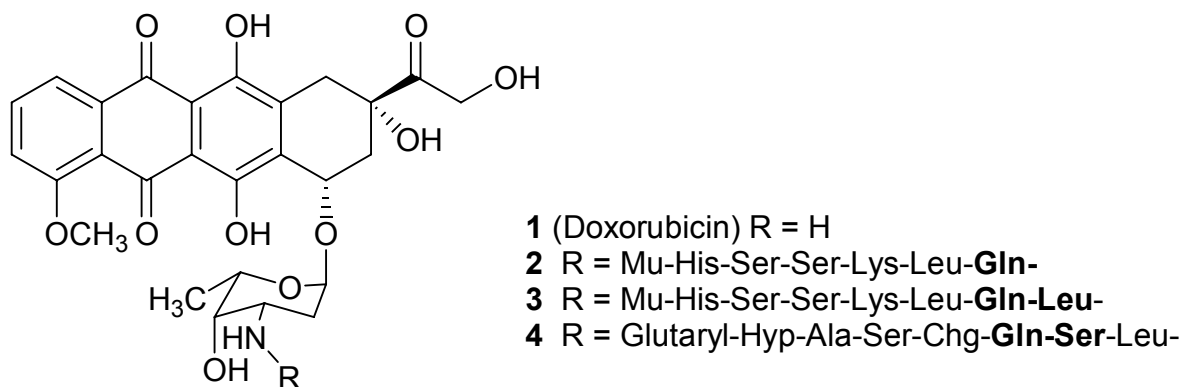
Figure 2. Chemical Structures of PSA-Specific Peptide-Doxorubicin Conjugates
P_1 and P1´ amino acids are indicated in bold.

The cytotoxic response of conjugate **3** was also measured by incubation of conjugate **3** in non-PSA-producing TSU cells, where there was no detectable cytotoxicity at concentrations up to 1 μM. However, adding enzymatically active PSA (30 μg/mL) to the incubation medium restored the prodrug's cytotoxicity against non-PSA-producing TSU cells with an IC_{50} value of 230 ± 5 nM whereas H-Leu-doxorubicin itself had an IC_{50} of 120 ± 4 nM against TSU cells. When PSA-positive PC-82 tumor-bearing mice were given the prodrug **3** at 4x the maximum tolerated dose (MTD) of doxorubicin, a 57% decrease *vs* control in tumor weight was observed.

Glutaryl-Hyp-Ala-Ser-Chg-Gln-Ser-Leu-doxorubicin

The peptide-doxorubicin conjugate **4** (L-377,202), Glutaryl-Hyp-Ala-Ser-Chg-**Gln-Ser-**Leu-doxorubicin (Hyp denotes *trans*-4-hydroxyl-*L*-prolyl, Chg denotes cyclohexyl-*L*-glycyl), showed promising results with greater than 20-fold selectivity against human prostate PSA-secreting LNCaP cells relative to non-PSA-secreting DuPRO cells. The prodrug had a rapid rate of hydrolysis by PSA ($t_{1/2} = 30$ min) to release cytotoxic H-Leu-doxorubicin at a substrate/PSA molar ratio of 100/1. Drug localization studies demonstrated that, compared to administration of doxorubicin, administration of L-377,202 led to lower doxorubicin levels in the heart, indicating the less cardiotoxicity of L-377,202. The prodrug L-377,202 also showed high tumor tissue distribution of doxorubicin and H-Leu-doxorubicin in xenograft models of prostate cancer, in which there was more H-Leu-doxorubicin than doxorubicin.[43] *In vivo* studies showed that L-377,202 was approximately 15 times more effective than doxorubicin when both were

used at their maximum tolerated doses (MTD). L-377,202 was able to reduce circulating PSA levels by 95% and tumor weight by 87% at a dose below its MTD, and caused approximately 6% body weight loss, while the equal molar of doxorubicin was ineffective in reducing PSA level and caused 22-28% body weight loss with substantial number of mice died. The greater efficacy and decreased gross toxicity of L-377,202 were at least partially attributable to its specific targeting on PSA-secreting tissues. However, the therapeutic usefulness of L-377,202 was limited by two apparent drawbacks: (1) only approximately 30% of the prodrug was metabolized to expected H-Leu-Dox in different laboratory animal models;[59] and (2) there was approximately 20% non-PSA-specific formation of doxorubicin observed in the blood of patients in a phase I clinical trial.[60]

Albumin-bound PSA-targeted Doxorubicin Prodrugs

Owing to a high metabolic turnover of tumor tissues and the enhanced vascular permeability of blood vessels of malignant tissues for circulating macromolecules, the plasma protein albumin preferentially accumulates in solid tumors. By using the plasma albumin as an anticancer drug carrier, the tumor-targeted drug delivery to tumor tissues could be achieved and the diffusion of cytotoxic agents into the healthy tissues would be therefore limited.[61] In January 2005, FDA approved Abraxane (albumin-bound paclitaxel), the first in the class of protein-bound drugs, for the treatment of breast cancer after failure of combination chemotherapy or relapse within six months of adjuvant chemotherapy. Recently, a dual-targeting prodrug strategy for improved prostate cancer

chemotherapy had been reported.[62,63] The design was based on the following features: (1) *in situ* bonding of a prodrug to endogenous plasma albumin after intravenous administration, (2) accumulation of the albumin-bound prodrug in the prostate cancer and (3) release of the cytotoxic species in the prostate cancer upon PSA-specific proteolysis.
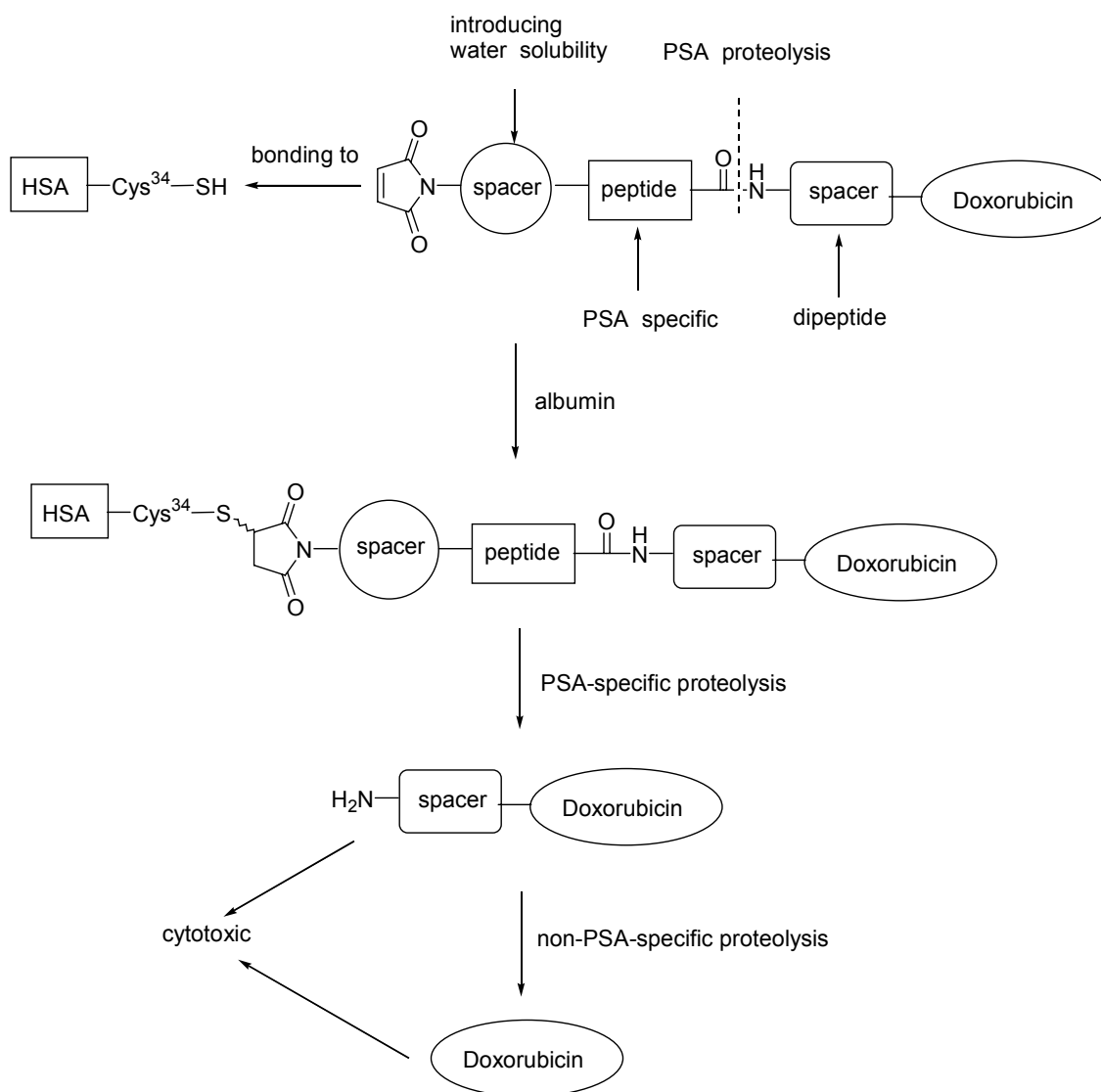
Figure 3. Proposed Mechanism of Albumin-Bound PSA-Activated Doxorubicin Prodrugs

The designed prodrugs consist of a maleimide moiety, a spacer, a PSA-specific peptide sequence, and a dipeptide-doxorubicin conjugate as shown in Figure 3. The prodrugs rapidly and selectively bound to human serum albumin (HSA) by forming a covalent C-S bond between the maleimide moiety and Cys[34] of HSA after incubation with human blood plasma. The selective bonding of prodrugs to HSA was due to the fact that free thiol groups are not usually present in the majority of circulating serum proteins except albumin; and the thiol group of Cys[34] is the most reactive thiol group in HSA because of its low pKa character, which is approximately 7 as compared to 8.5 and 8.9 for cysteine and glutathione, respectively.[64]

Figure 4. Chemical Structures of PSA4-Arg and PSA5
PSA cleavage site between amino acids is indicated in bold.

PSA4-Arg (**5**), EMC-Arg-Arg-Ser-Ser-Tyr-**Tyr-Ser**-Gly-Dox (EMC = ε-maleimidocaproic acid) and PSA5 (**6**), EMC-Arg-Ser-Ser-Tyr-**Tyr-Ser**-Arg-Dox, rapidly formed albumin-bound conjugates within 5 min after incubation with human blood plasma (Figure 4). PSA enzymatic assay showed that both albumin-bound PSA4-Arg and PSA5 were efficiently cleaved by PSA at P_1-P'_1 scissile bond between Tyr and Ser to release H-Ser-Gly-Dox and H-Ser-Arg-Dox, respectively. In cell culture experiments, the prodrugs were 70 to 100-fold less active against PSA-positive LNCaP cells than doxorubicin, presumably due to that the dipeptide-doxorubicin conjugates, H-Ser-Gly-Dox and H-Ser-Arg-Dox, were less cytotoxic than doxorubicin and the low concentrations of PSA present in the cell-conditioned medium of LNCaP cells (1 nM *vs* normal 1600-2800 nM).[65] However, PSA4-Arg and PSA5 significantly inhibited tumor growth in the PSA$^+$ xenograft model while negligible antitumor responses were observed in the PSA$^-$ xenograft model. *In vivo* activity studies showed that PSA5 had superior therapeutic index to PSA4-Arg. The main reason was presumably because the H-Ser-Arg-Dox cleaved from PSA5 was able to release more cytotoxic free doxorubicin upon non-PSA-specific proteolysis while the less cytotoxic H-Ser-Gly-Dox from PSA4-Arg was stable in PSA-positive prostate carcinoma tissues.

ii. Peptide-Vinblastine Analogue Conjugates

DNA-damaging cytotoxic agents like doxorubicin are more active in cells expressing the wild-type p53 protein, a tumor suppresser acting as a checkpoint in the cell cycles. In contrast, the cytotoxicity induced by microtubule-active agents like vinblastine (VIN) is

p53 independent. Considering that metastatic prostate cancer almost always contains p53 mutations, the treatment of advanced metastatic prostate cancer with PSA-activated vinblastine prodrugs should be more efficacious than PSA-activated doxorubicin prodrugs.

7 (Vinblastine) R = Ac
8 (dAcVIN) R = H
9 R = Ac-Hyp-Ser-Ser-Chg-**Gln-Ser**-Gly-
10 R = Ac-Hyp-Ser-Ser-Chg-**Gln-Ser**-Leu-
11 R = Ac-Hyp-Ser-Ser-Chg-**Gln-Ser**-Pro-
12 R = Ac-Hyp-Ser-Ser-Chg-**Gln-Ser**-Ser-Pro-
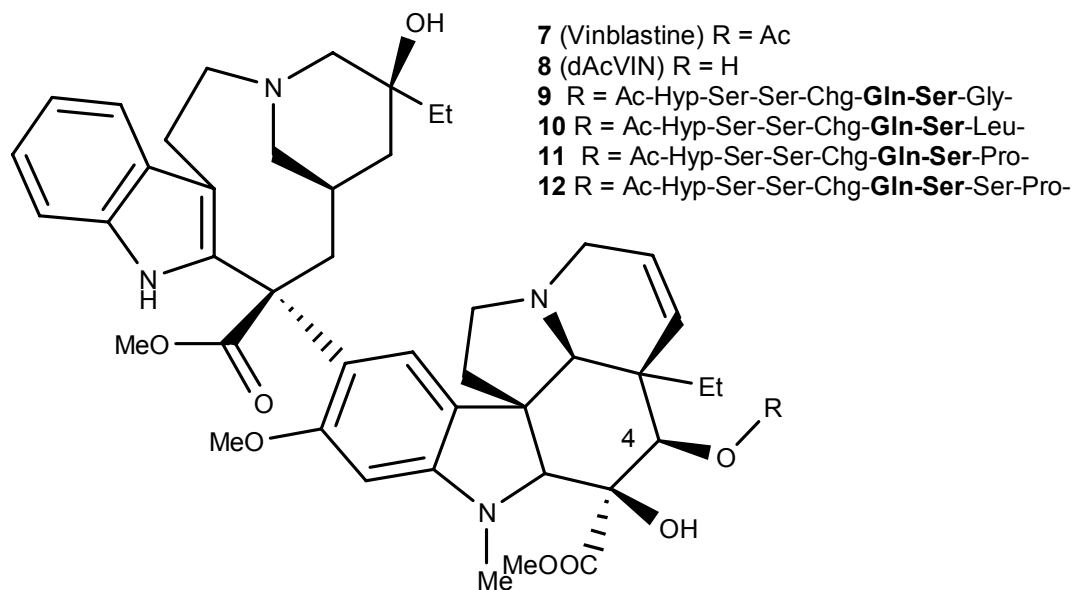
Figure 5. Chemical Structures of Vinblastine Prodrugs.

There was no cytotoxic efficacy *in vivo* for conjugates that were synthesized by coupling PSA-specific peptides with des-acetyl-vinblastine (dAcVIN) at C-23 via alkyl or cycloalkyl diamides. Efforts then focused on conjugates with the peptides linked to dAcVIN at C-4 (Figure 5). Similarly, an extra amino acid residue as a spacer was required to render the peptide-dAcVIN conjugates cleavable by PSA. While conjugates **9** and **10** were cleavable by PSA with t $\frac{1}{2}$ of 30 and 35 min respectively, the conjugate **11** was only 8% cleaved by PSA in 60 min. However, when an additional spacing serine

residue was inserted between the Pro- and Ser-, the resulting conjugate **12** was rapidly cleaved by PSA with a half-life of 12 min but was stable in human plasma. *In vitro* activity studies showed that conjugate **12** was over 10-fold more cytotoxic against PSA-positive LNCaP cells than against PSA-negative cells. *In vivo* nude mouse xenograft studies showed that the conjugate **12** was able to reduce the circulating PSA level by 99% and tumor weight by over 85% without causing host death.

Scheme 1. Proposed PSA-Induced "Chemical Release" of des-Acetyl-Vinblastine
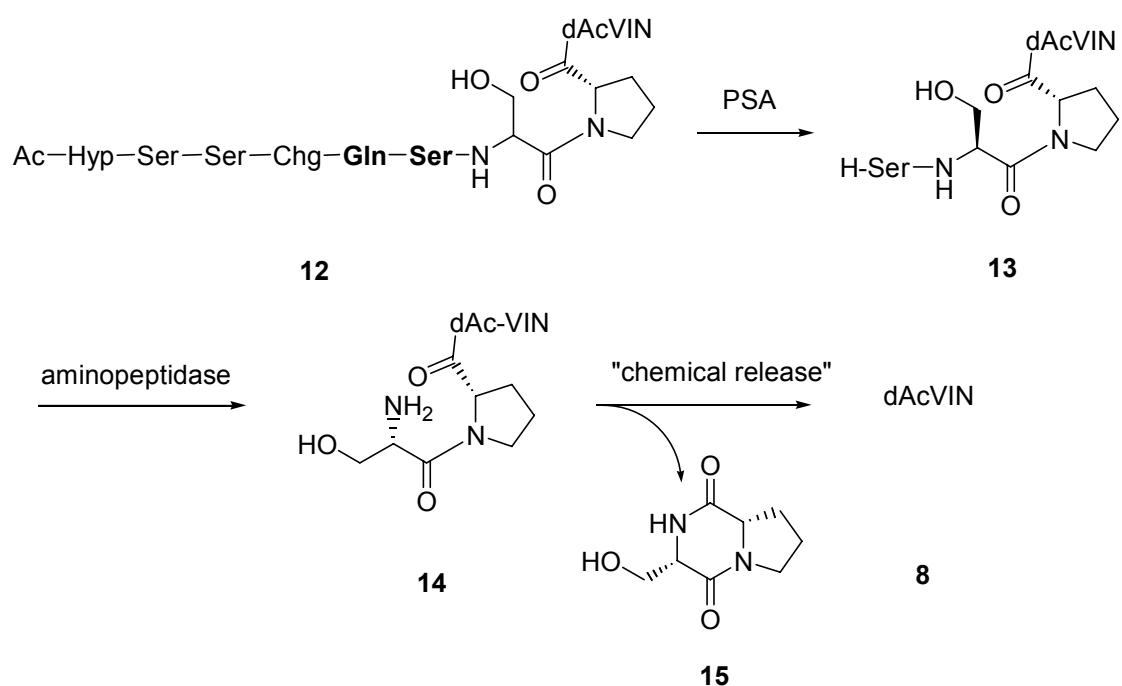
The superior activity of **12** was at least partially attributable to the "chemical release" of dAcVIN (**8**) from H-Ser-Pro-dAcVIN (**13**) after PSA proteolysis followed by non-PSA-specific cleavage (Scheme 1). The formation of diketopiperazine **15** served as a driving

force for the "chemical release" of dAcVIN, which is commonly seen in dipeptide esters, particularly if the C-terminal residue is a secondary amino acid.[66,67]

iii. Peptide-Paclitaxel Conjugates

Antimicrotubule taxanes have significant clinical activity in hormone-refractory prostate cancer.[68] Paclitaxel, a member of taxanes, has demonstrated efficacy in a variety of human tumors, including prostate cancer. However, the lack of selectivity and poor water-solubility limit its use in chemotherapy. Attempts have been made to convert paclitaxel into water-soluble prodrugs that can be activated by PSA-specific proteolysis.[52] Four peptide-paclitaxel conjugates were designed and synthesized by coupling paclitaxel to a PSA-specific water-soluble peptide, Mu-His-Ser-Ser-Lys-Leu-Gln-OH or Mu-Ser-Ser-Lys-Tyr-Gln-OH, via a self-immolative linker, either *para*-aminobenzyl alcohol (PABA) or ethylenediamine (EDA) as shown in Figure 6.

Although prodrugs **16** and **17** were stable in PSA enzymatic assay medium, they were unstable in the serum-containing medium because of the hydrolysis-labile carbonate functionality. Introduction of the carbamate functionality using an EDA linker in prodrugs **18** and **19**, however, increased the stability towards serum as well as the PSA-proteolysis rate of **18** and **19**. The prodrug **19** had the fastest rate of hydrolysis by PSA with a half-life of 6 h as compared to 14 h for **16**, 12 h for **17** and 10 h for **18**. The prodrug **19** was 3 to 5-fold more cytotoxic (IC$_{50}$ of ~1.0 μM) against the PSA-secreting CER22Rv1 cell line than the non-PSA-secreting DU145 and TSU cell lines.
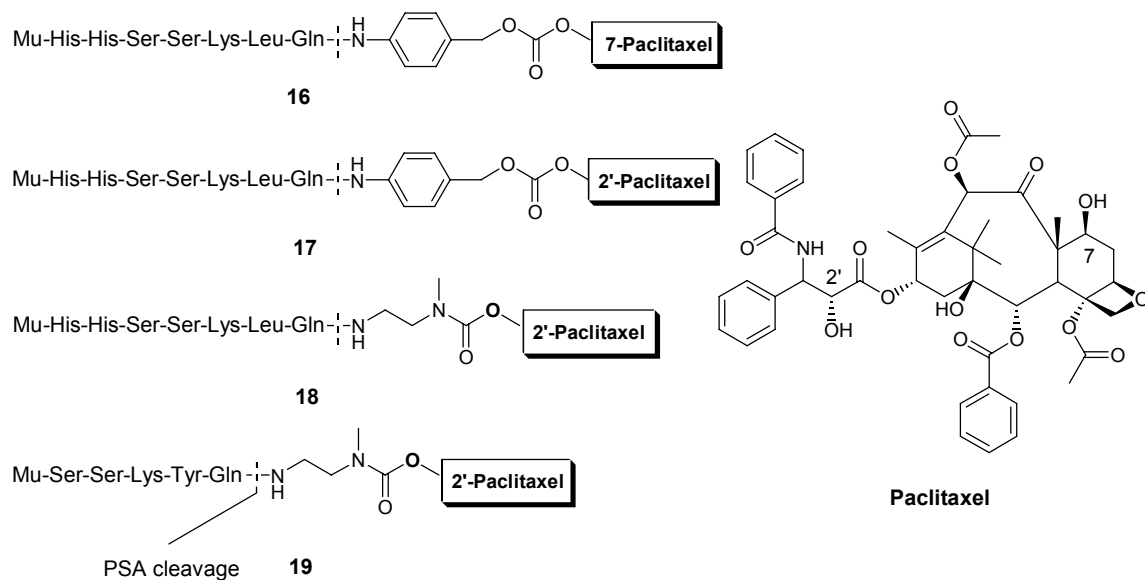
Figure 6. Chemical Structures of PSA-Activated Peptide-Paclitaxel Conjugates.

iv. Peptide-Fluorodeoxyuridine Conjugates

5-Fluoro-2′-deoxyuridine (FUDR) is an antimetabolite. It is first converted by thymidine kinase to FUDR-5′ phosphate *in vivo*, which in turn inhibits thymidylate synthase to interfere with DNA synthesis.[69] The cytotoxicity of FUDR, however, is not prostate cancer specific. To achieve selective cytotoxicity against prostate cancer, the FUDR was coupled with the PSA-specific peptide, Mu-His-Ser-Ser-Lys-Leu-Gln-OH, via a self-immolative linker H-Leu-Aib-OH[70] (Aib = α-Aminoisobutyrate) as shown in Scheme 2.[48] The resulting conjugate should have little or no cytotoxicity because the acylation of the 5′-hydroxy group prevents the 5′-phosphorylation of FUDR by thymidine kinase. Upon PSA-specific proteolysis, the free FUDR would be released through cyclization of the

linker. Enzymatic assays showed that the PSA proteolysis was not complete after 51 h

incubation with PSA at a molar ratio of 130/1 (prodrug/PSA). In the absence of PSA,

this conjugate was quite stable in the assay medium with no detectable FUDR formed

after 51 h incubation. *In vitro* colony survival assays indicated that the conjugate **20** had a

60-fold higher cytotoxicity (IC_{50} = 117 nM) in PSA-secreting LNCaP cells compared to

non-PSA-secreting TSU cells (IC_{50} = 7200 nM).

Scheme 2. Proposed Release Mechanism of Mu-HSSKLQL-Aib-FUDR

20

Mu-His-Ser-Ser-Lys-Leu-Gln-OH

PSA

21

22   (5-Fluoro-2'-deoxyuridine)
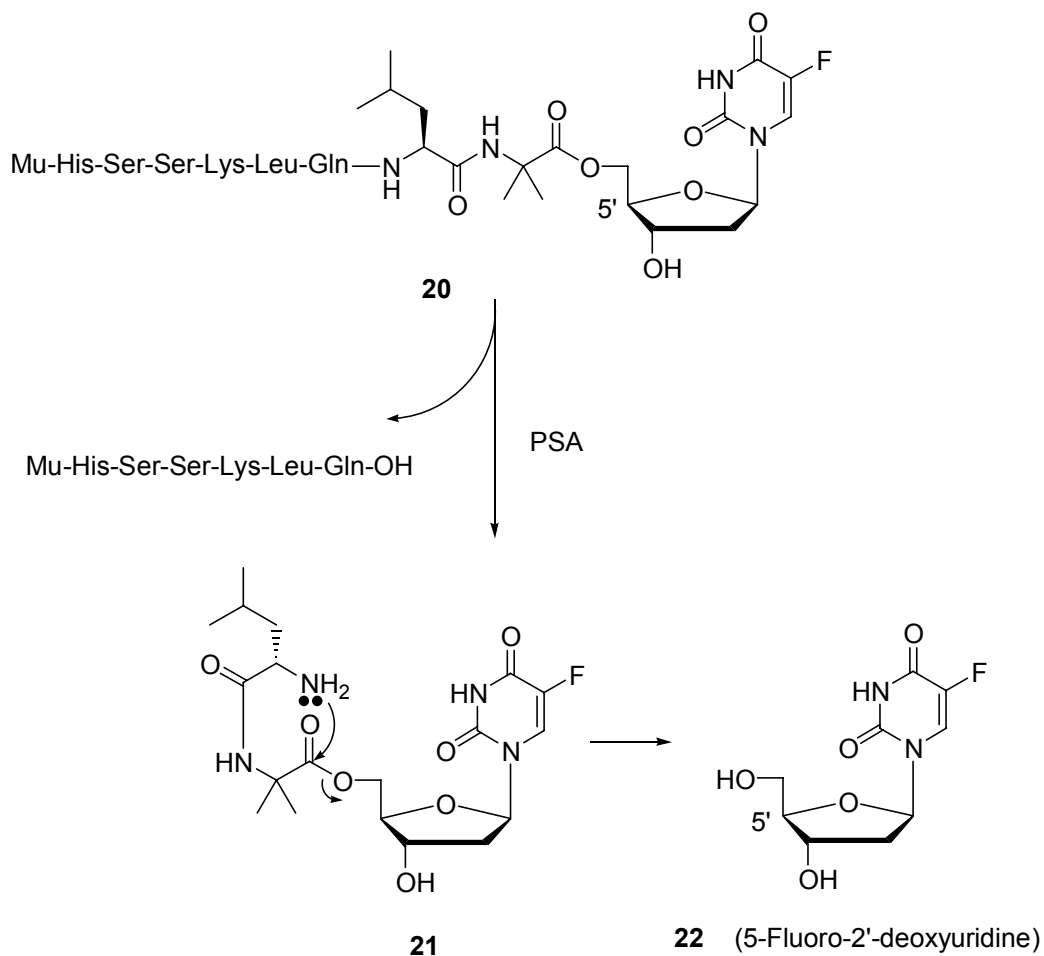
v. Peptide-Thapsigargin Analogue Conjugates

Because hormone-refractory prostate cancer (HRPC) has a lower growth fraction than other cancers, the standard anti-proliferative chemotherapy is relatively ineffective against slowly proliferating androgen-independent prostate cancer cells. In the most used LNCaP model, LNCaP cells respond very well to doxorubicin, paclitaxel or thapsigargin under normal growing conditions. However, when LNCaP cells grow with a much lower growth fraction in conditioned media, the death response induced by doxorubicin and paclitaxel is lost while thapsigargin (**23**) retains its ability to induce apoptosis.[44]

Thapsigargin (TG) is a potent inhibitor of the sarcoplasmic/endoplasmic reticulum Ca^{2+}-dependent ATPase (SERCA) pump. Inhibition of SERCA pump by thapsigargin leads to a rapid, 3 to 5- fold elevation in intracellular free Ca^{2+} due to emptying of the stored calcium pools within the endoplasmic reticulum (ER) through continuous and passive leakage of Ca^{2+} from the ER.[71] Depletion of the ER Ca^{2+} pool also generates a signal that induces a change in the permeability of the plasma membrane, leading to an influx of Ca^{2+} due to the high extracellular Ca^{2+} concentration.[72] Most importantly, thapsigargin is effective against both proliferative and quiescent cells by elevating intracellular free Ca^{2+} levels to induce apoptosis. Because the SERCA pump is present in every mammalian cell and is physiologically required for the endoplasmic reticulum in cells to function, this action mechanism of thapsigargin makes it unlikely to be selective for prostate cancer cells. Therefore, an inactive prodrug form of thapsigargin with a PSA-specific carrier

peptide would overcome this problem if thapsigargin is only liberated in the prostate cancer tissues via PSA-specific proteolytic digestion.
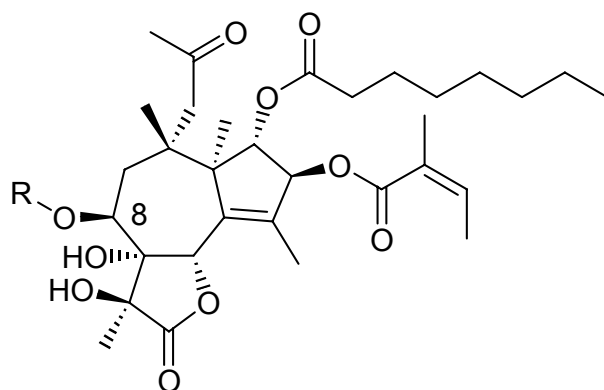
23 (Thapsigargin) R = CH$_3$CH$_2$CH$_2$CO-
24 12-Aminododecanoyl-thapsipargin R = H$_2$N(CH$_2$)$_{11}$CO-
25 R = Mu-His-Ser-Ser-Lys-Leu-**Gln-Leu**-

Figure 7. Chemical Structures of TG, 12ADT, and Mu-HSSKLQL-12ADT.
The P1 residue is indicated in bold

Among thapsigargin analogues derived from structural modifications, 12-aminododecanoyl-thapsigargin (12ADT) was identified as potent as thapsigargin towards SERCA pump inhibition and apoptotic activity. In addition, replacement of the 8-butanoyl group in thapsigargin with a 12-aminodocecanoyl group provided an amino group as an anchoring point to attach a peptide specific to PSA proteolysis (Figure 7). Insertion of a spacing amino acid between the peptide, Mu-His-Ser-Ser-Lys-Leu-Gln-OH (Mu-HSSKLQ), and 12ADT was essential to make the resulting conjugate cleavable by

PSA, which in turn released an amino acid-12ADT conjugate after proteolytic digestion. This amino acid-12ADT conjugate might be further converted to free 12ADT by another aminopeptidase. 12ADT was 3-fold less potent in SERCA inhibition and 40-fold less potent in apoptotic activity than thapsigargin. However, coupling of 12ADT with leucine, alanine, phenylalanine or serine improved the resulting conjugate's apoptotic activity by 4-40 folds. Among the amino acid-12ADT conjugates investigated, H-Leu-12ADT (L12ADT) had an equipotency of apoptotic activity and 3-fold less potency of SERCA pump inhibition compared to thapsigargin.

In vitro, conjugate **25** was cleaved by PSA to H-Leu-12ADT (L12ADT) with a k_{cat}/K_m of 21.9 $s^{-1}M^{-1}$. Most importantly, it was stable in human plasma with the observed <0.5% hydrolysis over 24 h. It showed over 100-fold higher cytotoxicity against PSA-secreting cells than against non-PSA-secreting cells. Continuous subcutaneous administration of conjugate **25** to mice led to nearly complete cessation of the PSA-expressing xenograft tumor growth over 40 days without discernible toxicity, substantial weight loss, and death. Furthermore, it had no effect on non-PSA-expressing xenograft tumors.[44] This conjugate **25** is currently under a phase I clinical trial.

vi. Peptide-Diazeniumdiolate Conjugates

Nitric oxide (NO) is a major mediator involved in many physiological processes. It may also act against many types of tumors by interacting with oxygen-derived radicals to form molecules that are able to nitrosate proteins, to modify their functions and to mediate

damages to DNA[73,74]. Diazeniumdiolates are compounds containing the [N(O)NO]⁻

structural unit, which is an excellent source for the controlled release of NO both *in vitro*

and *in vivo*.[74] A class of esterase-activated diazeniumdiolate prodrugs have shown

significant antileukemic activity *in vitro*.[75] Similarly, properly designed PSA-activated

diazeniumdiolate prodrugs would be able to selectively deliver toxic NO radicals to

prostate tumor tissues, leading to apoptosis of cancer cells. Diazeniumdiolate **29** was

conjugated to PSA-substrate peptides via a self-immolative 'acetal' linkage (Scheme 3).

Preliminary studies showed that conjugates **26-28** were cleavable by PSA to release NO

and stable at neutral pH.

Scheme 3. Proposed Mechanism of PSA-Activated Diazeniumdiolate Prodrugs
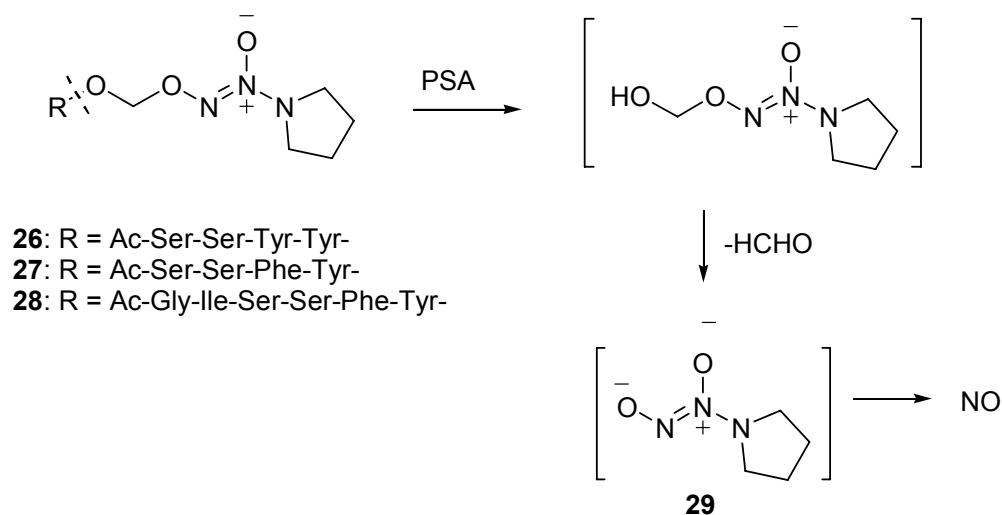
26: R = Ac-Ser-Ser-Tyr-Tyr-
27: R = Ac-Ser-Ser-Phe-Tyr-
28: R = Ac-Gly-Ile-Ser-Ser-Phe-Tyr-

vii. PSA-Activated Channel-Forming Toxin

Proaerolysin (PA) is a 53-kDa protein produced by the aquatic Gram-negative pathogen, *Aeromonas hydrophila*.[76] It exists in a form of water-soluble dimmer that binds to glycophosphatidylinositol-anchored proteins present on the surface of mammalian cells. After the carboxy-terminal inhibitory domain of PA is cleaved by ubiquitous membrane-bound proteases such as furins, the inactive Proaerolysin releases aerolysin that in turn rapidly oligomerizes and enters the membrane to form highly stable pores causing rapid cell death.[77] Cell viability assays showed that native PA was highly toxic *in vitro* with picomolar cytotoxicity but had no tumor-specific effects making it unsuitable for caner treatment. The native PA was then modified to produce a PSA-activated protoxin (PRX302), in which the original furin recognition sequence (-Lys-Val-Arg-Arg-Ala-Arg-) of PA was converted to a PSA-cleavable sequence (-His-Ser-Ser-Lys-Leu-Gln-).[51] This modification attenuated aerolysin activation in non-PSA-secreting cells by over 20-fold and in PSA-secreting cells by 5-fold. However, PRX302 still led to PSA-dependent decreases in cell viability at a picomolar concentration level. Single intratumoral injections of PRX302 produced nearly complete regression of PSA-positive human prostate cancer xenografts but not PSA-negative bladder cancer xenografts. In addition, a single injection of PRX302 into the PSA-producing monkey prostate caused extensive but organ-confined damage to the prostate with no morbidity. In contrast, little damage was observed following an injection of high-dose PRX302 into the non-PSA-producing dog prostate. A phase I trial is now warranted to assess toxicity of PRX302 in patients with rising PSA levels after prior definitive radiation therapy.

III. Summary

The current research on prodrugs based on PSA-specific activation has demonstrated that the PSA can be used as a prodrug-converting enzyme to achieve the site-specific release of cytotoxic agents at the prostate tumor site with fewer impacts on normal cells. A possible limitation of using PSA-activated prodrugs is that the prodrugs may also be activated in normal prostate. However, such activation would produce minimal problems because surgical removal of the prostate gland does not affect patient's overall health. In addition, androgen ablation induced by other therapies also activates apoptosis of normal as well as malignant prostate cells without producing toxic effects. Therefore, this limitation should not be clinically significant.

CHAPTER TWO

DESIGN, SYNTHESIS AND EVALUATION OF PSA-ACTIVATED

PEPTIDYLAMINOARYLMETHYL PHOSPHORAMIDE MUSTARDS

Our group has long-standing interests in prodrugs that target nitroreductase-based gene-directed enzyme prodrug therapy (GDEPT).[78-83] The enzyme under investigation is the *nfsB* gene product of *Escherichia coli*, an oxygen-insensitive flavin mononucleotide-containing nitroreductase (NTR).[84] The nitroreductase is capable of reducing certain aromatic nitro groups to the corresponding hydroxylamino or amino groups in the presence of NADH or NADPH. This enzyme can be delivered site-specifically to tumor cells by a bicistronic vector encoding for the *E. coli* nitroreductase. After a prodrug is administered, it is converted to the cytotoxic species by the *E. coli* nitroreductase expressed only in tumor cells. This strategy allows selective delivery of cytotoxic agents to tumor sites.[85,86] Therefore, it may overcome the problems associated with traditional chemotherapy, such as the side effects and limited maximum dose of anticancer drugs due to the lack of tumor selectivity.

Four classes of NTR-targeted prodrugs have been described, including 5-aziridinyl-2,4-dinitrobenzamide [87,88], dinitrobenzamide mustards[89-91], 4-nitrobenzylcarbamates[92-94], and nitroindolines[95] (Figure 8). We designed, synthesized and evaluated a series of nitroaryl phosphoramides, including cyclic and acyclic phosphoramides.[81,83] The rationale of our design was based on the "electronic property switch" that is triggered
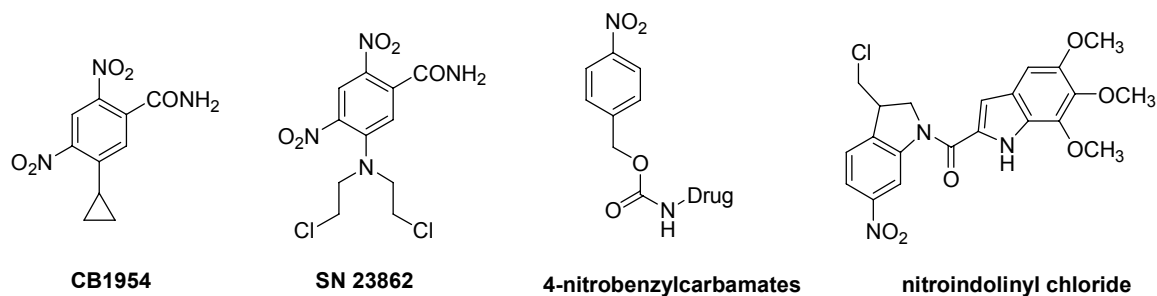
Figure 8. Structures of CB1954, SN 23862, 4-Nitrobenzylcarbamates and Nitroindolinyl Chloride.

by reduction of the electron-withdrawing nitro group (Hammett electronic parameter $\sigma_p =$ 0.78) to the electron-donating hydroxylamino ($\sigma_p = -0.34$) or amino group ($\sigma_p = -0.66$) as shown in Scheme 4. Upon reduction by nitroreductase, the resulting hydroxylamino or amino group facilitates the cleavage of benzylic C-O bond to release phosphoramide mustard (**33**) via a 1,6-elimination process.[96] This process has been extensively used for the targeted drug delivery and been well documented.[97]

Scheme 4. Activation Mechanism of Nitroreductase-Targeted 4-Nitroarylmethylphosphamide Mustards
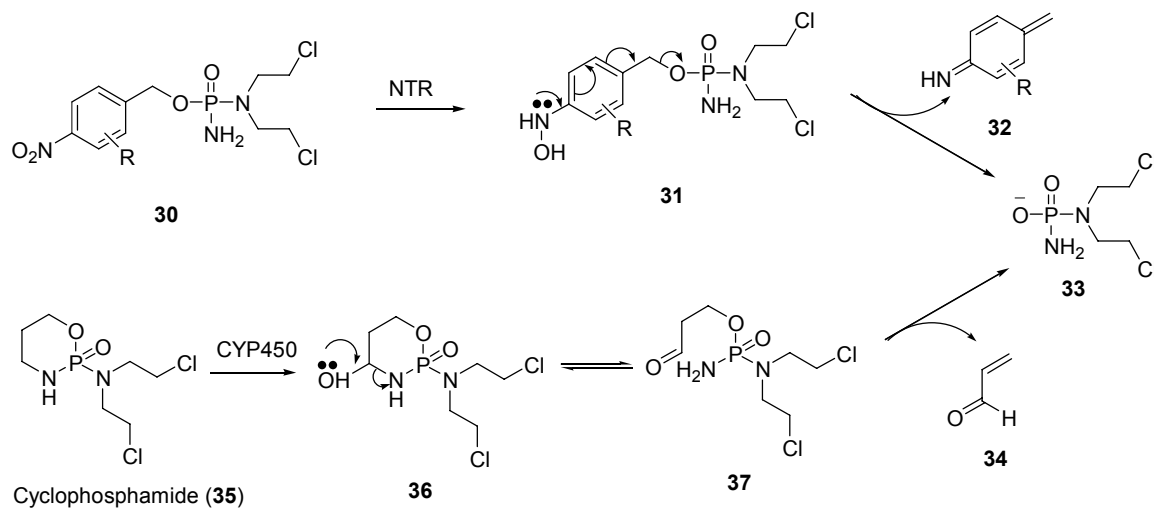
The released phosphoramide mustard (**33**) is the active metabolite of cyclophosphamide (**35**), an important anticancer drug that was synthesized over forty years ago and is still clinically used to treat a variety of cancers, especially slow-growing solid tumors for which there are few effective anticancer drugs are available.[98] Cyclophosphamide (**35**) itself is a prodrug that has to be activated by cytochrome P-450 (CYP450) in the liver (Scheme 4). The released phosphoramide mustard (**33**) is a strong alkylating agent that cross-links interstrand DNA and, ultimately is responsible for the cytotoxicity.[99-101] The byproduct acrolein (**34**) is related to hemorrhagic cystitis, a life-threatening side effect associated with cyclophosphamide treatment.[102] Our previously synthesized nitroarylmethyl phosphoramide mustards were shown to be excellent substrates of the *E. coli* nitroreductase and were highly cytotoxic against nitroreductase-expressing Chinese hamster fibroblast V79 cells and human ovarian carcinoma SKOV3 cells. Among them, 4-nitrobenzyl phosphoramide mustard (LH007) showed promising results in terms of cytotoxicity and selectivity against nitroreductase-expressing cancer cells. It was ~170,000x more cytotoxic towards the NTR^+ V79 cell line with an IC_{50} as low as 0.4 nM upon 72-hour expoure.[81] It was100-fold more active and 27-fold more selective over 5-aziridinyl-2,4-dinitrobenzamide (CB1954), a prodrug being evaluated clinically in combination with virally delivered nitroreductase.[103-107]

I. Design Principle and Proposed Activation Mechanism

PSA is produced in high levels by normal and malignant prostate cancer cells, and is only enzymatically active in extracellular microenvironment of prostate cells. In the presence of high concentration of Zn^{2+}, intracellular PSA is inactivated by the formation of complex with Zn^{2+}. Once entering the blood, PSA is inactivated by binding to serum protease inhibitors present. Therefore, PSA-activated prodrugs can be administered systemically via the blood without being activated in the systemic circulation due to inactivation of PSA by abundant serum protease inhibitors.

The current research on prodrugs based on PSA-specific activation has demonstrated that the PSA can be used as a prodrug-converting enzyme to achieve the site-specific release of cytotoxic agents at the tumor sites with fewer impacts on normal cells. Because PSA is sensitive to structural bulkiness at the cleavage site, direct coupling of the peptide substrate with an anticancer drug, such as doxorubicin and vinblastine, led to conjugates that were resistant to proteolytic cleavage by PSA. The insertion of 1-2 additional amino acids as a spacer between the P_1 site and the anticancer drug was required to improve the rate of PSA cleavage. Thus, upon proteolytic cleavage by PSA, the amino acid-drug or dipeptide-drug conjugate was released in the prostate tissue instead of the free drug. The conjugate was still in the form of prodrug with no or less cytotoxicity, requiring a post PSA-cleavage process to restore the original activity of the parent drug. Furthermore, the amino acid/dipeptide-drug conjugates can re-enter systemic circulation and spread to other tissues. Subsequent proteolysis of the conjugates by other proteases is often non-

specific, causing side effects and loss of selectivity due to release of the active drug in the blood and other tissues.

Our strategy is to insert a traceless linker between a PSA-substrate peptide and an anticancer agent, which would be only activated to release the cytotoxic agent after proteolytic cleavage of the peptide. By design, the cytotoxic agent is directly released at the site of the targeted tumor tissues without a post-metabolic process after PSA cleavage. In addition, instead of using big natural product anticancer agents like doxorubicin, vinblastine and thapsigargin, our design focuses on introducing phosphoramide mustard (**33**) as a cytotoxic agent to provide the designed prodrugs with "drug-like" properties according to the empirical Lipinski's rule of five.[108]

The goal of this project is to develop a site-specific activation delivery system that can be triggered by prostate-specific antigen. On the basis of results obtained in our nitroreductase-targeted GDEPT project, we postulated that, if we replace the nitro group with the peptidylamino functionality as shown in Scheme 5, the peptidylaminoarylmethyl phosphoramide mustard (**38**) could be activated through a 1,6-elimination process after PSA-mediated proteolysis. Among the short peptide substrates of PSA,[39,109] the pentapeptide, Glutaryl-Hyp-Ala-Ser-Chg-Gln-OH, is specific toward PSA proteolysis and not affected by extracellular proteases such as chymotrypsin, trypsin, urokinase, plasmin, thrombin and hk1.[110] This pentapeptide was used as a carrier of peptide-doxorubicin [43,110] and peptide-vinblastine prodrugs[47] for selectively killing PSA-secreting cells. Therefore, our design focused on Glutaryl-Hyp-Ala-Ser-Chg-Gln-aminoarylmethyl

phosphoramide mustards that would be specifically cleaved by PSA at P_1 glutamine residue to release the cytotoxic phosphoramide mustard (**33**) ultimately via the subsequent 1,6-elimination process.

Scheme 5. Proposed Activation Mechanism of Peptidylaminoarylmethyl Phosphoramide Mustards by PSA Proteolysis
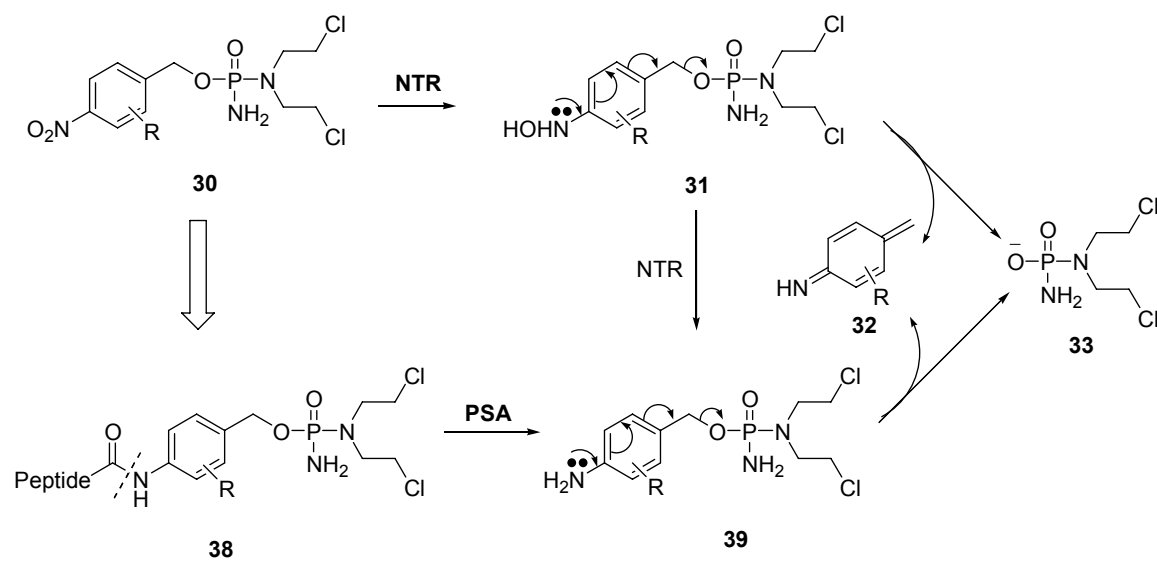
II. Methodology Development and Application of Selenocarboxylate/Azide Amidation

The retrosynthetic analysis of the peptidylaminoarylmethyl phosphoramide conjugates shown in Scheme 6 reveals 3 possible synthetic routes.

Scheme 6. Synthetic Routes to Peptidylaminoarylmethyl phosphoramide Mustards
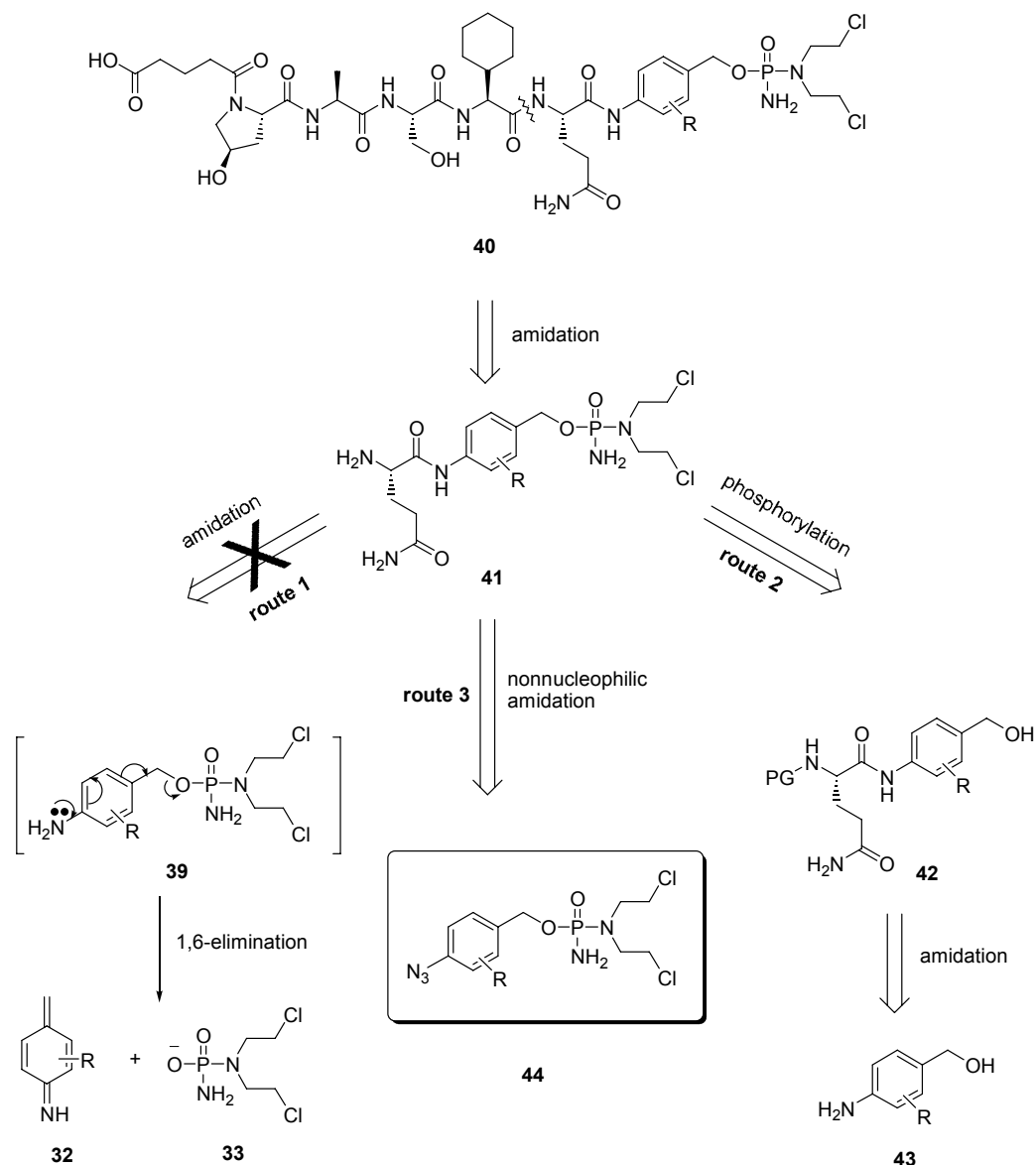
Route 1 is unlikely to be successful because the synthesis would go through a 4-aminoarylmethyl phosphoramide intermediate **39** that, however, is highly unstable due to its spontaneous decomposition via 1,6-elimination. As to route 2, our preliminary exploration was completely unsuccessful because phosphorylation of *N*-protected glutaminylaminobenzyl alcohol **42** failed to provide the desired product **41** using weak bases like pyridine or TEA. The requirement for strong bases capable of deprotonation of the hydroxyl group caused undesired *N*-phosphorylation of the carbamate functionality and the amide functionality. The lack of selectivity during phosphorylation caused the complexity of the reaction, and failed to afford the desired product in a reasonable yield. We, therefore, chose route 3 as our synthetic approach to the peptidylaminoarylmethyl phosphoramide mustards. To succeed, there is a need for a reliable non-nucleophilic amidation method, in which an azide can be coupled to a carboxylic acid directly to form the corresponding amide without going through an amine intermediate.

A. Overview of Non-Nucleophilic Amidation

Formation of an amide bond is usually achieved through the reaction of an activated carboxylic acid with an amine in which the amine acts as a nucleophile.[111] However, there are situations where free amines cannot be used because of either structural instability or the presence of functional groups that are incompatible with amines. In our design of peptidylaminoarylmethyl phosphoramide mustard conjugates, *N*-protected glutaminylaminoarylmethyl phosphoramide mustard **41** was proposed as a key intermediate. The retrosynthetic analysis reasoned that the nucleophilic amidation of 4-aminoarylmethyl phosphoramide mustard (**39**) would not work due to its spontaneous decomposition via a 1,6-elimination process as shown in scheme 6, and the non-nucleophilic amidation of 4-azidoarylmethyl phosphoramide mustard **44** was thus proposed.

Organoazides can react with carbonyl electrophile to afford amides in an extension of the Schmidt reaction (Scheme 7). In the presence of Brønsted acids, the reaction of organoazides with aldehydes and ketones is known as the Boyer reaction but it has very limited substrate scope.[112-114] Aubé and co-workers improved the reaction using Lewis acids as the catalyst to prepare lactams in excellent yields via the intramolecular Schmidt reaction.[115-117] The successful intermolecular Schmidt reaction of organoazides with ketones, however, was limited to cyclic ketones and hydroxyazides.[118-121] Because the phosphoryloxy moiety in the molecule **44** is labile to acid-catalyzed hydrolysis, the Schmidt reaction is apparently not a choice.

The reaction of organoazides with acyl donors in the presence of trialkyl phosphines is known as the Staudinger ligation (Scheme 7). The reaction takes place by forming an iminophosphorane, the intermediate of the Staudinger reduction,[122] followed by the acylation of this aza-ylide intermediate.[123-128] Recently, the modified Staudinger ligation[127,128], which forms an amide bond starting from an azide and a phosphine-linked ester/thio ester in the form of $R'COO-C_{n=1,2}-PR_2$ or $R'COS-C_{n=1,2}-PR_2$, has been successfully used in N-glycosylation,[129-134] peptide ligation[135-138] and lactamization.[139] The reaction involves a 5 or 6-membered intramolecular transacylation of an iminophosphorane followed by hydrolysis to form an amide. The Staudinger ligation favors aliphatic azides while for aromatic azides, especially those bearing electron-withdrawing substituents, the reactions are very slow and may fail.[140] Furthermore, when the Staudinger ligation is incomplete or fails, the iminophosphorane intermediate will be converted to the corresponding amine by hydrolysis in an aqueous medium or during aqueous workup without the possibility of recovering the azide starting material. It was also reported that the azides could react directly with carboxylic acids to form the corresponding amide in the presence of a trialkyl phosphine. The proposed mechanism suggested that the reaction was involved in a three-component complex instead of a typical iminophosphorane intermediate.[141-143]

The amidation reaction of thio acids with azides has recently attracted broad attention. Acetylation of organic azides with thioacetic acid was first reported by Just in 1980.[144] It was postulated as a conventional nucleophilic acylation reaction between thioacetic acid and the amine formed via *in situ* reduction of the azide by the adventitious hydrogen

sulfide, which was then regenerated during the acylation reaction.[145] However, recent results from Williams' group suggested a new mechanism that involved the formation of a thiatriazoline intermediate followed by a retro-[3+2] cycloaddition to form the amide product (Scheme 7).[146] Two mechanistic pathways were proposed for the formation of the thiatriazoline intermediate: for electron-deficient azides, the thiatriazoline is formed via a stepwise linear coupling of the thio acid with the azide followed by intramolecular cyclization; and for electron-rich azides, the thiatriazoline is formed via a concerted intermolecular [3+2] cycloaddition reaction between the thio acid and the azide. Several applications and modifications of this Williams thio acid/azide amidation have been reported.[147-151] However, the thio acid/azide amidation usually gives low yields for electron rich and sterically hindered azides, and requires high reactant concentration and temperature to achieve a satisfactory conversion rate.[146] This promoted us to develop a new amidation method with azides that can be carried out under mild conditions and applicable to amino acids and peptides.

Selenium shares some of the same chemical properties with sulfur but the larger and more easily polarizable selenium atom makes it more nucleophilic than sulfur. For example, selenophenolate was found to react with methyl iodide ~7 times faster than thiophenolate in a S_N2 displacement reaction.[152] We postulated that selenocarboxylic acids would also be more reactive than thio acids and potentially facilitate the amide formation with azides. Moreover, Knapp and co-workers reported that, while a sterically hindered 2-azidopiperidine derivative was entirely unreactive toward thioacetic acid in refluxing chloroform in the presence of 2,6-lutidine, it efficiently reacted with

selenoacetic acid to form the corresponding acetamide in a yield of 75% under the same reaction conditions.[153] Therefore, selenocarboxylate/azide amidation is an attractive reaction for us to prepare amides without going through an amine intermediate.

Scheme 7. Schimdt Reaction, Staudinger Ligation and Williams Amidation
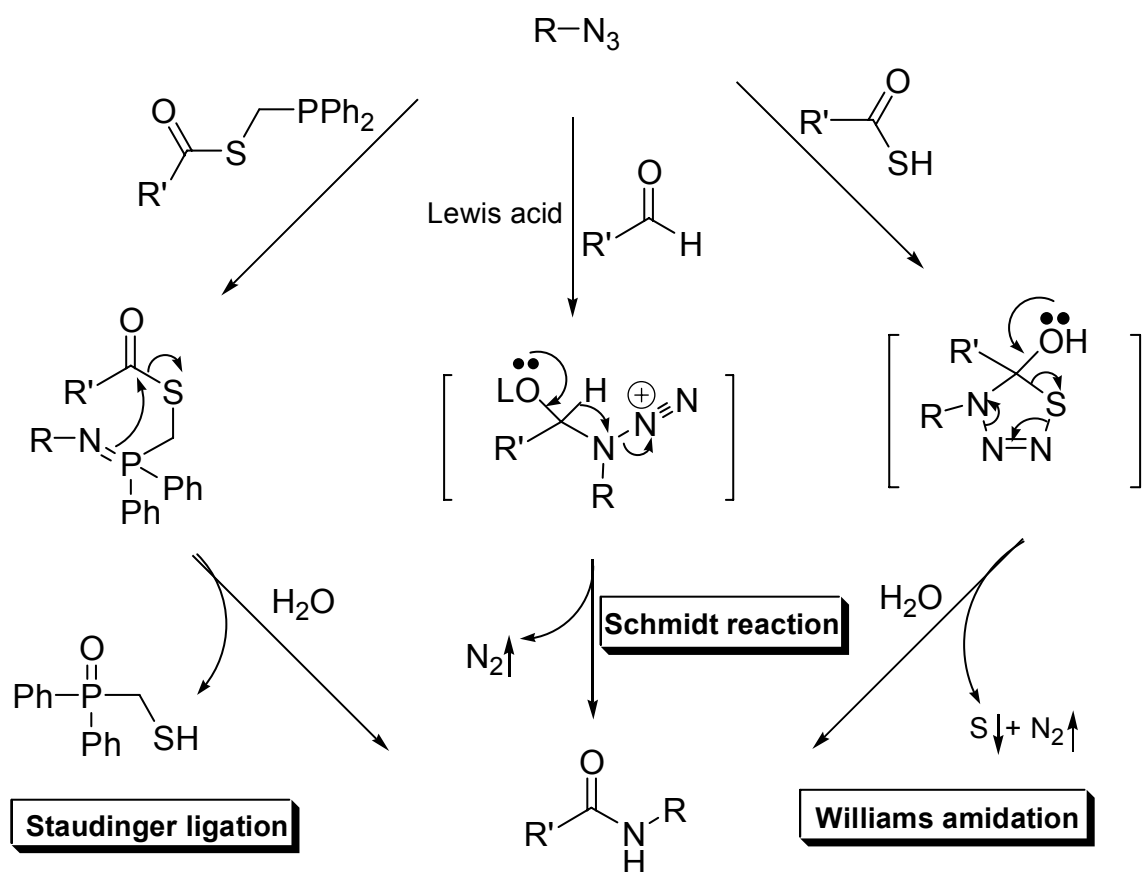
B. Selenocarboxylate/Azide Amidation using Benzeneselenocarboxylate as a Model Compound.

Exploration of Reaction Conditions. Selenocarboxylic acids are known to be unstable and readily oxidized to diacyl diselenides upon exposure to air. However, their corresponding alkali metal and trialkylammonium salts are relatively stable, especially for aromatic selenocarboxylates. For example, no significant change occurred in potassium 4-methylbenzeneselenocarboxylate when it was exposed to air for 5 hours. Under oxygen-free conditions, most aromatic selenocarboxylate salts can be stored at −17 °C for at least one month.[154] Thus, benzeneselenocarboxylate is an ideal model compound to react with various organoazides to explore the selenocarboxylate/azide amidation. Selenocarboxylates have to be prepared *in situ* because they are extremely labile to air due to oxidation. On the basis of that diacyl selenides are relatively stable and readily prepared; moreover, aromatic diacyl selenides can be purified by silica gel flash column chromatography, dibenzoyl selenide was first used as a precursor of benzeneselenocarboxylate. For the amidation reaction, potassium benzeneselenocarboxylate was generated *in situ* by mixing dibenzoyl selenide with stoichiometric amount of potassium methoxide in DMSO/EtOAc (1:1) at 5 °C under nitrogen atmosphere (Conditions A). DMSO was used to increase the solubility of potassium methoxide. After the addition of azide, the reaction was allowed to gradually warm to room temperature and was stirred for 0.5-2 h until TLC and/or LC-MS showed the disappearance or no further decrease of the starting azide.

Series of homologous aromatic azides bearing various electron-donating and electron-withdrawing functionalities were selected to explore the scope of the amidation reaction and to give a better assessment of the electronic and steric effects on the reaction outcome. It was found that electron-deficient azides were much more reactive than electron-rich azides. Aromatic azides bearing electron-withdrawing groups such as NO_2, Cl, CN, acetyl, COOH and COOMe gave excellent yields while phenyl azide and aromatic azides bearing electron-donating groups such as methoxy, methyl, and hydroxymethyl gave lower yields of desired amides with most of the azide starting materials recovered (Table 1). The reactions were highly chemoselective and very clean, giving >90% yields based on the recovery of starting azides. No significant side reactions were observed. All unreacted azides could be easily recovered. The lower conversion yields for the less reactive azides were partially due to the short lifetime of benzeneselenocarboxylate. It was found that potassium benzeneselenocarboxylate had a half-life of 25 min in the presence of DMSO (Figure 9), which was used as a co-solvent to increase the solubility of potassium benzeneselenocarboxylate. The mild oxidizing property of DMSO, however, accelerated the decomposition of benzeneselenocarboxylate, which adversely affected the yield of product.

Organic amine salts of selenocarboxylate have better solubility in organic solvents than the corresponding metal salts. Diisopropylethylammonium benzeneselenocarboxylate was then prepared to explore a set of reactions conditions to increase the solubility and stability of selenocarboxylates. Diisopropylethylammonium benzeneselenocarboxylate was prepared by the treatment of dibenzoyl diselenide with a stoichiometric amount of

piperidine in the presence of diisopropylethylamine in acetonitrile (Conditions B). The half-life of diisopropylethylammonium benzeneselenocarboxylate was found to be 11.3 h at 25 °C (Figure 9). This was an improvement of 27 times in stability if compared to the half-life of 25 min under conditions A using DMSO as a co-solvent. Even when the temperature was raised to 55 °C, the half-life of the benzeneselenocarboxylate was 1.4 h, still nearly 3.4-time longer than previous reaction conditions A. The improved stability of benzeneselenocarboxylate allowed us to decrease the amount of the selenocarboxylate from 2.0 equiv to 1.2 equiv for electron-deficient azides to provide comparable yields. For electron-rich azides, the reaction temperature was raised up to 55 °C to afford much better yields (Table 1).

These model reactions of benzeneselenocarboxylate with various azides indicated that the selenocarboxylate/azide amidation reaction was highly chemoselective and very clean; and was compatible with a variety of functional groups including hydroxy, ketone, carboxylic acid, ester, and cyano. Excellent yields were obtained when electron-deficient aromatic azides were used. The selenocarboxylate/azide amidation offered the advantage of mild reaction conditions without going through the nucleophilic and basic free amine intermediates.

What limited the application of selenocarboxylate/azide amidation was the lack of a practical method to prepare selenocarboxylates. The known methods of preparing selenocarboxylates include the treatment of trimethylsilyl selenocarboxylates with alkali metal fluorides,[155,156] the reaction of acyl chlorides with alkali metal selenides,[157] the

reaction of diacyl selenides or diacyl diselenides with alkali metal hydroxide,[158] alkali metal methoxide,[159] or piperidine[160] , and the reaction of carboxylic acids with Woollin's reagent, [PhP(=Se)Se]$_2$[161] (Scheme 8).

Scheme 8. Common Methods to Generate Selenocarboxylates *in situ*
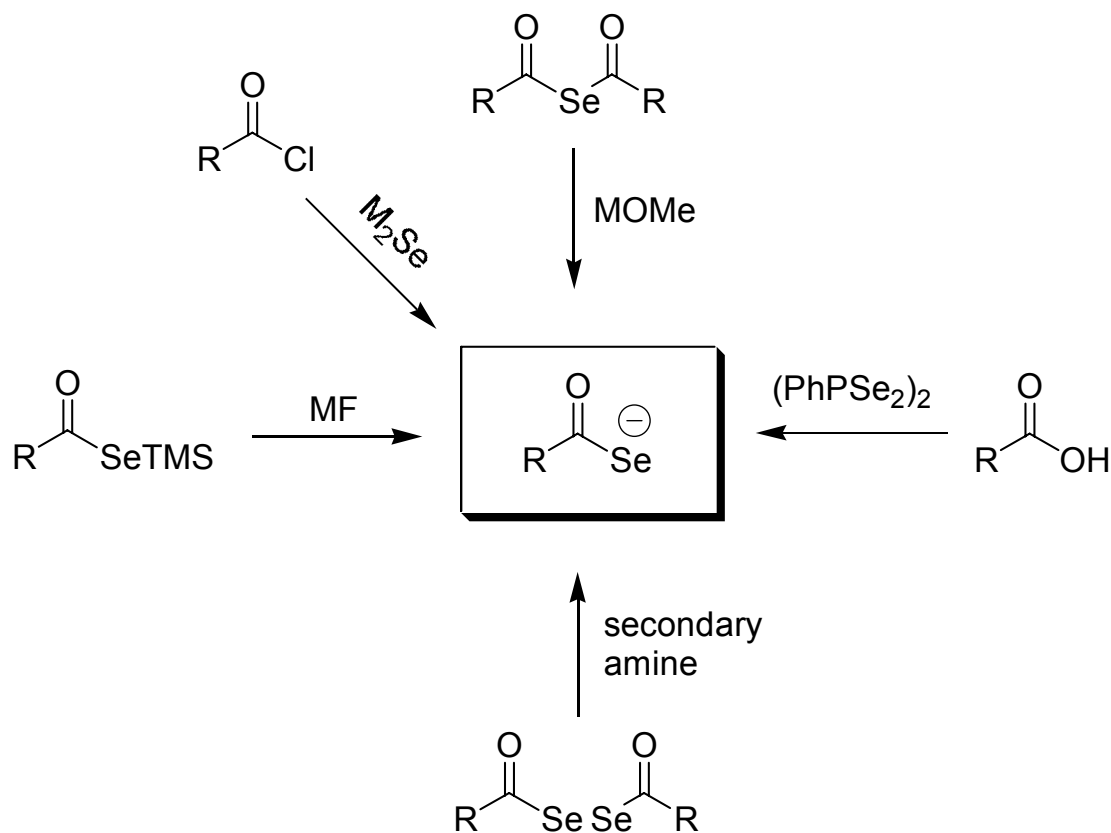
However, all of the above methods for the preparation of selenocarboxylates have disadvantages. For example, trimethylsilyl selenocarboxylic esters are highly moisture sensitive; alkali metal selenides are poorly soluble in organic solvents; starting from diacyl selenides or diacyl diselenides is not economical as half of the carboxylate equivalents are wasted. Although Woollins' reagent can directly convert carboxylic acids

to the corresponding selenocarboxylic acids in refluxing toluene, such high reaction temperature is not suitable for amino acids and peptides. Therefore, our primary goal was to develop a practical method to prepare various selenocarboxylates from carboxylic acids directly under much milder conditions and a general one-pot amidation procedure that is applicable to amino acids and peptides.

LiAlHSeH was first synthesized and reported by Ishihara et al.[162] It is a powerful selenating reagent capable of preparing a wide-range of selenium-containing compounds. LiAlHSeH can smoothly convert activated carboxylates, including acyl chlorides, mixed anhydrides and OBt esters, to the corresponding selenocarboxylates under very mild conditions (Scheme 9).

Scheme 9. Exploration of Selenocarboxylate/Azide Amidation Using Different Methods

48a: LG = -Cl
48b: LG = -OCOOR
48c: LG = -OBt
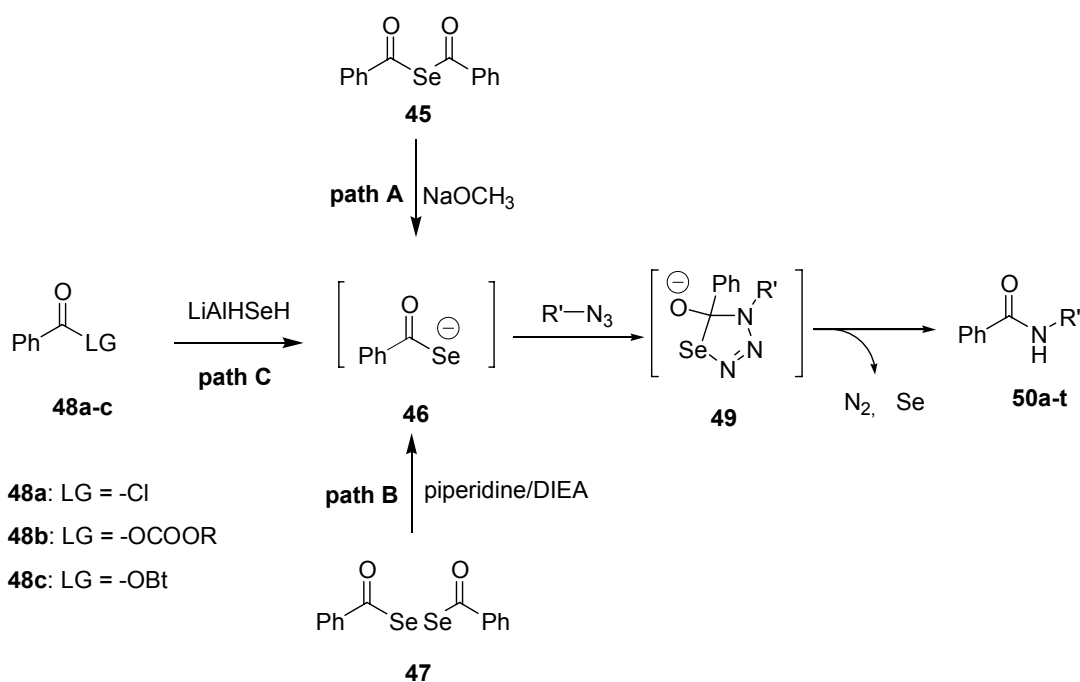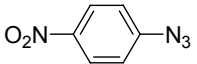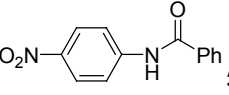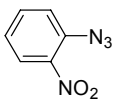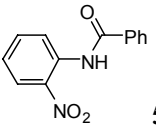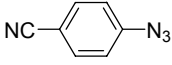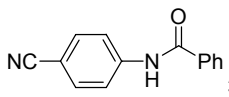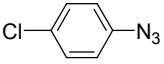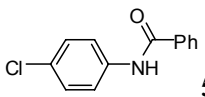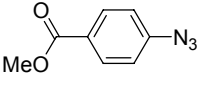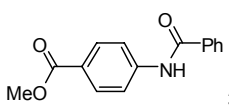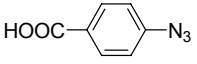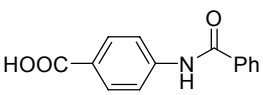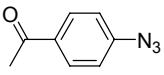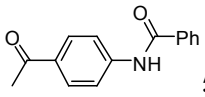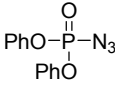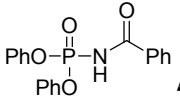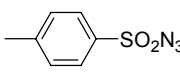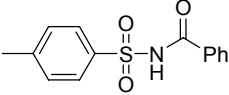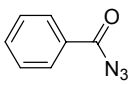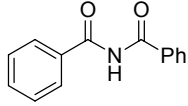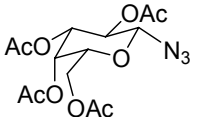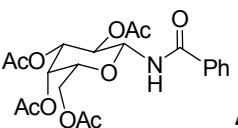
The preparation of LiAlHSeH entailed treating LiAlH$_4$ with a stoichiometric amount of selenium in THF at 0 °C under nitrogen atmosphere to give a gray LiAlHSeH suspension.[162] LiAlHSeH reacted readily with the freshly prepared mixed anhydride at 0 °C to give the corresponding selenocarboxylate, which could be used directly for the amidation reaction. A general one-pot procedure was developed for the selenocarboxylate/azide amidation reaction (Conditions C). First, the carboxylic acid was activated with isopropyl chloroformate in THF at 0 °C in the presence of *N*-methylpiperidine to form the corresponding mixed anhydride. Then, the mixed anhydride solution was added to the freshly prepared suspension of LiAlHSeH in THF via cannula under nitrogen atmosphere. The reaction started immediately with the release of CO$_2$ to form the corresponding selenocarboxylate *in situ*. A solution of the azide was then added to the above selenocarboxylate solution via syringe. The reaction was monitored using TLC and/or LC-MS and worked up after the disappearance of or no further decrease of the starting azide. Isopropyl chloroformate was found to be a better choice over other common chloroformates (e.g., methyl chloroformate, ethyl chloroformate and isobutyl chloroformate) as the resulting mixed anhydride, acyl isopropyl carbonate, was more stable and relatively more resistant to hydrolysis. Stability kinetic studies showed that the half-life of benzeneselenocarboxylate was 16 h at 25 °C and 10 h at 55 °C under the reaction condition C, which was a significant improvement over previously described conditions A and B.

Effects of Azides on the Amidation Reaction. Overall, electron-deficient azides were more reactive than electron-rich azides. For electron-deficient azides, 1.1 equiv of benzeneselenocarboxylate was sufficient to give excellent conversion to the corresponding amides with isolated yields of 81-98% (entries 1-10, Table 1). For less reactive electron-rich azides, 2.0 equiv of benzeneselenocarboxylate and mild heating were used to achieve good yields (entries 11-20, Table 1). The yield of selenocarboxylate/azide amidation correlated well with the stability and solubility of the selenocarboxylate in the reaction medium.[163,164] For highly reactive electron-deficient azides, the reactions were complete in a very short time. Thus, the increased half-life of selenocarboxylate did not seem to offer any benefits for electron-deficient azides as similar overall yields were obtained under the present conditions C compared to the previously described conditions A and B (entries 1, 3 and 6, Table 1). Electron-withdrawing groups at the *para* or *ortho* position to the azido group appeared to stabilize the transition state and/or intermediate due to delocalization of the negative charge on nitrogen through resonance effects, and thus facilitated formation of the amide bond. Kinetic studies using LC-MS monitoring of the amidation reaction indicated that the reaction was slower when the nitro group was at the *ortho* position than at the *para* position, suggesting a steric hindrance effect. However, moving the nitro substituent from the *para* to *ortho* position in the starting azide did not affect the overall yield of amidation (entry 2, Table 1), For benzoyl azide, the desired amide **50j** was obtained in 81% yield under conditions C as compared to 51% yield under conditions B[164] (entry 10, Table 1). For 2,3,4,6-tetra-*O*-acetyl-*β*-D-galactopyranosyl azide, the desired product **50k** was prepared in 71% yield (entry 11, Table 1). For the less reactive azides, reactions

under conditions A generally led to lower yields due to the shortest half-life of the selenocarboxylate as compared to reactions under conditions B and C (entries 12-16). For 4-methoxylphenyl azide, the corresponding amide **50o** was obtained in 63% yield under conditions C compared to 65% under conditions B[164] and only 7% under conditions A[163] (entry 15). Similarly, 4-azido-benzyl alcohol gave the desired product **50p** with an improved yield of 70% compared to 56%[164] and 44%[163] under conditions B and A, respectively (entry 16). The more electron-rich 4-aminophenyl azide provided 54% yield of *N*-(4-aminophenyl)benzamide (**50n**) under both conditions A and B (entry 14). The successful amidation of 4-azidobenzyl acetate to 4-benzamidobenzyl acetate **50q** in 68-76% yield (entry 17) suggested that the amidation did not involve *in situ* reduction of the azide to the corresponding amine prior to amide bond formation. Otherwise, the reduction would have led to the formation of polymerized quinonimine methide instead of the desired amide as discussed earlier and depicted in Scheme 6. Aliphatic 6-[(*tert*-butyldiphenylsilyl)oxy]hexyl azide also reacted with benzeneselenocarboxylate to form the desired amide **50t** in 62% yield under conditions C (entry 20).

Under conditions C, we were able to apply mild heating to accelerate the amidation process for the less reactive azides and, thus, were able to improve the amidation yields. Although conditions B and C showed comparable yields for both electron-deficient and electron-rich azides, the easy adaption of conditions C to the one-pot procedure starting directly from carboxylic acids provides a straightforward, practical and efficient route to the selenocarboxylate/azide amidation reaction that can be applicable to amino acids and peptides.

Table 1. Amidation of Benzeneselenocarboxylate with Azides under Different Conditions

Entry	Azide	Amide product	Conditions[a]	T(^{o}C)	Yield[b] (%)
1	O$_2$N— —N$_3$	50a	A	25	98
			B	25	95
			C	25	96
2	N$_3$ / NO$_2$	50b	A	25	95
			B	25	93
3	NC— —N$_3$	50c	A	25	98
			B	25	96
			C	25	94
4	Cl— —N$_3$	50d	A	25	96
			B	25	95
5	MeO$_2$C— —N$_3$	50e	A	25	98
			B	25	87
6	HOOC— —N$_3$	50f	A	25	87
			B	25	89
			C	25	91
7	acetyl— —N$_3$	50g	A	25	88
8	PhO–P(O)(OPh)–N$_3$	50h	B	25	88
			C	25	95
9	—SO$_2$N$_3$	50i	B	25	96
			C	25	98
10	PhC(O)N$_3$	50j	B	55	51
			C	55	81
11	AcO sugar N$_3$	50k	C	55	71

Entry	Azide	Product	Conditions	Temp	Yield[b]
12	phenyl azide	PhC(O)NH–Ph **50l**	A	25	25
			B	55	40
13	H$_3$C–C$_6$H$_4$–N$_3$	H$_3$C–C$_6$H$_4$–NHC(O)Ph **50m**	A	25	7
14	H$_2$N–C$_6$H$_4$–N$_3$	H$_2$N–C$_6$H$_4$–NHC(O)Ph **50n**	B	55	54
			C	55	54
15	MeO–C$_6$H$_4$–N$_3$	MeO–C$_6$H$_4$–NHC(O)Ph **50o**	A	25	7
			B	55	65
			C	55	63
16	HOCH$_2$–C$_6$H$_4$–N$_3$	HOCH$_2$–C$_6$H$_4$–NHC(O)Ph **50p**	A	25	44
			B	55	56
			C	55	70
17	AcOCH$_2$–C$_6$H$_4$–N$_3$	AcOCH$_2$–C$_6$H$_4$–NHC(O)Ph **50q**	A	55	76
			B	55	68
			C	55	70
18	(F, HOCH$_2$) aryl azide	**50r**	B	55	78
19	(F, HOCH$_2$) aryl azide	**50s**	B	55	37
20	TBDPSO–(CH$_2$)$_6$–N$_3$	TBDPSO–(CH$_2$)$_6$–NHC(O)Ph **50t**	C	55	62

[a]General conditions: **A**, in DMSO/EtOAc (1/1, v/v) with benzeneselenocarboxylate prepared by treating dibenzoyl selenide with 1 equiv of KOMe; **B**, in acetonitrile with benzeneselenocarboxylate prepared by treating diacyl diselenide with 1 equiv of piperidine in the presence of 1 equiv of diisopropylethylamine; **C**, in THF with benzeneselenocarboxylate prepared by treating the mixed anhydride with LiAlHSeH.

[b]Isolated yields based on azides

Stability of the Selenocarboxylate. The stability of benzeneselenocarboxylate was measured by monitoring the amide formation between benzeneselenocarboxylate and 4-toluenesulfonyl azide under the present reaction conditions. The amide product, *N*-(4-toluenesulfonyl)benzamide, was then analyzed by HPLC to determine the amount of benzeneselenocarboxylate that remained in solution. To ensure fast and quantitative consumption of all benzeneselenocarboxylate remained in solution at a given time point, 2 equivalents of 4-toluenesulfonyl azide were used. Complete and quantitative amidation was achieved within 5 min as determined by HPLC. Such fast formation of product allowed us to accurately measure the amount of benzeneselenocarboxylate present during our stability study.
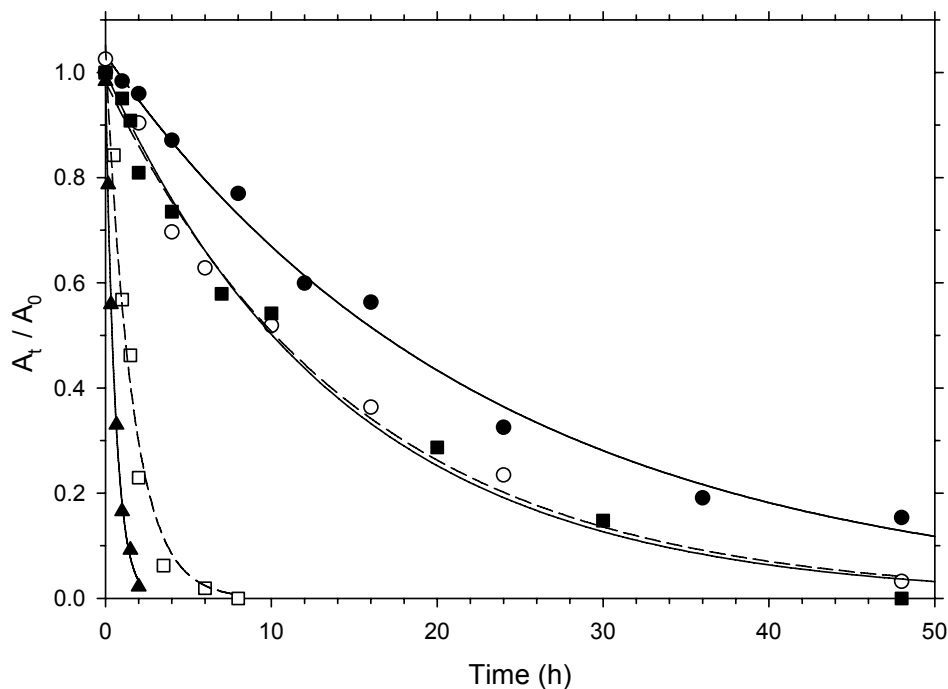
Figure 9. Stability of Benzeneselenocarboxylate under Different Reaction Conditions

Conditions A, in DMSO/EtOAc (1/1 v/v) at r.t. ($-\blacktriangle-$); Conditions B, in acetonitrile at r.t. ($-\blacksquare-$) and 55 °C (---□---); Conditions C, in THF at r.t. ($-\bullet-$) and 55 °C (---○---).

Figure 9 illustrates the stability profiles of benzeneselenocarboxylate under different reaction conditions. The half-life of benzeneselenocarboxylate was found to be 16 h/25 °C in THF under conditions C as compared to 11 h in acetonitrile under conditions B and 25 min in DMSO/EtOAc[163] under conditions A. When the temperature was raised to 55 °C, the half-life of benzeneselenocarboxylate was around 10 h in THF under conditions C as compared to 1.4 h in acetonitrile under conditions B. The longer half-life of the selenocarboxylate under conditions C presumably was due to the presence of trace amounts of reducing agents in the reaction mixture, which probably delayed the oxidation/decomposition of selenocarboxylates caused by the trace amount of oxygen present in the solvent. This, thus, benefited the amidation reactions that require longer time and mild heating. Although the stability of the selenocarboxylate did not present a problem for the faster amidation reactions with electron-deficient azides, it significantly affected the overall yields of amidation for electron-rich azides. Under conditions C, the amidation yields for the less reactive electron-rich azides were improved by the increased half-life of the selenocarboxylate.[164]

Mechanisms of Selenocarboxylate/Azide Amidation. Our experimental results clearly demonstrated that the yields of selenocarboxylate/azide amidation dependent primarily upon the electronic properties of the azides. Electron-deficient azides reacted with selenocarboxylates much faster and gave better yields than electron-rich azides. This was in apparent contrast to the "*in situ* reduction and acylation" mechanism where electron-rich azides would give more nucleophilic amines that in turn should facilitate the nucleophilic acylation and afford higher yields of amide formation than electron-deficient

azides. Furthermore, when benzeneselenocarboxylate was incubated with 4-cyanoaniline, there was no detectable amide formation while 4-cyanophenyl azide gave a 94% yield of amide **50c**. In addition, we were able to successfully synthesize 4-benzamidobenzyl acetate (**50q)** from 4-azidobenzyl acetate, suggesting that there was no *in situ* reduction of the azide otherwise the spontaneous decomposition of 4-aminobenzyl acetate would lead to the polymerized quinonimine methide instead of the amide product.

On the basis of the careful mechanistic studies, two pathways leading to the formation of a thiatriazoline intermediate were proposed for Williams thio acid/azide amidation.[146] Depending on the electronic properties of azide, a thiatriazoline intermediate formed via a stepwise or concerted mechanism. By analogy, the selenocarboxylate/azide amidation likely proceeded through the corresponding selenatriazoline intermediate **53**. As shown in Scheme 10, a stepwise mechanism, path A, could be operative. Bimolecular union of the terminal nitrogen of the electron-deficient azide with selenium of the selenocarboxylate followed by an intramolecular cyclization formed the selenatriazoline intermediate **53**. Alternatively, a concerted [3+2] cycloaddition, path B, gave the selenatriazoline intermediate **53** before decomposition of **53** via a retro-[3+2] cycloaddition to the amide product. The observed solvent effects and electronic effects of azide substrate were consistent with these mechanisms. The amidation reaction proceeded faster in polar solvents, indicating the involvement of a polar transition state that could be stabilized by polar solvents. Electron-withdrawing groups on azides stabilized the transition state **52** by, presumably, delocalization of the negative charge on the nitrogen and, therefore, facilitated the amidation reaction through the path A linear mechanism. For the electron-

rich azides, the amidation reaction might proceed through the path B concerted [3+2] cyclization mechanism and was much slower, requiring longer reaction time at elevated temperature.

Scheme 10. Proposed Mechanisms of Selenocarboxylate/Azide Amidation
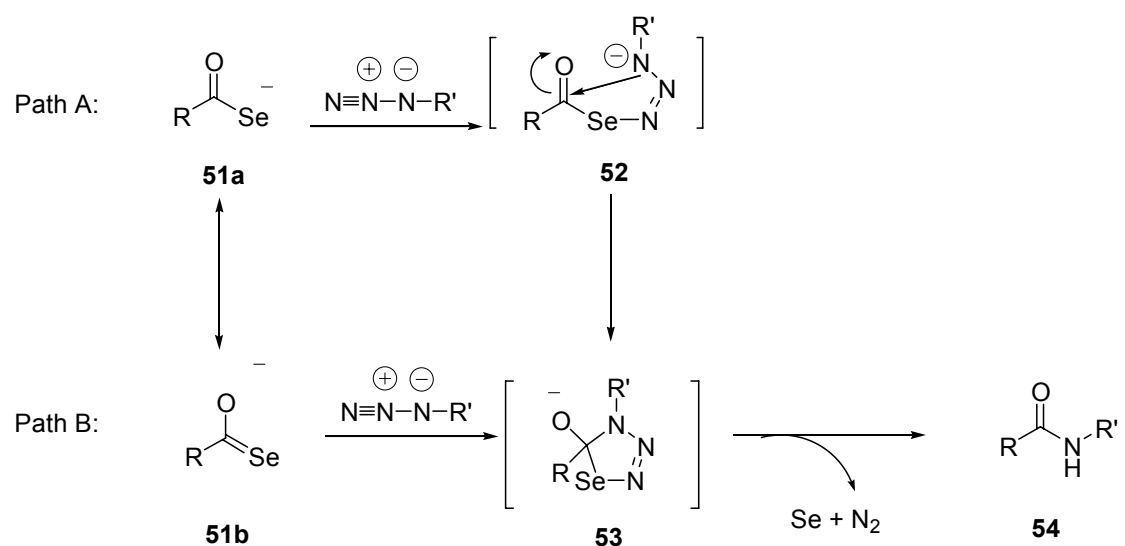
C. Application of Selenocarboxylate/Azide Amidation to Amino Acids/Peptides

To demonstrate the general applicability of selenocarboxylation of various *N*-protected amino acids and short peptides with LiAlHSeH, 4-cyanophenyl azide, a representative electron-deficient aromatic azide, was used to react with the selenocarboxylates generated *in situ* because the electron-deficient aromatic azides reacted more readily with selenocarboxylates.[163,164] As shown in Table 2, various amino acids all gave excellent yields (~ 90%) of the desired amide products (entries 1-8) with the exception of Fmoc-glutamine, which gave only 70% isolated yield because of partial dehydration (entry 9). For dipeptides, Boc-Leu-Trp-OH and Boc-Ser(Ac)-Phe-OH and the tripeptide, Boc-Asn-Leu-Trp-OH, the desired amidation products were obtained in 83-92% yields (entries 10-12). The high yields of the desired amide products demonstrated that the *N*-protected amino acids were effectively converted to the corresponding selenocarboxylates in this one-pot amidation procedure. Furthermore, common amino protecting groups such as Boc, Fmoc, Cbz, acetyl and OBzl were well tolerated under the reaction conditions.

Amino Acid Derivatization Analysis. To determine whether the present amidation conditions would cause significant racemization, compound **55a** was hydrolyzed with 6N HCl followed by derivatization with *o*-phthaldialdehyde (OPA) and *N*-Boc-L-cysteine (NBC) whereas NBC provided better separation of the derivatized D- and L-phenylalanines over *N*-Acetyl-L-cysteine (NAC)[165] presumably due to the increased steric bulkiness of the Boc group as compared to acetyl group.

Table 2. The Three-Step Amidation of 4-Cyanophenyl Azide with Amino Acids and Peptides[a]
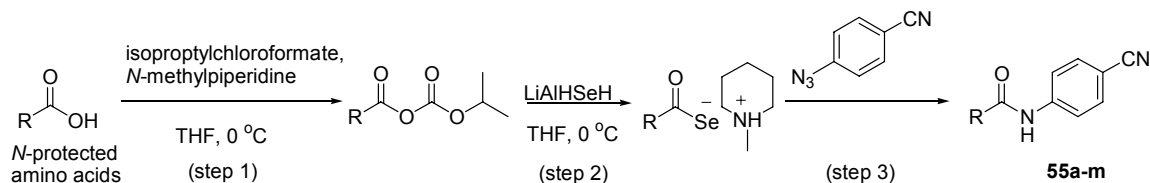
Entry	Amino acid or peptide	Amide product	Yield (%)[b]
1	Z-Phe-OH	Z-Phe—N(H)—C₆H₄—CN **51a**	85
2	Z-Ser(Bzl)-OH	Z-Ser(Bzl)—N(H)—C₆H₄—CN **51b**	89
3	Z-Gln-OH	Z-Gln—N(H)—C₆H₄—CN **51c**	90
4	Z-Met-OH	Z-Met—N(H)—C₆H₄—CN **51d**	88
5	Boc-Glu(OBzl)-OH	Boc-Glu(OBzl)—N(H)—C₆H₄—CN **51f**	89
6	Boc-Pro-OH	Boc-Pro—N(H)—C₆H₄—CN **51g**	90
7	Boc-Val-OH	Boc-Val—N(H)—C₆H₄—CN **51h**	89
8	Fmoc-Trp-OH	Fmoc-Trp—N(H)—C₆H₄—CN **51i**	90
9	Fmoc-Gln-OH	Fmoc-Gln—N(H)—C₆H₄—CN **51j**	70
10	Boc-Leu-Trp-OH	Boc-Leu-Trp—N(H)—C₆H₄—CN **51k**	87
11	Boc-Ser(Ac)-Phe-OH	Boc-Ser(Ac)-Phe—N(H)—C₆H₄—CN **51j**	92
12	Boc-Asn-Leu-Trp-OH	Boc-Asn-Leu-Trp—N(H)—C₆H₄—CN **51m**	83

[a]General conditions: Amino acid or peptide (1.1 mmol), isobutyl chloroformate (1.1 mmol) and
N-methylpiperidine (1.1 mmol), THF, 0 °C, 20 min; LiAlHSeH (1.1 mmol), 5 °C, 30 min;
4-cyanophenyl azide (1.0 mmol), THF, r.t., 3 h.

[b]Isolated yield

As shown in Figure 10, the resulting isoindole derivatives were separated by reversed phase HPLC and compared with L-phenylalanine and D-phenylalanine isoindole derivatives. The observed racemization was ~1.5%, which might be caused by the step involving activation of the carboxylic acid. It has been shown that the general coupling methods, including mixed anhydride, HOBt/DCC, HBTU/HOBt, and BOP/HOBt, would cause racemization when applied to peptide synthesis.[166] The observed racemization in the present procedure was from the activation of the carboxylic
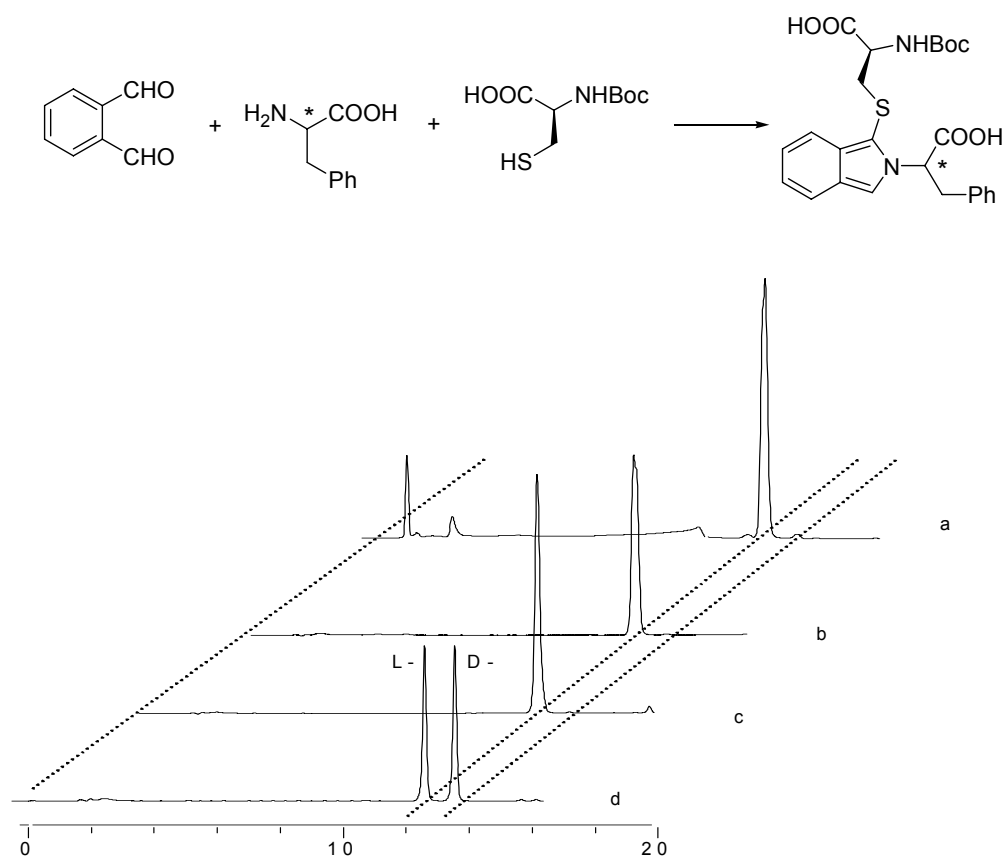
Figure 10. OPA/NBC Derivatization of Phenylalanine.

a. Acid hydrolysis of *N*-Cbz-*N'*-(4-cyano)phenyl-L-phenylalaninamide **55a** followed by OPA/NBC derivatization; **b.** Acid hydrolysis of *N*-Cbz-L-Phenylalanine followed by OPA/NBC derivatization as a control; **c.** Acid hydrolysis of *N*-Cbz-*N'*-benzyl-L-phenylalaninamide followed by OPA/NBC derivatization as a control; **d.** OPA/NBC derivatization of DL-phenylalanine as a standard.

acid with isopropyl chloroformate. To confirm this assumption, N-Cbz-N´-benzyl-L-phenylalaninamide was synthesized by activation of Z-L-phenylalanine with isopropyl chloroformate followed by the treatment with benzylamine. The obtained amide was then used as a control in our acid hydrolysis and OPA/NBC derivatization studies. It was observed that the obtained N-Cbz-N'-benzyl-phenylalaninamide contained ~1.5% D-isomer, indicating the racemization ratio during the activation step. Acid hydrolysis and OPA/NBC derivatization studies indicated that the racemization most likely occurred in the step of formation of the mixed anhydride rather than the following generation of selenocarboxylate and amidation steps.

Solvent Effects. THF was the solvent of choice for the preparation of LiAlHSeH. If CH_2Cl_2 was used instead, the reaction of $LiAlH_4$ with selenium could not occur. For the amidation step, both protic and aprotic solvents could be used as co-solvents. Overall, we found that the selenocarboxylate/azide amidation proceeded faster in polar solvents. As shown in Table 3, in comparison with the reaction in neat THF (entry 1, Table 3), mixing with polar organic solvents including acetone, methanol and acetonitrile accelerated the reaction but there were no significant effects on the overall yields (entries 2-4, Table 3). Increasing the ratio of acetonitrile from 25% to 50% shortened the reaction time slightly from 1.5 h to 1.0 h (entries 4 *vs* 5, Table 3). But further increasing acetonitrile to 75% slightly slowed the reaction back to 2.0 h (entries 5 *vs* 6, Table 3). This could be because of the decreased solubility of the highly lipophilic azide in the presence of too much polar solvent leading to heterogeneity of the reaction mixture. It should also be noted that the presence of water did not adversely affect the amidation reaction and good overall yield

of 89% was obtained when a mixed solvent of THF and water (3:1, v/v) was used as the

solvent in the 3rd amidation step (entry 7, Table 3).

Table 3. Effect of Solvents on Reaction Time and Yield of the Amidation Reaction
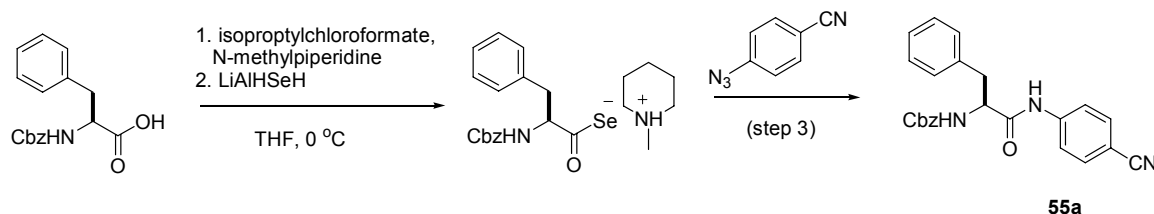
Entry	Solvent system used in step 3	Reaction time[a] (h)	Yield (%)[b]
1	THF	3	85
2	THF/CH$_3$COCH$_3$ (3:1, v/v)	1.5	87
3	THF/MeOH (3:1, v/v)	1.0	88
4	THF/CH$_3$CN (3:1, v/v)	1.5	89
5	THF/CH$_3$CN (1:1, v/v)	1.0	92
6	THF/CH$_3$CN (1:3, v/v)	2.0	91
7	THF/H$_2$O (3:1,v/v)	1.5	89

[a]General conditions: Z-Phe-OH (1.1 mmol), isobutyl chloroformate (1.1 mmol) and
N-methylpiperidine (1.1 mmol), THF, 0 °C, 20 min; LiAlHSeH (1.1 mmol); 4-cyanophenyl azide
(1.0 mmol), r.t.

[b]Isolated yields based on azides

Selenocarboxylation of Amino Acids/Peptides with NaHSe. Klayman and Griffin reported that, in protic solvents, selenium reacted rapidly with sodium borohydride to generate sodium hydrogen selenide (NaHSe) according to equation (1) and (2).[167] The selenium present in such a solution was in the form of hydrogen selenide ions (HSe⁻, >99%) and as selenide ions (Se^{2-}, < 0.5%). The obtained sodium hydrogen selenide could be directly used as its alcoholic or aqueous solution without isolation.

$$4\ NaBH_4\ +\ 2\ Se\ +\ 7\ H_2O\ \longrightarrow\ 2\ NaHSe\ +\ Na_2B_4O_7\ +\ 14\ H_2 \quad (1)$$

$$NaBH_4\ +\ Se\ +\ 3EtOH\ \longrightarrow\ NaHSe\ +\ B(OEt)_3\ +\ 3\ H_2 \quad (2)$$

Commercially available Z-Gly-OSu was first used for the model reaction. The procedure included the preparation of NaHSe solution as described by Klayman, generation of the corresponding amino selenocarboxylates *in situ* by mixing the stoichiometric amount of Z-Gly-OSu ester with NaHSe, and amidation with *p*-nitrophenyl azide. NaHSe reacted rapidly with Z-Gly-OSu to produce the corresponding Selenocarboxylate, Z-Gly-SeNa. The reaction was complete within 0.5 h at 0 °C. Although aliphatic selenocarboxylates were generally thought to be more unstable than aromatic selenocarboxylates, to our surprise, the acid form of Z-Gly-SeH could be seen in LC-MS. Figure 11 shows a Z-Gly-SeH peak at 3.08 min (UV_{detect} = 280 nm) with the observed m/z of 267.95, 268.95, 269.95, 271.95 and 273.95 corresponding to [^{76}M-H]⁻, [^{77}M-H]⁻, [^{78}M-H]⁻, [^{80}M-H]⁻, and [^{82}M-H]⁻ respectively. Selenium has six naturally-occurring isotopes, five of which are stable: ^{74}Se (0.89%), ^{76}Se (9.37%), ^{77}Se (7.63%), ^{78}Se (23.77%), and ^{80}Se (49.61%). The last three also occur as fission products, along with ^{79}Se and ^{82}Se (8.73%) that are

considered as stable due to their very long half-lives.[168] The correct isotope abundance ratio further confirmed that the molecule contained selenium. After confirmation of the completion of selenocarboxylation, a solution of *p*-nitrophenyl azide in THF was added via syringe. The reaction started immediately with the precipitation of gray selenium and the formation of nitrogen gas, and was completed within 2 h at room temperature. Figure 12 shows the result of reaction of Z-Gly-SeNa produced *in situ* with *p*-nitrophenyl azide at 30 min (UV$_{detect}$ = 280 nm). The peak at 6.05 min is related to the desired Z-Gly-*p*NA with the mass of 442.10 corresponding to [M-H+TFA]$^-$.
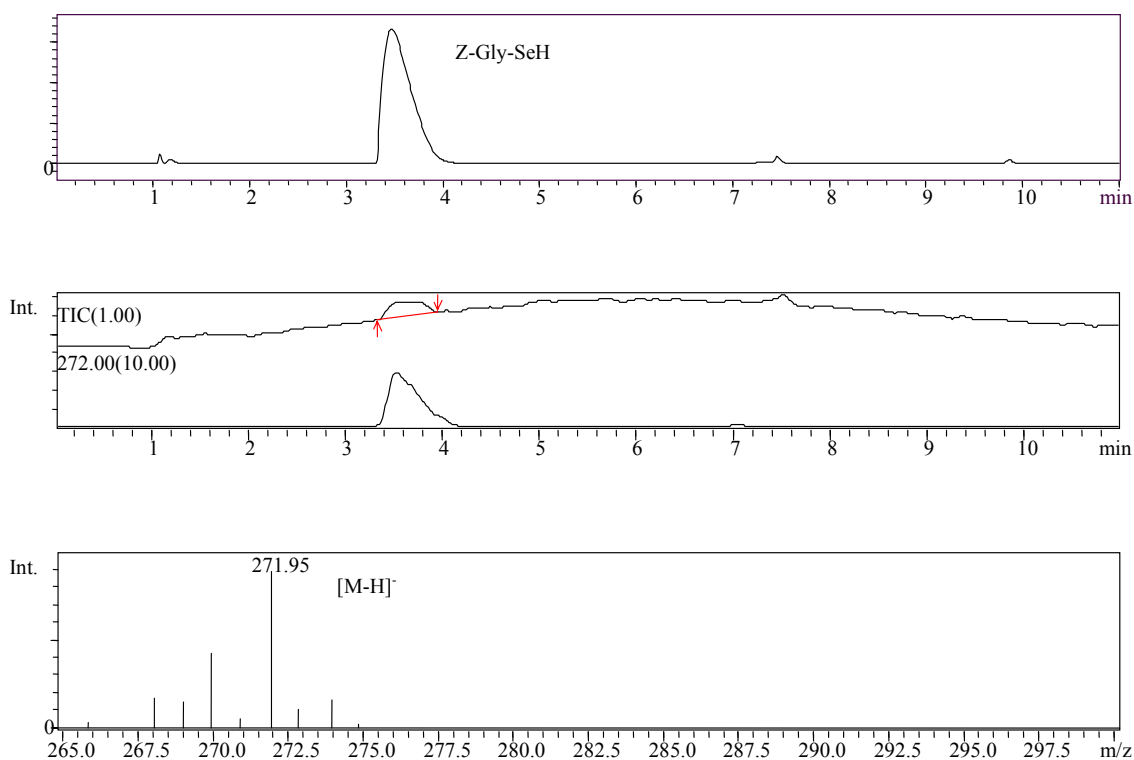
Figure 11. Selenocarboxylation of Z-Gly-OH by Reacting NaHSe with Z-Gly-OSu to Afford Z-Gly-SeH
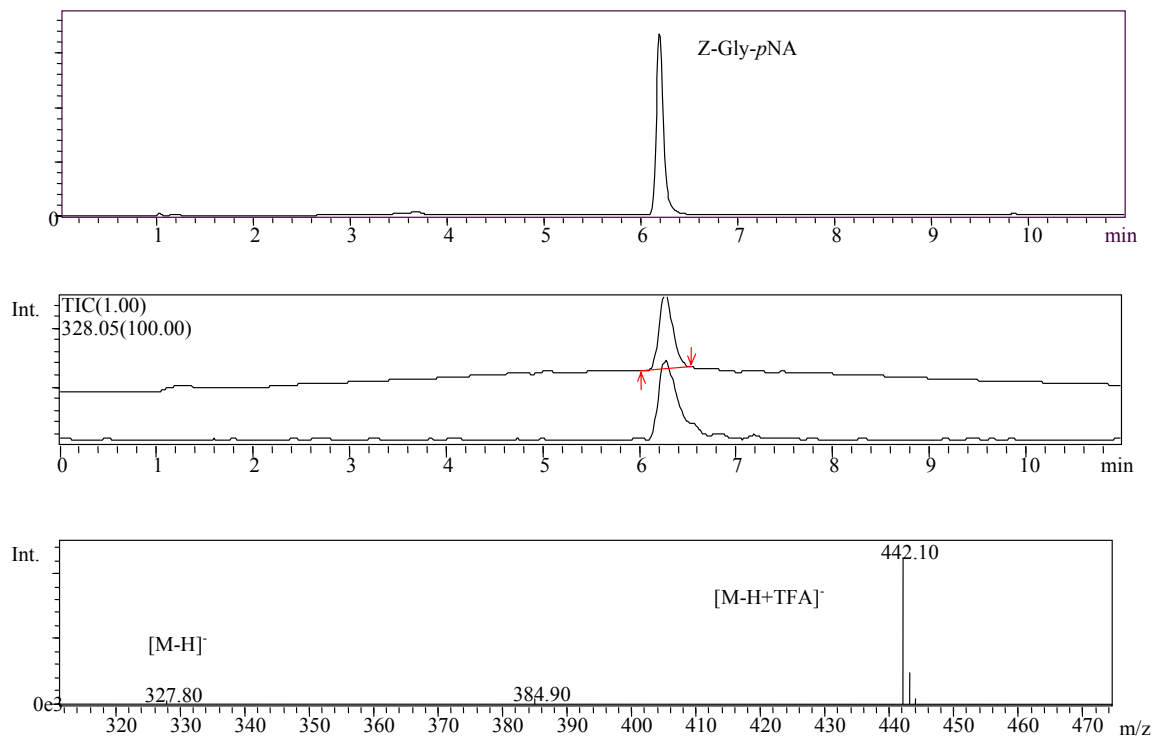
Figure 12. Reaction of Z-Gly-SeNa Generated *in situ* with *p*-Nitrophenyl Azide to Form Z-Gly-*p*NA

Synthesis of Amino Acid-*p*-Nitroanilides and Amino Acid-7-Amino-4-methylcoumarins via Selenocarboxylate/Azide Amidation. Chromogenic and fluorogenic amino acid/peptide conjugates are often used as substrates in assays for protease activity and specificity.[169] Proteolytic cleavage of the amino/peptide conjugates liberates the free chromophore or fluorophore, allowing the convenient determination of the cleavage rate of individual substrates by using a spectrophotometer such as an UV or fluorescence photometer. *p*-Nitroaniline is among the most commonly used chromogenic reagents, which is attached to an amino acid/peptide through an amide bond linkage. However, the synthesis of amino acid/peptide *p*-nitroanilide (*p*NA) conjugates is

particularly problematic due to the poor nucleophilicity of the aromatic amino group, which is further deactivated by the electron-withdrawing nitro group.

Direct acylation of *p*-nitroaniline using common peptide synthesis coupling methods, including DCC[170], HOBt activated ester[171], acyl chloride[172] and mixed anhydride[173-176] methods, did not afford satisfactory yields. Phosphorus trichloride,[177] phosphorus pentaoxide[178,179] and phosphorus oxychloride[180] methods were then developed to improve the acylation yields. However, these methods use unfavorable anhydrous pyridine as a solvent to suppress potential removal of Boc protecting group of amino acids/peptides. Reiter reported an alternative method, involving acylation of *p*-(Boc-amino)aniline followed by selective removal of the Boc protecting group and oxidation of the free amino to nitro.[181] This method, however, is not applicable to methionine, tyrosine, tryptophan and cysteine, which are sensitive to oxidation conditions.

Nishi and co-workers reported that the condensation of amino acids with *p*-nitrophenyl isocyanate provided moderate yields of *p*-nitroanilides.[182] However, commercially available *p*-nitrophenyl isocyanate contained degradation products during the period of storage, and these impurities needed to be removed before use. In addition, a significant amount of hydantoin by-product was found in the reaction mixture. Addition of DMAP improved the amidation yields but the formation of hydantoin by-product also increased.[183] A modified procedure using Curtius rearrangement with DPPA was reported by Shioiri to minimize the above side reaction, affording moderate to excellent yields (54-95%) dependent on amino acids, but the investigation was limited to Boc protected

amino acids with only three examples provided.[184] Although several attempts have been made to improve the synthesis of amino acid *p*-nitroanilides, a general method applicable to full range of amino acids is still needed.

Selenocarboxylate/azide amidation is highly chemoselective and mild, and works very efficiently for electron-deficient azides, such as *p*-nitrophenyl azides and sulfonyl azides. Therefore, it could be a potential solution to solve the problem of synthesizing highly electron-deficient aromatic amides such as *p*-nitroanilides. Furthermore, *p*-nitrophenyl azide could be readily prepared and stored in the dark for a long period of time without degradation. A 3-step one-pot procedure of selenocarboxylate/azide amidation was published and described earlier, in which *N*-protected amino selenocarboxylates were prepared by the treatment of mixed anhydrides of *N*-protected amino acids with LiAlHSeH[162] and then reacted with azides through selenatriazoline intermediate.[185] Recently, we developed an improved route to *N*-protected amino selenocarboxylates by reaction of activated *N*-protected amino acids with sodium hydrogen selenide (NaHSe) generated *in situ*, and a one-pot procedure for preparation of amino acid-*p*NA conjugates using selenocarboxylate/azide amidation strategy. The typical procedure included mixing of *N*-protected amino acid-OSu esters with the stoichiometric amount of freshly prepared NaHSe followed by addition of *p*-nitrophenyl azide. The selenocarboxylation was generally complete within 0.5 h at 0 °C. However, for sterically hindered amino acids such as isoleucine and threonine, the selenocarboxylation was slower and required room temperature for completion. The amount of amino acid-OSu esters was slightly in excess (1.2 equiv) relative to *p*-nitrophenyl azide.

As shown in Table 4, Z, Boc, Fmoc and Trt protecting groups were all well tolerated under the present reaction conditions. All amino acid-pNA conjugates were obtained in excellent yields (88% - 98%). Hydroxyl group of tyrosine and threonine did not need to be protected and no significant undesired intermolecular esterification was observed. The desired p-nitroanilides were obtained in the yields of 90% and 91% respectively. Furthermore, an aqueous solution of NaHSe was prepared according to equation (2) and reacted with Z-Gly-OSu in 50% aqueous THF to produce water-soluble Z-Gly-SeNa. The subsequent amidation in 50% aqueous THF with p-nitrophenyl azide afforded the desired Z-Gly-pNA in a yield of 95% (entry 1), indicating that the reaction also could be carried out in the presence of water. Z-Tyr-pNA was obtained in a yield of 88% in 50% aqueous THF and in a yield of 90% in THF/2-propanol (1/1). When reacting Fmoc-Ile-OSu with NaHSe, the higher reaction temperature (room temperature instead of 0 ^{o}C) was required to complete the reaction, indicating a steric hindrance effect. However, once the Fmoc-Ile-SeNa was formed, it quickly reacted with p-nitrophenyl azide to provide Fmoc-Ile-pNA in a yield of 90%. This suggested that the steric hindrance effect of selenocarboxylates did not play a significant role in the amidation step. Furthermore, the indole unit of tryptophan did not need protection and was well tolerated without affecting the amidation reaction (entry 7, Table 4). This newly developed method certainly has advantages of the ease of handling, mild reaction conditions, high yields, and compatibility with the protecting groups commonly used in amino acid and peptide chemistry such as Fmoc, Boc, Cbz, and Trt.

Table 4. Synthesis of Amino Acid *p*-Nitroanilides through Selenocarboxylation of Amino Acid-OSu Esters with NaHSe Followed by Amidation with *p*-Nitrophenyl Azide

Entry	Amino acid	Product		Yield [a]
1	Z-Gly-OSu	Z-Gly—N(H)—C$_6$H$_4$—NO$_2$ **56a**		98% / 95%[b]
2	Z-Tyr-OSu	Z-Tyr—N(H)—C$_6$H$_4$—NO$_2$ **56b**		90% / 88%[b]
3	Fmoc-Thr-OSu	Fmoc-Thr—N(H)—C$_6$H$_4$—NO$_2$ **56c**		91%
4	Fmoc-Ile-OSu	Fmoc-Ile—N(H)—C$_6$H$_4$—NO$_2$ **56d**		90%
5	Boc-Phe-OSu	Boc-Phe—N(H)—C$_6$H$_4$—NO$_2$ **56f**		91%
6	Fmoc-Met-OSu	Fmoc-Met—N(H)—C$_6$H$_4$—NO$_2$ **56g**		92%
7	Fmoc-Trp-OSu	Fmoc-Trp—N(H)—C$_6$H$_4$—NO$_2$ **56h**		94%
8	Fmoc-His(Trt)-OSu	Fmoc-His(Trt)—N(H)—C$_6$H$_4$—NO$_2$ **56i**		91%

[a] Reaction conditions: NaHSe (1.2 eq) and amino acid-OSu (1.2 eq) in THF/2-PrOH at 0 °C, then *p*-nitrophenyl azide (1.0 eq), 2h, r.t..

[b] Reaction conditions: NaHSe (1.2 eq) and amino acid-OSu (1.2 eq) in THF/H$_2$O at 0 °C, then *p*-nitrophenyl azide (1.0 eq), 2h, r.t..

For amino acid-OSu esters that were not commercially available or difficult to prepare, a 3-step one-pot procedure starting from N-protected amino acids was developed, in which the amino acids were first activated by formation of the corresponding mixed anhydride, and then were converted to the their selenocarboxylates by NaHSe followed by amidation with *p*-nitrophenyl azide.

Table 5. Three-Step One-Pot Selenocarboxylate/Azide Amidation to Synthesize Amino Acid *p*-Nitroanilides[a]
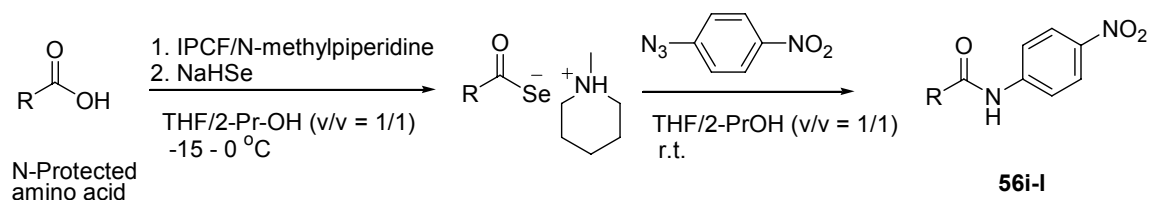
Entry	Amino acid	Product		Yield (%)[b]
1	Boc-Arg-OH.HCl	Boc-Arg—NH—⟨ ⟩—NO$_2$	56i	81
2	Boc-Gln-OH	Boc-Gln—NH—⟨ ⟩—NO$_2$	56j	91
3	Z-Ser-OH	Z-Ser—NH—⟨ ⟩—NO$_2$	56k	86
4	Boc-Ser-Phe-OH	Boc-Ser-Phe—NH—⟨ ⟩—NO$_2$	56l	89

[a]General conditions: Amino acid or peptide (1.1 mmol), isobutyl chloroformate (1.1 mmol) and N-methylpiperidine (1.1 mmol), THF, 0 °C, 20 min; LiAlHSeH (1.1 mmol), 5 °C, 30 min; *p*-nitrophenyl azide (1.0 mmol), THF, r.t., 2 h.

[b] Isolated yield

Table 5 summarizes the results of such attempts. Isopropyl chloroformate was chosen to activate amino acids because the corresponding mixed anhydrides were relatively resistant to hydrolysis or alcoholysis, especially at low temperature. By using this 3-step procedure, we could successfully synthesize N^α-protected arginine p-NAs that are of special interests since they usually are starting materials for the synthesis of chromogenic substrates of trypsin-type serine proteases. Due to the presence of guanido group, the synthesis of N^α-protected Arg-pNA has been particularly troublesome until now. Boc-Arg-OH.HCl was used directly without protecting the guanido group for the selenocarboxylate/amidation reaction. We found that Boc-Arg-OH.HCl could be activated with isopropyl chloroformate and the activated form was smoothly converted to the corresponding selenocarboxylate followed by the reaction with p-nitrophenyl azide to afford Boc-Arg-p-nitroanilide in a yield of 81%. By using the same method, Boc-Gln-pNA, Z-Ser-pNA and Boc-Ser-Phe-pNA were obtained in a yield of 91%, 86% and 89% respectively. It was not necessary to protect the hydroxy group of serine if the reaction temperature was carefully controlled below 0 °C. Such low temperature also limited the potential dehydration of the amide moiety, which often occurred for asparagine and glutamine.

Incorporation of N-protected amino acids with fluorogenic 7-amino-4-methylcoumarin (AMC) is similarly problematic with p-nitroaniline due to the low nucleophilicity of 7-aromatic amino group. Hence, this newly developed selenocarboxylate/azide amidation strategy would also provide an easy access to amino acid-AMC conjugates. As summarized in Table 6, the amino acid-AMC conjugates were obtained in excellent

yields of 82%-92%, which were slightly lower than the yields of *p*-nitroanilides prepared under the same reaction conditions. This was consistent to our previously observed trend that more electron-deficient azides would give better yields.

Table 6. Synthesis of Amino Acid 7-Amino-4-methylcoumarin (AMC) Conjugates through Selenocarboxylation of Amino Acid-OSu Esters with NaHSe Followed by Amidation with 7-Azido-4-methylcoumarin

Entry	Amino acid	Product	Yield (%)[a]
1	Z-Gly-OSu	**57a**	92 (89)[b]
2	Z-Tyr-OSu	**57b**	86 (84)[b]
3	Boc-Phe-OSu	**57c**	86
4	Fmoc-Met-OSu	**57d**	82
5	Fmoc-Trp-OSu	**57e**	82
6	Fmoc-His(Trt)-OSu	**57f**	82

[a]General conditions: NaHSe (1.2 eq) and amino acid-OSu (1.2 eq) in THF/2-PrOH at 0 °C, then 7-azido-4-methylcoumarin (1.0 eq), 2h, r.t.

[b]General conditions: NaHSe (1.2 eq) and amino acid-OSu (1.2 eq) in THF/H$_2$O at 0 °C, then 7-azido-4-methylcoumarin (1.0 eq), 2h, r.t..

D. Summary

Selenocarboxylate/azide amidation provides an attractive alternative method to the conventional nucleophilic acylation of amine when an amide bond needs to be formed without going through an amine intermediate. The reaction is highly chemoselective and clean, and can be carried out under alcoholic and aqueous conditions. The reaction also represents a traceless coupling between a carboxylic acid and an azide. Selenocarboxylate/azide amidation is complementary to the Staudinger ligation, as the Staudinger ligation favors electron-rich azides and selenocarboxylate/azide amidation works more effectively on electron-deficient azides. However, the lack of practical preparation of selenocarboxylates limited the application of this type of amidation reaction.

Convenient one-pot procedures were developed to form selenocarboxylates by reacting the mixed anhydrides of carboxylic acids with LiAlHSeH or NaHSe under mild conditions. They were effective over a range of carboxylic acids, including amino acids and peptides, and overcame disadvantages of other methods of generating selenocarboxylates. These easy-to-handle procedures to form selenocarboxylates directly from carboxylic acids facilitated the selenocarboxylate/azide amidation and made this type of amidation reaction very practical. They should also benefit other reactions related to selenocarboxylates. Excellent yields of amides were obtained for electron-deficient azides and significantly improved yields were achieved for the less reactive azides due to the dramatically increased stability of selenocarboxylates under the reaction conditions

present. We also developed a convenient method to efficiently synthesize amino acid-*p*NAs/AMCs, which are important synthons to synthesize chromogenic/fluorogenic protease substrates through segment condensation or stepwise elongation. This method had many advantages, including reproducibility, high yields, cleanness, short reaction time, mild reaction conditions, and compatibility with a wide range of organic and aqueous solvents. It also provided a new efficient method to synthesize highly electron-deficient amides, which were usually difficult to prepare due to the poor nucleophilicity of the amine reactants.

III. 4-Nitroarylmethyl Phosphoramide Mustards for NTR-Activated Prodrugs

A. Design Principle

Cyclophosphamide (CP) is one of the more successful anticancer agents developed over the past few decades. Attempts in developing more selective cyclophosphamide derivatives have led to the development of phosphoramide prodrugs incorporating a variety of specific activation mechanisms, including acid-sensitive hexenopyranoside aldo-phosphoramide,[186] hypoxia-selective nitroheterocyclic phosphoramides[187,188] and indolequinone phosphoramidates for DT-diaphorase activation.[189]

Our efforts focused on the design of phosphoramides incorporating site-specific activation mechanisms by strategically placing a nitro group for bioreductive activation to move the activation site from liver to the tumor tissues. Upon exposure to the Nitroreductase in the presence of NADH and NADPH, the nitro group would be reduced to a hydroxylamino group and further to an amino group. The electronic property switch from electron-withdrawing nitro to electron-donating hydroxylamino and amino would cause cleavage of the benzylic C-O bond in phosphoramide functionality, and thus promote the release of phosphoramide mustard (**33**), the active metabolite of cyclophosphoramide (Scheme 11). These nitroarylmethyl phosphoramide mustards were identified as excellent substrates of *E. coli* nitroreductase. *In vitro* cell culture assays showed that they were highly cytotoxic against NTR$^+$ cell lines but had marginally negligible cytotoxicity against NTR$^-$ cell lines.[81,83]

Scheme 11. Proposed Activation Mechanism of 4-Nitroarylmethylphosphoramide Mustards

cross-linking DNA strands leading to cytotoxicity
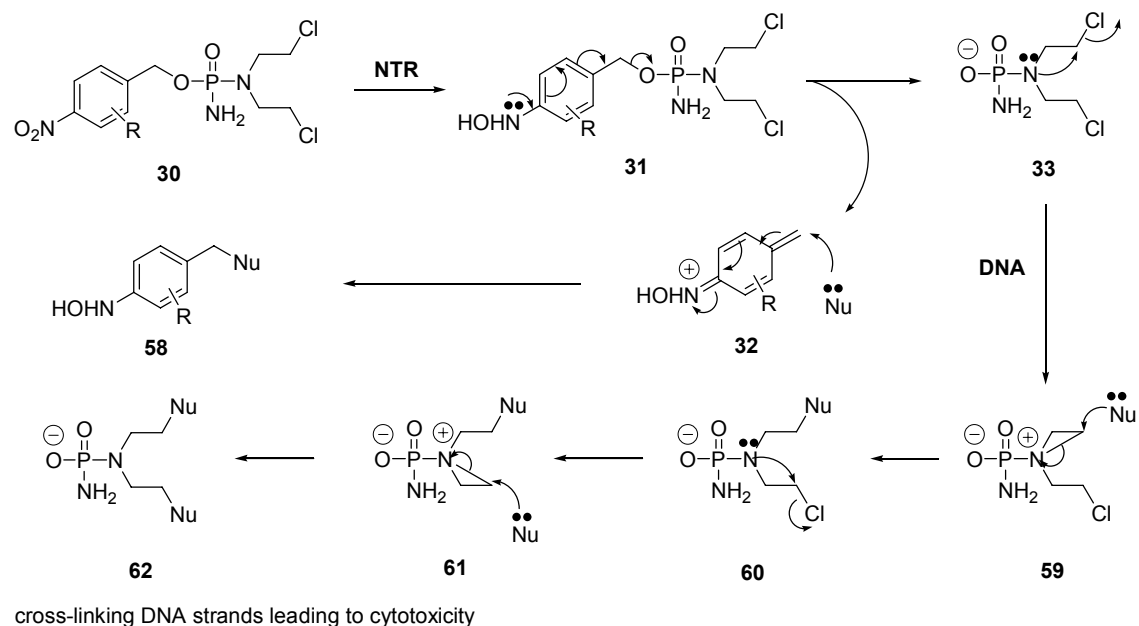
Previous SAR studies demonstrated that the benzylic C-O bond was crucial for activation of the prodrug.[81,83] Replacement of benzylic oxygen with nitrogen caused significant loss of the cytotoxicity as well as the selectivity. Among a series of nitrobenzyl phosphoramide mustards synthesized in our laboratory, 4-nitrobenzyl phosphoramide mustard (LH007) showed excellent activity with IC_{50} as low as 0.4 nM and a selectivity ratio of 170,000 against nitroreductase expressing V79 cells upon 72 h exposure. It was 100x more active and 27x more selective than 5-aziridinyl-2,4-dinitrobenzamide (CB1954), a Nitroreductase-targeted prodrug under phase II clinical trials.

It is unlikely that all tumor cells will be transfected by the vector and thus not all tumor cells will express the prodrug-converting enzyme. Subsequently, some tumor cells would

not be exposed to the active agent released from the parent prodrug upon enzymatic activation. Therefore, the ideal active agent should be able to diffuse into the intercellular fluid and kill neighbouring cells in the tumor. This action is termed the bystander effect, which is crucial to the success of gene-directed prodrug therapy as it amplifies the effect of the drug. 4-Nitrobenzyl phosphoramide mustard showed a better bystander effect with a TE_{50} value of 3.3% compared to 4.5% for CB1954. This result suggested that the hydroxylamine intermediate was able to penetrate through cellular membranes and deliver the cytotoxic phosphoramide mustard into neighboring cells.

To discover analogues with the improved selectivity and bystander effect, we performed SAR studies on the lead compound LH007, 4-nitrobenzyl phosphoramide mustard. In addition, these nitroarylmethyl phosphoramide mustards were ideal model compounds for PSA-activated peptidylaminoarylmethyl phosphoramide mustards because they shared a same linker, 4-aminoarylmethyl alcohol, to release phosphoramide mustard upon activation. We were interested in introduction of electron-withdrawing groups like fluoro into the aromatic ring in order to decrease the electron density of the benzene ring, which in turn would modulate the stability and the release kinetics of phosphoramide mustard via 1,6-elimination. Slower release of phosphoramide mustard would give the hydroxylamine intermediate more time to penetrate cellular membranes and release the cytotoxic phosphoramide mustard inside of neighboring tumor cells and, therefore, improve the bystander effect that was important for prodrugs to succeed. In addition, replacement of the aromatic hydrogen with the more hydrophobic fluorine would

increase the lipophilicity of the hydroxylamine intermediate, which further could facilitate the penetration of cellular membranes and enhance the bystander effect.

B. Results and Discussion

The synthesis of substituted 4-nitrobenzyl phosphoramide mustards **30a-e** was accomplished starting from substituted 4-nitrobenzoic acids **63a-e** as shown in Scheme 12. Our initial attempt to reduce methyl 2-fluoro-4-nitrobenzoate with DIBAL at −78 °C in THF afforded only 40% of the desired product with nearly 50% of the starting material recovered. Increasing the amount of DIBAL or reaction temperature failed to improve the yield because of the undesired reduction of nitro group. By using the modified McGeary's procedure[190], we were able to obtain the required alcohols in the yields >90%. In this process, the carboxylic acids **63a-e** were converted to the corresponding hydroxybenzotriazoyl (OBt) esters and then were reduced to alcohols **64a-e** with sodium borohydride in THF. However, adding sodium borohydride to the OBt ester solution caused a significant side reaction in which the formed alcohol reacted with the unconsumed OBt ester to produce the corresponding ester. Addition of the solution of each OBt ester dropwise to the suspension of sodium borohydride in THF was crucial to achieve the high yield of product with good purities. The alcohols **64a-e** prepared by the modified procedure were sufficiently pure and directly used for the next step reaction without the need of column purification. The substituted 4-nitrobenzyl phosphoramide mustards **30a-e** were synthesized via a 3-step one-pot procedure in which the alcohols

were first deprotonated by n-BuLi followed by phosphorylation with bis(2-chloroethyl)phosphoramidic dichloride and then aminolysis with ammonia.

Scheme 12. Synthesis of 4-Nitroarylmethylphosphoramide Mustards
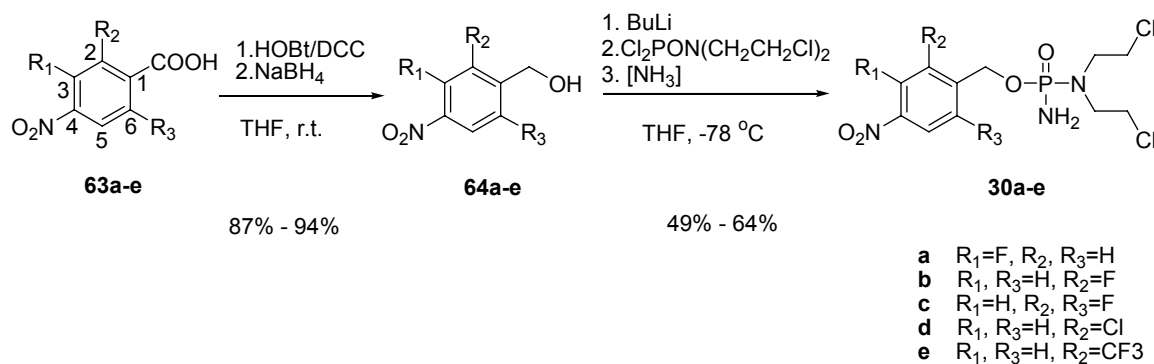
While substituted benzoic acids **63a,b,d,e** were commercially available, 2,6-difluoro-4-nitrobenzoic acid (**63c**) had to be synthesized starting from 3,4,5-trifluoro-nitrobenzene (**65**) as shown in Scheme 13. Nucleophilic substitution of the 4-fluorine with sodium dimethyl malonate in the presence of sodium hydride afforded dimethyl 2-(2,6-difluoro-4-nitrophenyl)malonate (**66**) in a yield of 76%. The intermediate **66** was then oxidized with potassium permanganate in 1N KOH aqueous solution to afford the desired product, 2,6-difluoro-4-nitrobenzoic acid (**63c**), in a yield of 91%.

Scheme 13. Synthesis of 2,6-Difluoro-4-nitrobenzoic Acid
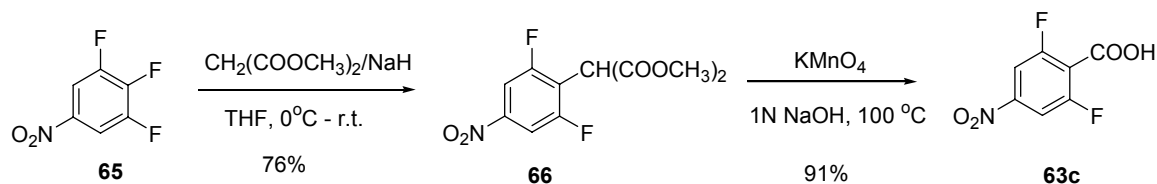
Antiproliferative Activity in Cell Culture. Compounds **30a-e** were evaluated for their cytotoxicity against cells expressing or not expressing the *E. coli* nitroreductase. Two types of cells, the V79 Chinese hamster fibroblast cells and the SKOV3 human ovarian carcinoma cells, were used for antiproliferative activity assays. The NTR$^-$-V79 cells were transfected with vector only, while the NTR$^+$-V79 cells were transfected with a bicistronic vector encoding for the *E. coli* nitroreductase and puromycin resistance as a selective marker. The NTR-expressing SKOV3 cells (SKOV3-NTR and SKOV3-NfsA) were used to compare with untransfected SKOV3 cells (SKOV3-GFP). The V79 cells were exposed to the test compounds for 72 h and the SKOV3 cells were exposed to the test compounds for 18 h. CB1954 and 4-nitrobenzyl phosphoramide mustard were used as controls.

According to the results shown in Table 7, introduction of fluorine into the 3-postion, *meta* to benzylic carbon as in **30a**, caused an over 10-fold decrease in cytotoxicity against NTR-expressing V79 cells and a 2-fold decrease in cytotoxicity against NTR-expressing SKOV3 cells, representing a 9 to 10-fold decrease in selectivity as compared to 4-nitrobenzyl phosphoramide mustard (LH007). This may be attributed to the inductive effect of fluorine: the electron-withdrawing fluorine decreased the electron density of benzene ring, making it less susceptible to 1,6-elimination and release of the cytotoxic phosphoramide mustard. However, introduction of fluorine into the 2-position, *ortho* to benzylic carbon as in **30b**, did not affect the cytotoxicity towards both NTR$^+$ V79 and NTR$^+$ SKOV3 cells. This suggested that the resonance effect of fluorine facilitated the release of phosphoramide mustard. Replacement of 2-fluorine with chlorine as in **30d** and

trifluoromethyl group as in 3**0e** caused a 10 to 20-fold decrease in cytotoxicity towards NTR^+ V79 cells as well as the selectivity due to the decreased electron density of benzene ring. Introduction of two fluorines into the 2-position and 6- position as in **30c** retained the subnanomolar cytotoxicity against NTR^+ V79 cells. However, the selectivity was decreased due to a 4-fold increase in cytotoxicity against NTR^- V79 cells.   The selectivity of **30c** was 1.4-fold lower towards V79 cells and 3-fold lower towards SKOV3 cells as compared to that of **30b**.   The different IC_{50} values between V79 cells and SKOV3 cells could be due to the different NTR expression levels between two cell lines. Another contributory factor could be a greater DNA repairing capability or resistance to DNA damage-induced apoptosis in the SKOV3 cells. The extent of bystander effect was critical to the success of GDEPT. The bystander effect was then measured by quantitating the percentage of activator (NTR^+) cells in a mixed population of NTR^+ and NTR^- cells to produce an IC_{50} midway between those in either NTR^+ or NTR^- cell type alone.[191] The results showed that the lead, 4-nitrobenzyl phosphoramide mustard (LH007), has a slightly improved bystander effect with TE_{50} of 1.6% over CB1954 with TE_{50} of 2.8%. The introduction of fluorine further improved the bystander effect by 2 folds as shown in Table 7. The excellent bystander effect and selectivity suggested that fluorinated 4-nitrobenzyl phosphoramide mustards were better candidates over CB1954 for use in combination with nitroreductase in GDEPT.

Table 7. *E. coli* Nitroreductase Activation of 4-Nitroarylmethyl Phosphoramide Mustards in NTR$^+$ and NTR$^-$ Cancer Cells

Compd.	V79 cells,[e] 72 h exposure [a]			SKOV3 cells,[e] 18 h exposure [a]				
	IC$_{50}$,[b] NTR$^-$	IC$_{50}$,[b] NTR$^+$	ratio [c]	IC$_{50}$,[b] NTR$^-$	IC$_{50}$,[b] NTR$^+$	ratio	IC$_{50}$,[b] 25% NTR$^+$ 75% NTR$^-$	TE$_{50}$
CB1954	254	0.036	7,000	486	0.4956	981	4.26	2.8%
LH007	67	0.0004	170,000	943	0.099	9523	0.98	1.6%
30a (3-F)	48	0.003	16,000	246	0.2056	1198	0.48	0.7%
30b (2-F)	49	0.0004	120,000	266	0.08	3290	0.39	0.8%
30c (2,6-diF)	26	0.0008	20,000	ND[d]	ND[d]	ND[d]	ND[d]	ND[d]
30d (2-Cl)	50	0.002	13,000	140	0.1249	1121	ND[d]	ND[d]
30e (2-CF$_3$)	17	0.004	12,000	172	0.3057	565	ND[d]	ND[d]

[a] Cells were exposed to each test compound, and a standard cell viability assay was performed at the end of indicated incubation period. Initially, the maximum concentration used was 100 μM in the case of V79 cells and 1000 μM in the case of SKOV3 cells. When necessary, assays were repeated at higher drug concentrations to obtain accurate IC$_{50}$ values.

[b] IC$_{50}$ values are the concentration in μM required to reduce cell number to 50% of control after the cells were exposed to the drug for the indicated time. The standard errors of all assays were within 10% of the mean between replicates at a given concentration and 10-23% for the fitted IC$_{50}$ values.

[c] Ratio of IC$_{50}$ values (NTR$^-$/NTR$^+$) as an indication of activation by *E. coli* nitroreductase.

[d] Not determined.

[e] Cell lines: V79 (Chinese hamster fibroblast) and SKOV3 (human ovarian carcinoma).

In summary, series of substituted 4-nitrobenzyl phosphoramides were designed to fine tune the release kinetics of cytotoxic phosphoramides and to be more lipophilic than LH007 with aims of improving the bystander effect. Introduction of fluorines into the benzene ring improved the bystander effect by 2 folds as compared to LH007 due to increased lipophilicity contributed by the hydrophobic property of fluorine. While

introduction of fluorine into the *meta* position to benzylic carbon led to a significant decrease in cytotoxicity against NTR$^+$ cells, introduction of fluorine into the *ortho* position to benzylic carbon retained the same subnanomolar level of cytotoxicity as LH007. This suggested that the release of drug was affected by both inductive effect and resonance effect of fluorine: the electron-withdrawing fluorine prevented the 1,6-elimination process by decreasing the electron density of the benzene ring through its inductive effect; and fluorine also acted also as a electron donor through its resonance effect to facilitate the 1,6-elimination process. Introduction of chlorine or trifluoromethyl group into the *ortho* position to the benzylic carbon, however, led to a 10 to 20-fold loss of cytotoxicity against NTR$^+$ cells, suggesting a predominant electron-withdrawing inductive effect. Clearly, the rate of releasing phosphoramide mustard via the 1,6-elimination process correlated to the electron density of the aromatic ring. Further studies have been undertaken to modulate the electron density by replacement of the benzene ring with a heteroaromatic ring.

IV. Prostate-Specific Antigen Targeted Prodrugs

NTR-activated 4-nitroarylmethyl phosphoramide mustards are ideal model compounds for PSA-targeted peptidylaminoarylmethyl phosphoramide prodrugs because they share a same drug releasing mechanism as shown in Scheme 5. The release of cytotoxins from both types of prodrugs is essentially based on the "electronic property switch" that is triggered by the targeted enzymes. Upon reduction of nitro by NTR or proteolytic cleavage by PSA, the resulting electron-donating hydroxylamino or amino would facilitate the cleavage of the benzylic C-O bond to release active phosphoramide mustard (**33**) via the 1,6-elimination process. Furthermore, the easiness of synthesizing 4-nitroarylmethyl phosphoramide mustards makes it possible to provide large number of derivatives for SAR studies within a short period of time.

SAR studies on 4-nitroarylmethyl phosphoramide mustards indicated that electron-withdrawing inductive effect of fluorine prevented the 1,6-elimination process by decreasing the electron density of aromatic ring and, thus, caused a decrease in cytotoxicity. Introduction of fluorine into the *ortho* position to benzylic carbon, however, was capable of restoring the cytotoxicity by the electron-donating resonance effect of fluorine. Furthermore, the decreased electron density of aromatic ring would prevent undesired release of drug prior to enzymatic activation and, thus, improve stability. Fluorinated 4-nitrobenzyl phosphoramides had improved bystander effect because of increased lipophilicity by introduction of hydrophobic fluorine. 2-Fluoro-4-nitrobenzyl phosphoramide mustard (**30b**) was the best compound representing a balance of the

desired bystander effect, cytotoxicity and selectivity. Because the activation of PSA-targeted prodrugs takes place extracellularly, the extent of intracellular access and neighboring cell killing should be very important to the success of PSA-targeted prodrug therapy. Therefore, fluorinated prodrugs targeting PSA were designed to be more lipophilic with aims of improving the bystander effect and stability as well (Scheme 13).

By design, conjugation of a phosphoramide mustard moiety with a PSA-specific peptide via a traceless linker would lead to a biologically poorly active compound; the cytotoxicity of phosphoramide mustard would be restored after proteolytic cleavage of the peptide by PSA. Glutaryl-Hyp-Ala-Ser-Chg-Gln-OH was one of the PSA-specific substrates, which was used by Merck to couple with H-Ser-Leu-Doxorubicin to yield L-377,202, a drug candidate that was tested in a phase 1 clinical trial. The resulting peptide-doxorubicin conjugate was effectively cleaved by PSA with a half-life of around 30 min and had good water-solubility due to the presence of a free carboxyl group. We, therefore, chose this pentapeptide to couple with the phosphoramide mustard moiety via a traceless linker **67a-e**.

As discussed in the section II of Chapter 2, retrosynthetic analysis of peptidylaminoarylmethyl phosphoramide mustards revealed a synthetic route that would go through a nonnucleophilic amidation of azide as shown in Scheme 6. Most importantly, our laboratory has successfully developed a new methodology of Selenocarboxylate/azide amidation, which makes a convergent synthetic pathway eventually possible. As shown in Scheme 14, the designed peptide conjugate prodrugs

40a-e would be synthesized by coupling the tetrapeptide, Fm-glutaryl-Hyp-Ala-Ser-Chg-OH, with glutaminylaminoarylmethyl phosphoramide mustards **41a-e** via a segment condensation strategy. The latter **41a-e** could be easily synthesized through the selenocarboxylate/azide amidation by reacting various 4-azido-arylmethyl phosphoramide mustards **44a-e** with the selenocarboxylate form of *N*-protected glutamine.

Scheme 14. Retrosynthetic Analysis of Glutaryl-Hyp-Ala-Ser-Chg-Gln-NH-arylmethyl Phosphoramide Mustards
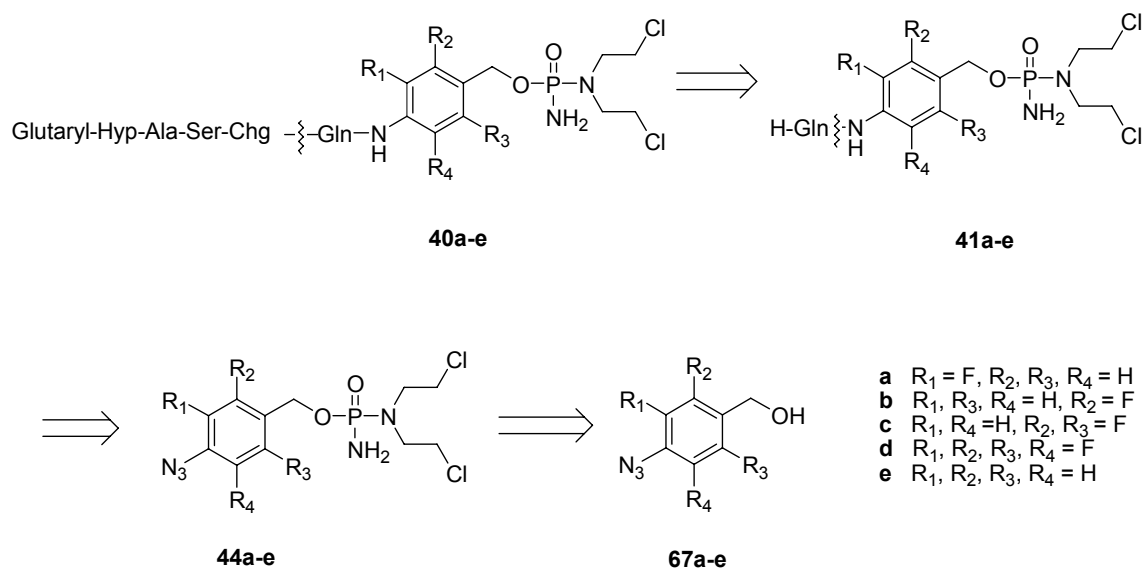
A. Synthesis of Peptidylaminoarylmethyl Phosphoramide Mustards

*Synthesis of 4-azido-arylmethyl phosphoramide mustards **44a-e***

The synthesis of 4-azido-benzyl phosphoramide mustard **44e** started from commercially available 4-aminobenzyl alcohol (**43e**) through diazotization and azide displacement. 4-Azidobenzyl alcohol (**67e**) was obtained in a yield of 78% after flash column chromatography. The desired 4-azido-benzyl phosphoramide mustard (**44e**) was synthesized via a 3-step one-pot procedure (Scheme 15): 4-azidobenzyl alcohol was first treated with 1.0 equiv of n-BuLi at −78 °C to remove the alcoholic proton followed by the phosphorylation with 1.2 equiv of bis-(2-chloroethyl)phosphoramidic dichloride and then aminolysis with ammonia. The desired product **44e** was obtained in a yield of 55%.

Scheme 15. Synthesis of 4-Azido-benzyl Phosphoramide Mustard
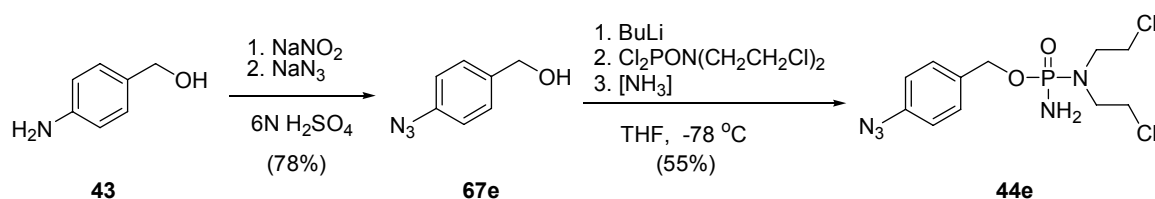
The synthesis of fluorosubstituted derivatives is summarized in Scheme 16. For 2-fluoro, 3-fluoro and 2,6-difluoro substituted derivatives, the synthesis started from their corresponding nitroaromatic acids which were commercially available. Briefly, the nitro group was converted to the amino group by catalytic hydrogenation affording nearly

quantitative yields of corresponding 4-aminobenoic acid derivatives **68a-c**. Then, the

amino group was converted to an azido group using the standard diazotization/azide

protocol to afford the corresponding 4-azidobenzoic acid derivatives **69a-d** in yields of

80 - 90%. Using the modified McGeary's procedure, the carboxylic acid group was

selectively reduced by sodium borohydride in THF to an alcohol without reduction of the

azido group, affording the corresponding alcohols **66a-d** in yields of 70% - 86%. Then,

the obtained fluorosubstituted 4-azidobenzyl alcohols **66a-d** were converted to the

corresponding 4-benzyl phosphoramides **44a-d** using the 3-step one-pot procedure

described earlier.

Scheme 16. Synthesis of 4-Azido-arylmethyl Phosphoramide Mustards

a R_1 = F, R_2, R_3, R_4 = H
b R_1, R_3, R_4 = H, R_2 = F
c R_1, R_4 = H, R_2, R_3 = F
d R_1, R_2, R_3, R_4 = F
e R_1, R_2, R_3, R_4 = H
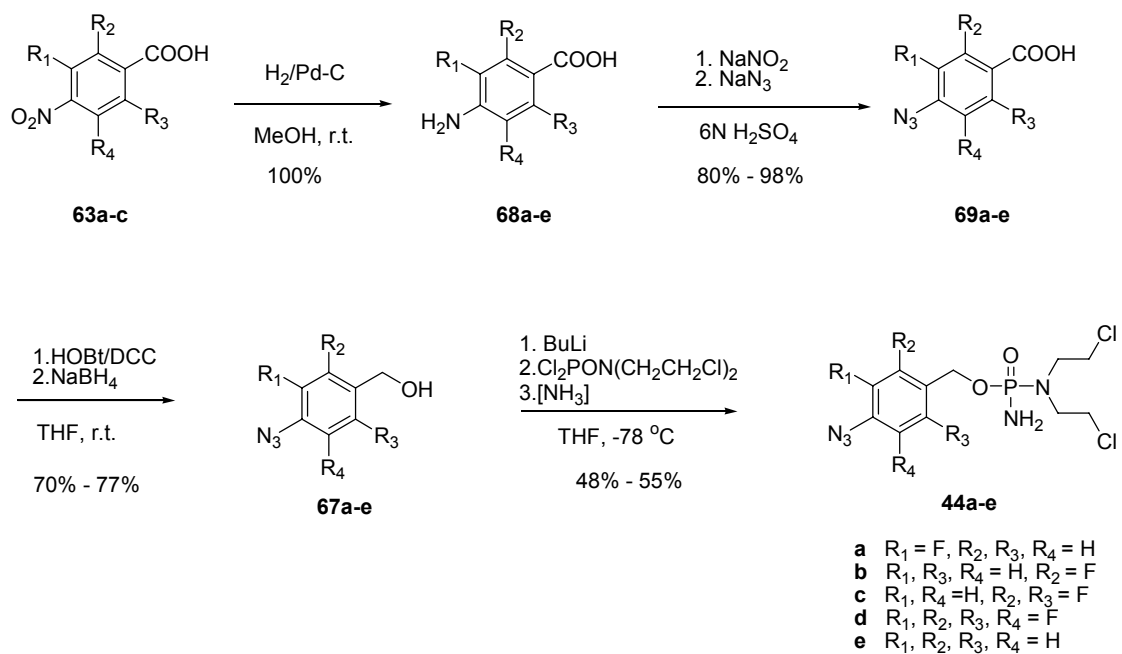
*Synthesis of 4-glutaminylaminoarylmethyl phosphoramide mustards **41a-e***

We have developed a one-pot selenocarboxylate/azide amidation procedure for directly coupling a *N*-protected amino acid with an azide to form an amide. Herein, the same strategy was used to synthesize *N*-protected glutaminylaminobenzyl phosphoramide mustards. 4-Azidobenzyl phosphoramide mustard **67e** was used as a model compound to explore the suitable reaction conditions. Boc-glutaminylaminobenzyl phosphoramide mustard, Z-glutaminylaminobenzyl phosphoramide mustard, and Fmoc-glutaminylaminobenzyl phosphoramide mustard were successfully synthesized in moderate yields. However, removal of Boc- and Cbz- protecting group was troublesome due to the liability of phosphoryl functionality to the deprotection conditions. Although deprotection of Fmoc-glutaminylaminobenzyl phosphoramide mustard did not present any problem, it required a polar aprotic solvent to dissolve Fmoc-glutamine. TFA-glutamine was soluble in THF, and could be easily prepared in a yield of 84% yield by the treatment of L-glutamine with S-ethyl trifluoroacetate.[192] Furthermore, the TFA protecting group could be readily removed by the treatment with K_2CO_3 or ammonia. We, thus, used TFA-glutamine as a starting amino acid to prepare glutaminylaminoarylmethyl phosphoramide mustards **41a-e**.

The synthesis of TFA-glutaminylaminobenzyl phosphoramides **71a-e** started from the selenocarboxylation of TFA-glutamine by the treatment of the mixed anhydride of TFA-glutamine with freshly prepared LiAlHSeH. The *in situ* generated selenocarboxylate of TFA-glutamine was used directly to react with various 4-azidoarylmethyl phosphoramide

mustards **44a-e**. The results were summarized in Scheme 17. It clearly indicated that the electron-deficient azides, 4-azido-2,3,5,6-tetrafluorobenzyl phosphoramide mustard (**44d**) and 4-azido-2,6-difluorobenzyl phosphoramide mustard (**44c**) provided the highest yields of 87% and 72% respectively. 4-Azido-2-fluorobenzyl phosphoramide mustard (**44b**) afforded a better yield of 55% over 4-Azido-benzyl phosphoramide mustard (**44e**) (25%) due to the introduction of electron-withdrawing fluorine. However, introduction of fluorine into the *ortho* position to the azido group as in **44a** did not improve the yield. This could be due to that the *ortho*-fluoro group acted as an electron donor through resonance effect, indicating that, in addition to inductive effect, the resonance effect also affected the rate of selenocarboxylate/azide amidation. The TFA protecting group was smoothly removed by the treatment of TFA-glutamine conjugates with 4.0 equiv of K_2CO_3 in aqueous acetonitrile at room temperature without significant hydrolysis of the phosphoryloxy moiety. The glutaminylaminoarylmethyl phosphoramide mustards **41a-e** were purified with flash column chromatography affording 74%-85% yield and their structures were confirmed by LC/MS and NMR.

Scheme 17. Synthesis of Glutaminylaminoarylmethyl Phosphoramide Mustards

71a-e	**41a-e**
a R_1 = F, R_2, R_3, R_4 = H, 20%	**a** R_1 = F, R_2, R_3, R_4 = H, 74%
b R_1, R_3, R_4 = H, R_2 = F, 55%	**b** R_1, R_3, R_4 = H, R_2 = F, 76%
c R_1, R_4 =H, R_2, R_3 = F, 72%	**c** R_1, R_4 =H, R_2, R_3 = F, 85%
d R_1, R_2, R_3, R_4 = F, 87%	**d** R_1, R_2, R_3, R_4 = F, 78%
e R_1, R_2, R_3, R_4 = H, 25%	**e** R_1, R_2, R_3, R_4 = H, 77%
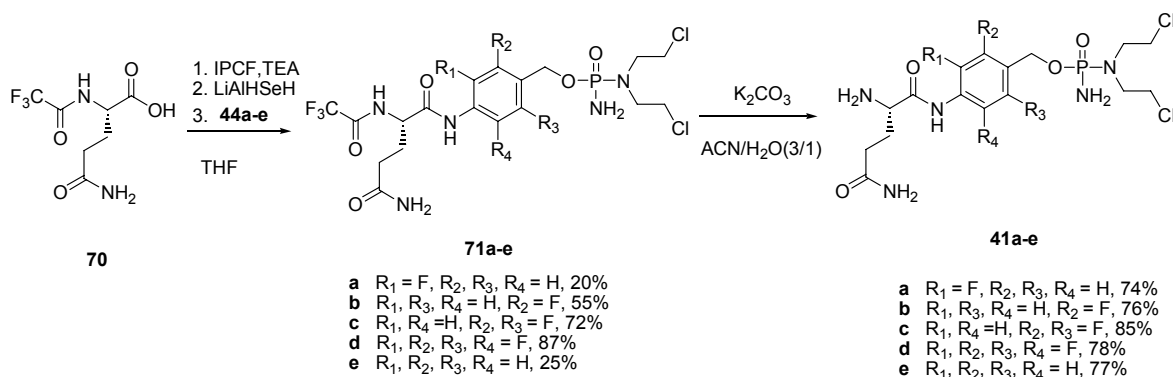
Solid-Phase Synthesis of Fm-glutaryl-Hyp-Ala-Ser-Chg-OH (72)

The pentapeptide, Fm-glutaryl-Hyp-Ala-Ser-Chg-OH (**72**), was synthesized using Fmoc chemistry on Wang resin, 4-hydroxymethylphenoxy resin. Briefly, Fmoc-cyclohexylglycine was first attached to the Wang resin using DMAP/DIC protocol. The resin was then capped by acetic anhydride. Subsequent *N*-Fmoc-amino acids were activated and coupled using HBTU/DIEA protocol. After each cycle of coupling, the *N*-terminal Fmoc protecting group was removed by the treatment with 20% piperidine in NMP. A Kaiser ninhydrin test was performed to determine the completion of each coupling and deprotection. The cleavage of peptide from the resin was achieved using 95% TFA in CH_2Cl_2. The cleaved peptide was then purified by semi-preparative reversed phase HPLC.

Synthesis of Glutaryl-Hyp-Ala-Ser-Chg-Gln-aminoarylmethyl Phosphoramide Mustards ***40a-e***

As shown in Scheme 18, the tetrapeptide **72** was first activated by formation of its OBt ester using HBTU/DIPEA protocol, followed by coupling with H-Gln-aminoarylmethyl phosphoramide mustards **41a-e** in NMP. The reaction process was monitored by LC/MS. The conjugated products were collected as white solids by precipitation from 5% aqueous $NaHCO_3$. The peptide conjugates obtained were immediately dissolved in 50% acetonitrile in methanol and treated with 10 equivalents of diethylamine at room temperature. After completion of the reaction as monitored by LC/MS, the solvents were

evaporated under reduced pressure. The residues were washed with diethyl ether and then

subjected to semi-preparative reversed phase HPLC.

Scheme 18. Synthesis of Glutaryl-Hyp-Ala-Ser-Chg-Gln-aminoarylmethyl Phosphoramide
Mustards **40a-e**

72

1. HBTU/DIPEA, **41a-e**
2. 10 eq DEA

40a-e

a R_1 = F, R_2, R_3, R_4 = H, 28%
b R_1, R_3, R_4 = H, R_2 = F, 38%
c R_1, R_4 =H, R_2, R_3 = F, 40%
d R_1, R_2, R_3, R_4 = F, 30%
e R_1, R_2, R_3, R_4 = H, 30%
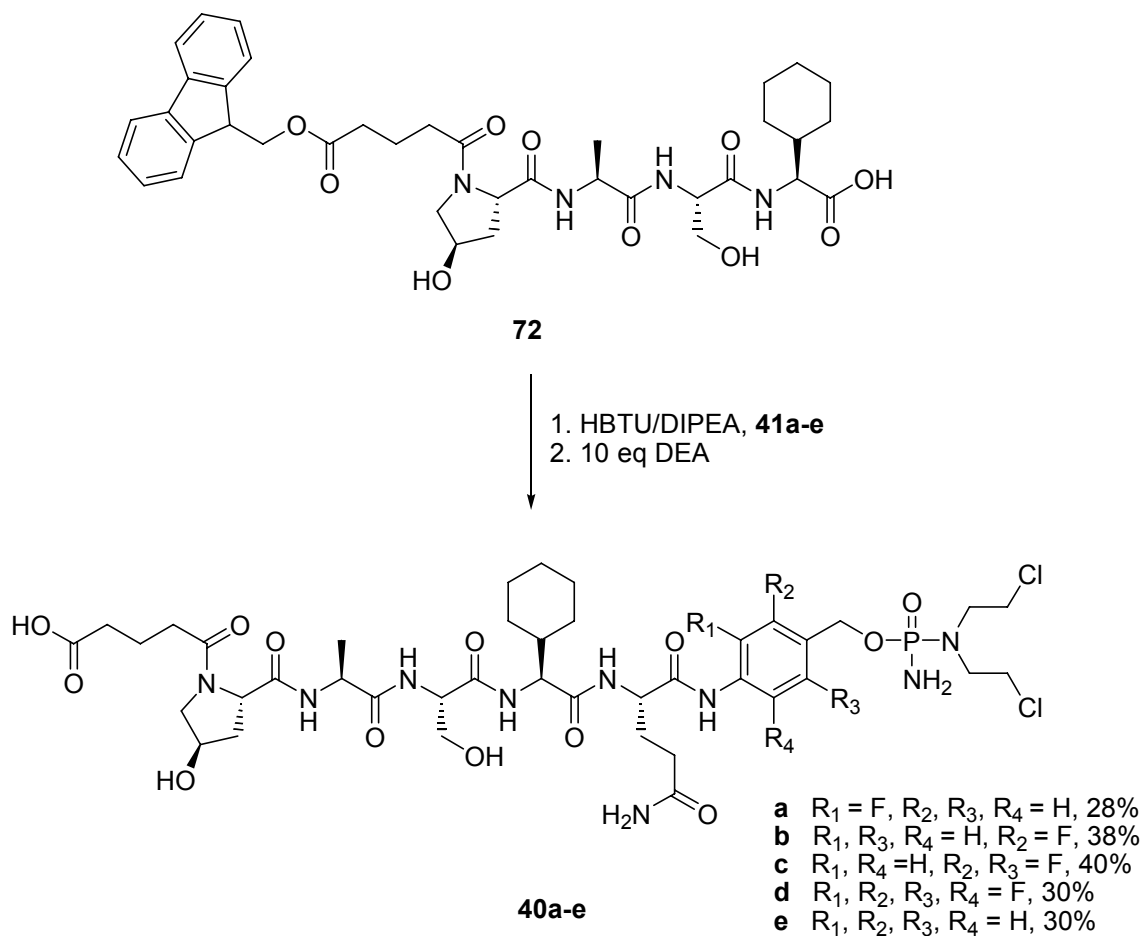
B. Results and Discussion

i. Stability Study of Peptidylaminoarylmethyl Phosphoramide Mustards 40a-e

The stabilities of peptidylaminoarylmethyl phosphoramide mustards **40a-e** were determined under conditions employed for both PSA enzyme assays and cell-culture assays. PSA enzyme assays were performed in a buffer containing 10 mM Tris/HCl and 0.01% TWEEN-20$^{®}$ at pH 8.0, and cell-culture assays were performed in a culture medium at pH 7.4. All substrates were incubated at 37 °C in the PSA assay buffer and a Na$_2$HPO$_4$/NaH$_2$PO$_4$ buffer (pH 7.4) mimicking the cell culture conditions, respectively. Aliquots were withdrawn at various time intervals and stored frozen prior to HPLC analysis. The half-lives were calculated based on the disappearance of substrates and are summarized in Table 8. Glutaryl-Hyp-Ala-Ser-Chg-Gln-aminobenzyl phosphoramide **40e** had a shortest half-life of 44 h in the phosphate buffer at pH 7.4 (Figure 13) and 46 h in the Tris.HCl buffer at pH 8.0 (Figure 14), respectively. Introduction of fluorine into the 2-, 2,6-, and 2,3,5,6-position of benzene ring increased the stabilities of resulting **40b-d** by average 2.4-fold, 2.8-fold and 3.5-fold in both buffers. Introduction of fluorine into the 3-position (*ortho* to the amino group) of benzene ring, however, dramatically increased the stability of **40a** by over 10-fold. The degradation products were found to be the corresponding peptidylaminoarylmethyl alcohols according to LC-MS analysis. There were two possible pathways of degradation: the breakage of P–O bond due to the hydrolysis of phosphoryloxy functionality or 1,6-elimination followed by nucleophilic
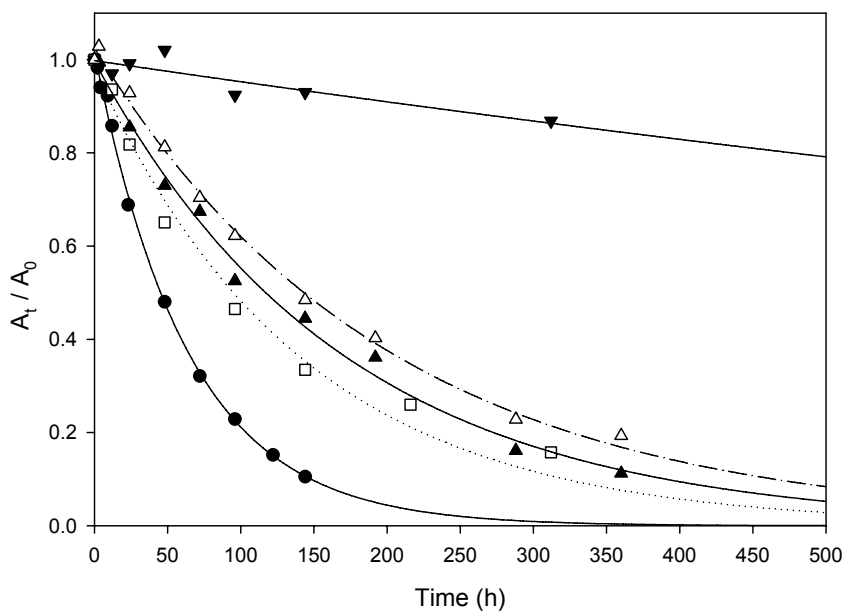
Figure 13. Stabilities of Peptidylaminoarylmethyl Phosphoramide Mustards **40a-e** in a Phosphate Buffer (pH 7.4) at 37 $^{\circ}$C.

40a (—▼—), **40b** (···□···), **40c** (—▲—), **40d** (—·–△–·—), **40e** (—●—).
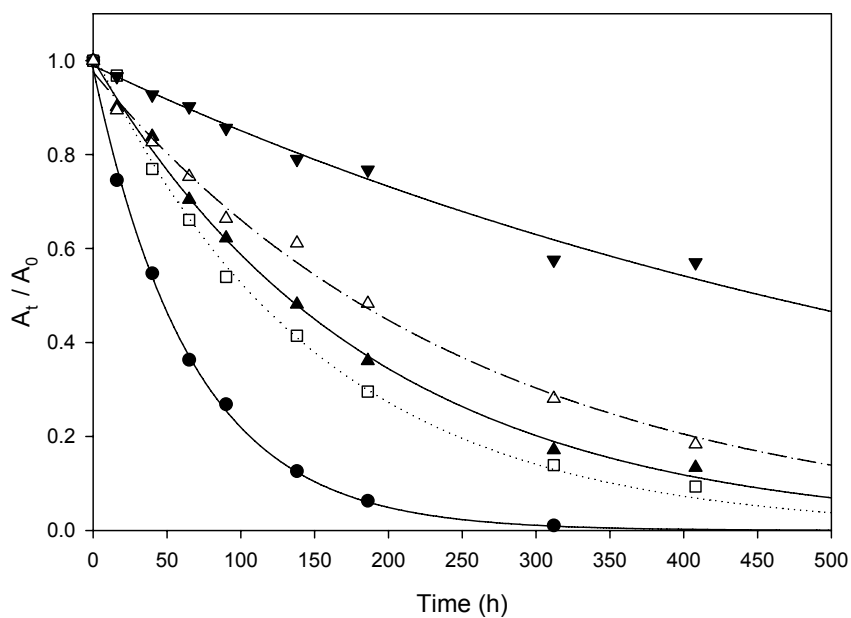
Figure 14. Stabilities of Peptidylaminoarylmethyl Phosphoramide Mustards **40a-e** in a Tris Buffer (pH 8.0) at 37 $^{\circ}$C.

40a (—▼—), **40b** (···□···), **40c** (—▲—), **40d** (—·–△–·—), **40e** (—●—).

addition of water to the resulting quinonimine methides. After 3 days incubation of 4-nitrobenzyl phosphoramide mustard in the same phosphate buffer (pH 7.4) at 37 $^{\circ}$C, there was no detectable degradation observed, indicating that the phosphoryloxy functionality was stable toward hydrolysis. Therefore, the degradation of peptide conjugates most likely was due to 1,6-elimination. It also provided a reasonable explanation why introduction of fluorines into the benzene ring generally enhanced the stability of resulting conjugates. That was presumably because the electron-withdrawing property of fluorine effectively decreased the electron density of the aromatic ring, which the 1,6-elimination process relied on. In other words, increasing the electron density of aromatic ring would accelerate the rate of 1,6-elimination, and decreasing the electron density of aromatic ring would slow the rate of 1,6-elimination and, thus, improve stability.

ii. PSA Enzymatic Study of Peptide Conjugates

The peptidylaminoarylmethyl phosphoramide mustards **40a-e** were evaluated as substrates of PSA at an enzyme/substrate molar ratio of 1/100, while L-377,202, Glutaryl-Hyp-Ala-Ser-Chg-Gln-Ser-Leu-Doxorubicin, was used as a control. The stock solution of each substrate was prepared as a 10 mM solution in DMSO. The substrates were then incubated with 1 mol% of PSA at 37 °C in a buffer containing 10 mM Tris/HCl and 0.01% TWEEN-20$^{\circledR}$ with pH 8.0. Aliquots were withdrawn at various time intervals, quenched by acetonitrile (20%), and stored frozen prior to HPLC analysis. All these peptide conjugates were cleaved by PSA in a time-dependent manor as monitored by HPLC analysis. The pentapeptide segment, Glutaryl-Hyp-Ala-Ser-Chg-Gln-OH, was

confirmed by LC/MS showing the mass of 669.32 corresponding to [M-H]⁻. As shown in Figure 15, for the control substrate, L-377,202, the complete disappearance of substrate was observed within 2 h with a half-life of ~ 30 min. This half-life value was consistent to the previously reported 30 min in the literature.[41] However, for all peptidylaminoarylmethyl phosphoramide mustards, the substrate concentrations did not reach to zero after 5-hour incubation and did not further decrease after 3 h. This may be due to inactivation of PSA upon the release of activated alkylating phosphoramide mustard (**33**) or electrophilic quinonimine methides.
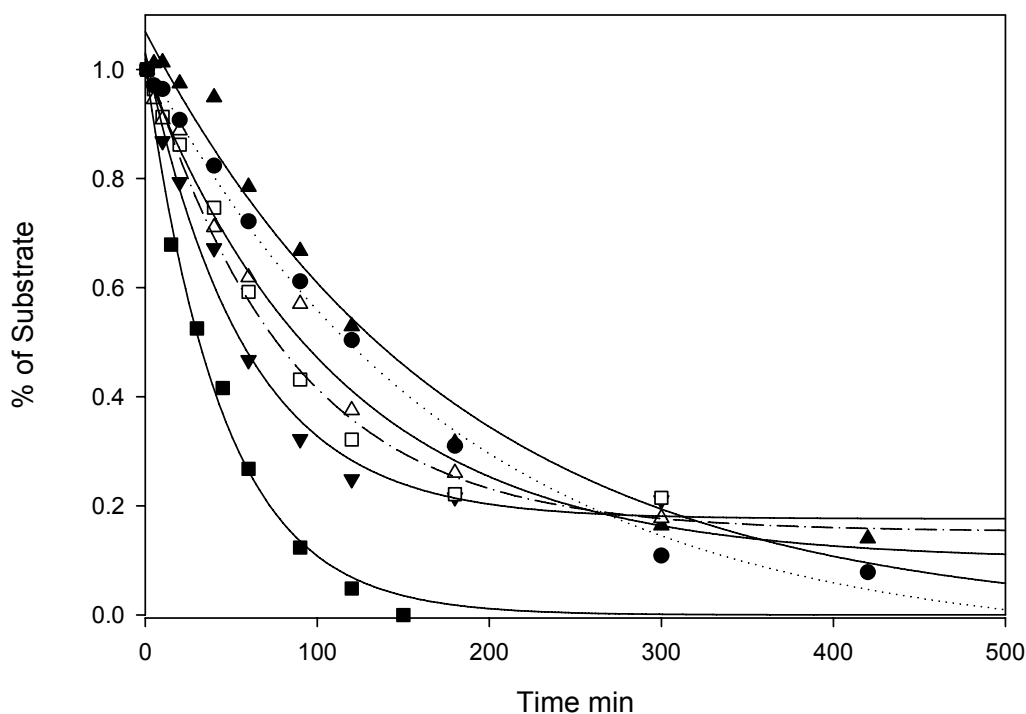
Figure 15. The Disappearance of Peptidylaminoarylmethyl Phosphoramide Mustards during PSA Enzymatic Hydrolysis.

Each conjugate was incubated with PSA by an enzyme/substrate ratio of 1/100 in a buffer (pH 8.0) containing 50 mM Tris/HCl, 10 mM CaCl₂ and 0.1% TWEEN-20 at 37.0 °C. L-377,202 (—■—), **40a** (—▼—), **40b** (—·–□–·—), **40c** (—▲—), **40d** (—△—), **40e** (···●···).

iii. Antiproliferative Activity Study of Peptide Conjugates

The antiproliferative activities of peptidylaminoarylmethyl phosphoramide mustards were evaluated by the standard MTT assay performed in PSA-expressing LNCaP cells and non-PSA-expressing DU145 cells, while L-377,202 was used as a control. Cells were maintained in RPMI 1640 medium supplemented with 10% FBS, 100 units/mL penicillin G and 100 units/mL streptomycin sulfate and split at 80% confluence followed by trypsinization and subcultured at 1:6 in the medium changed every 72 h. Cells harvested by trypsinization were resuspended in a serum-free medium containing 2% (v/v) TCM and plated in 96-well microtiter plates with ~ 5,000 cells in 0.1 ml medium per well. After 48 h incubation, serial dilutions of the test compounds were added to the cells. Medium alone was used as the negative control while L-377,202 was used as the positive control. Each compound was evaluated in triplicate and MTT assay was performed 3 days after addition of the test compounds. The absorbance at 570 nm (reference 650 nm) was read using a Dynatech MR5000 microtiter reader. The antiproliferative activity assay for each compound was performed at least twice. The IC_{50} values for **40a-e** were calculated and are summarized in Table 8. As expected, DU145 cell line (PSA-negative) was not sensitive to L-377,202 and prodrugs **40a-d**. The prodrug **40e** was cytotoxic towards DU145 cells having an IC_{50} of 35 μM because it was the least stable compound with a half-life of 44 h in the phosphate buffer (pH 7.4) similar to the cell culture conditions. After 72-h incubation with DU145 cells prior to MTT assay, over 60% of **40e** was decomposed with the release of cytotoxic phosphoramide mustard. Except the prodrug **40d**, all prodrugs were cytotoxic towards the PSA-positive LNCaP cell line.

Table 8. Stability, PSA Cleavage, and Antiproliferative Activity of Peptide Conjugates **40a-e**

Peptide-prodrugs	$t_{1/2}$ (h)[a]			IC_{50} (µM)		Selectivity
	PSA⁻ (PH 7.4)	PSA⁻ (PH 8.0)	PSA⁺	DU145 PSA⁻	LNCaP PSA⁺	
L-377,202	NA	NA	0.6	> 100	1.1	> 90
40a (3-F)	> 300h	465	0.66	> 100	29.0	> 3
40b (2-F)	108	105	0.95	> 100	5.3	> 19
40c (2,6-diF)	118	131	2.1	> 100	20.0	> 5
40d (2,3,5,6-tetraF)	136	178	1.3	> 100	> 100	NA
40e	44	46	2.1	35.0	11.0	3

Prodrug **40b** showed the highest cytotoxicity against LNCaP cells with an IC_{50} of 5.3 µM, followed by **40e** (IC_{50} = 11.0 µM), **40c** (IC_{50} = 20.0 µM), and **40a** (IC_{50} = 29.0 µM). The lack of cytotoxicity of **40d** was presumably due to the fact that the 1,6-elimination process was prevented by introduction of four electron-withdrawing fluorines making the aromatic ring highly electron-deficient and, thus, the release of phosphoramide mustard was blocked.

To confirm this hypothesis, 4-azido-2,3,5,6-tetrafluorobenzyl phosphoramide mustard (**44d**) was reduced by hydrogenation in the presence of 10% Pd-C in ethyl acetate. As expected, there was no 1,6-elimination upon reduction of azido to amino. The reaction was quite clean, providing the corresponding 4-amino-2,3,5,6-tetrafluorobenzyl phosphoramide mustard (**73**) as the only product. Figure 16 represents the LC-MS report of catalytic hydrogenation of **44d**, in which the mass of 398.05 corresponds to $[M+H]^+$, 420.10 corresponds to $[M+Na]^+$ and 461.10 corresponds to $[M+Na+CH_3CN]^+$. The

isotope abundance ratio indicates that there are two chlorines in the molecule. The structure of **73** was further confirmed by ^{1}HNMR and ^{13}CNMR.
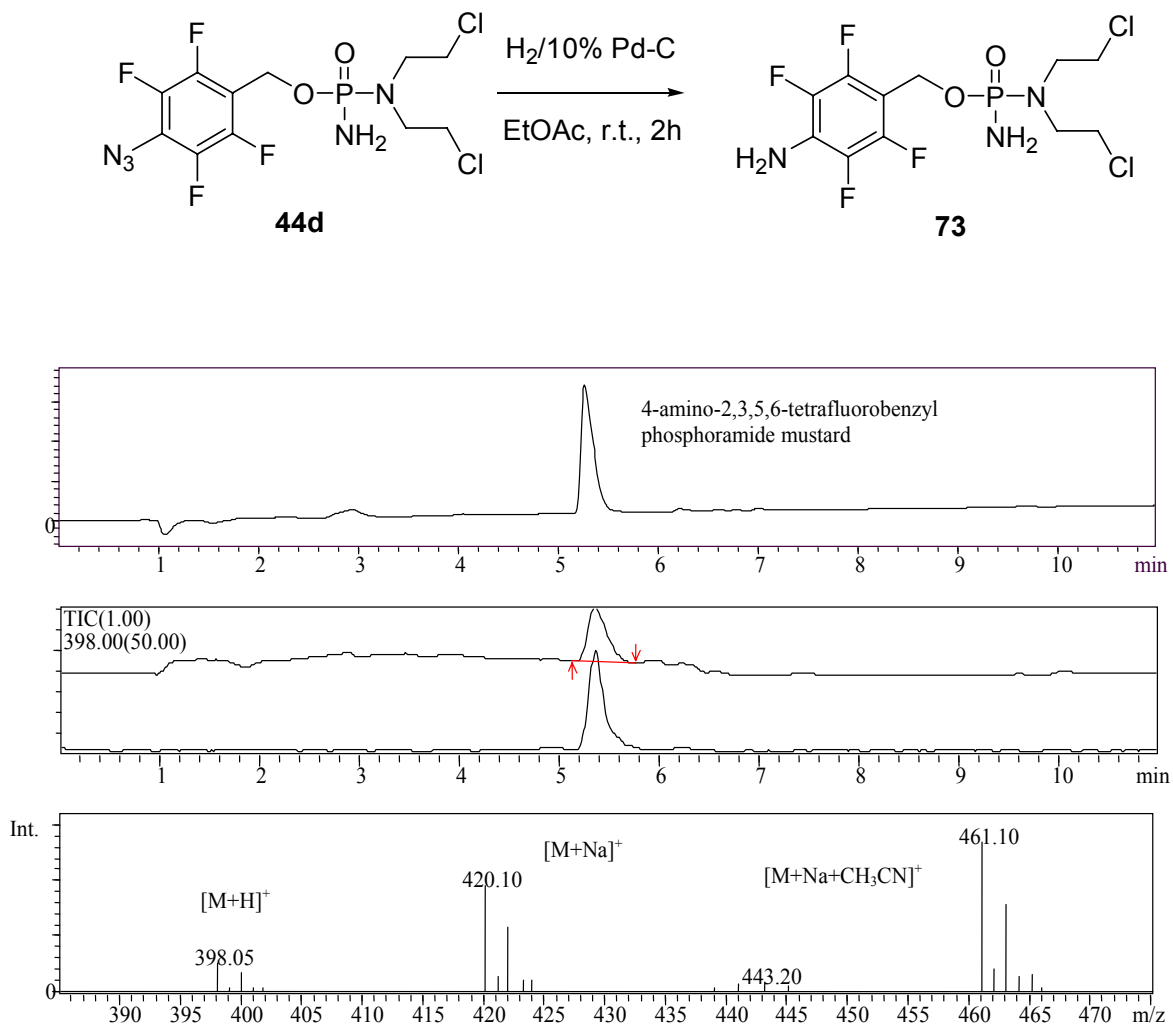
Figure 16. Reduction of 4-Azido-2,3,5,6-tetrafluorobenzyl Phosphoramide Mustard to Stable 4-Amino-2,3,5,6-tetrafluorobenzyl Phosphoramide Mustard

V. Summary

We designed, synthesized and evaluated peptidylaminoarylmethyl phosphoramide mustards as prodrugs for site-specific activation by PSA in prostate cancer cells. The design principle was based on proteolytic cleavage of peptide to activate the linker that releases cytotoxic phosphoramide mustard via a 1,6-elimination process. This 1,6-elimination mechanism was successfully applied in our previous nitroreductase-based prodrug design. All evaluated peptide conjugates were substrates of PSA according to PSA enzyme assay. *In vitro* antiproliferative activity assay of these peptide conjugates showed promising results in terms of cytotoxicity and selectivity. Structure-activity relationship studies on these peptidylaminoarylmethyl phosphoramide mustards indicated that introduction of electron-withdrawing fluorines into the benzene ring improved the stability of resulting peptide conjugates under conditions used for PSA enzyme assay and *in vitro* antiproliferative activity assay. However, introduction of fluorine into the *ortho* position to benzylic carbon was crucial to retain the cytotoxicity of compounds. Introduction of fluorine into the *meta* position to benzylic carbon caused a significant decrease in cytotoxicity. This trend was observed in both nitroreductase-based prodrugs and PSA-based prodrugs. The peptide conjugate **40b**, Glutaryl-Hyp-Ala-Ser-Chg-Gln-NH-(2-F)benzyl phosphoramide mustard, was identified as the best compound representing a balance of the desired stability, PSA cleavage, antiproliferative activity, and selectivity. However, introduction of four fluorines to the benzene ring simply led to the loss of cytotoxicity towards both PSA expressing LNCaP cells and PSA non-expressing DU145 cells even though the PSA enzyme assay clearly indicated the

cleavage of the peptide conjugate. It suggested that decreasing the electron density of benzene ring too much would adversely affect the drug release rate although the stability was improved. Further studies on modulation of the electron density on benzene ring will be performed to optimize the stability and the rate of 1,6-elimination upon proteolytic cleavage and, therefore, to achieve the needed balance between the stability prior to proteolytic activation and the drug release kinetic profile.

CHAPTER THREE

EXPERIMENTAL SECTION

General methods

Moisture-sensitive reactions were performed in oven-dried glassware under a positive pressure of argon or nitrogen. Air and moisture sensitive materials were transferred via syringe or cannula under argon or nitrogen atmosphere. Solvents were either ACS reagent grade or HPLC grade and used directly without further purification unless otherwise stated: THF and dichloromethane were dried by pressure filtration under nitrogen through activated alumina; *N,N*-dimethylformamide was dried and redistilled over calcium hydride. Reagents purchased were ACS grade or better and used without further purification unless otherwise stated: the concentration of n-BuLi in hexane was measured by using diphenylacetic acid protocol before use. All reactions were magnetically stirred and monitored by thin-layer chromatography (TLC) using Whatman polymer-backed F_{254} silica gel plates and/or Shimadzu 2010 LC-MS system. Flash column chromatography was performed using silica gel (Merck 230-400 mesh) or using a Teledyne ISCO CombiFlash Companion Automated Flash Chromatographic System with prepacked silica gel columns. Solid-phase synthesis of peptides was performed on an Advanced ChemTech automated peptide synthesizer. Lyophilization was performed on a Savant lyophilizer. Yields were based on the chromatographically pure compounds. Melting points were determined on a Mel-Temp capillary apparatus. Infrared spectra were recorded with Thermo-Nicolet Avatar 360 FTR spectrometer and the absorbance is reported in reciprocal centimeters (cm^{-1}). All ^1H and ^{13}C NMR spectra were recorded on a Varian Gemini 200 MHz spectrometer at ambient temperature and calibrated using

residual undeuterated solvents as the internal reference. The following abbreviations were used to indicate the multiplicities: s = singlet; d = doublet; dd = doublets of doublet; dt = doublets of triplet; t = triplet; td = triplets of doublet; q = quartet; m = multiplet; br = broad.

The reactions were monitored using Shimadzu LCMS-2010 system equipped with a Chromolith SpeedROD RP-18e column (50x4.6 mm). Solvent A was 0.1% HCOOH/H_2O and solvent B was 0.1% HCOOH/CH_3CN. The gradient was 10-90% of solvent B over 10 min with a flow rate at 1 mL/min. The kinetic studies were performed on a Waters symmetry C_{18} column (3.5 μm, 4.6 x 150 mm) at 1 mL/min with a gradient of 10-80% of acetonitrile containing 0.1% trifluoroacetic acid over 15 min on a HP1090 system. The peptidylaminoarylmethyl phosphoramide mustards were purified using Gilson automated preparative HPLC system equipped with a Keystone Hypersil-C18 (5.0 μm, 20 x 150 mm) at 12 mL/min with a linear gradient of 30-90% of acetonitrile containing 0.1% trifluoroacetic acid over 10 min.

I. Selenocarboxylate/Azide Amidation

Method A using diacyl selenide: To a solution of dibenzoyl selenide (2.0 mmol) in EtOAc (20 mL) was added a suspension of KOMe (2.0 mmol) in DMSO (20 mL) at 5 °C under nitrogen atmosphere. The resulting mixture was stirred for 10 minutes at 5 °C. Then, the starting azide (1.0 mmol) was added into the above mixture. The reaction was allowed to gradually warm to room temperature. The reaction was poured into ice water

when TLC showed the disappearance or no further decrease of the starting azide. The gray selenium powder was removed by filtration. The filtrate was then extracted with EtOAc. After removal of solvents, the crude product was purified by flash column chromatography (FCC) on silica gel. Structures were confirmed using ^{1}H NMR, ^{13}C NMR and LC-MS.

Method B using dibenzoyl diselenide: To a solution of dibenzoyl diselenide (1.2 mmol), the azide (1.0 mmol), and DIEA (1.2 mmol) in acetonitrile (10 mL) was added piperidine (1.2 mmol) at 25 ^{o}C under nitrogen atmosphere. The resulting mixture was stirred for 2 hours. For electron-rich azides, the reactions were carried out at 55 ^{o}C in the presence of 2.0 equiv of benzeneselenocarboxylate. The reaction was poured into water when TLC showed the disappearance or no further decrease of the starting azide. The gray selenium powder was removed by filtration. The filtrate was then extracted with EtOAc. After removal of solvents, the crude product was purified by flash column chromatography (FCC) on silica gel.

Method C using carboxylic acids. (1) Preparation of LiAlHSeH: LiAlHSeH was prepared essentially following literature procedure and used immediately.[162] Briefly, to a suspension of LiAlH$_4$ (44mg, 1.1 mmol) in anhydrous THF (10 mL) was added selenium powder (88 mg, 1.1 mmol) at one portion at 0 °C. The mixture was stirred at 0 °C for 20 min under nitrogen atmosphere and ready to be used. (2) One-pot amidation procedure: To a solution of carboxylic acid (1.1 mmol) and *N*-methylpiperidine (0.134 mL, 1.1 mmol) in THF (10 mL) was added a 1.0 M solution of isopropylchloroformate in toluene

(1.1 mL, 1.1 mmol) at 0 °C under nitrogen atmosphere. The resulting mixture was stirred for 20 minutes at 0 °C. Then, the obtained mixed anhydride solution was slowly added into the prepared LiAlHSeH solution via cannula over a period of 5 min. The reaction mixture was stirred for additional 30 min below 5 °C under nitrogen atmosphere. Then, a solution of azide (1.0 mmol) in THF (1 mL) was added into the above selenocarboxylate solution via syringe. For electron-deficient azides, the amidation reaction was carried out at 0 °C to room temperature. For electron-rich azides, 0.5 mmol of the azide were used and the reaction was carried out at 55 °C. When TLC and/or LC-MS showed the disappearance of the starting azide or no further change of the reaction mixture, the reaction mixture was filtered through a Celite pad that was rinsed with EtOAc (3x25 mL). The combined organic phase was washed with 5% $NaHCO_3$, water and brine, and dried over anhydrous Na_2SO_4. After removal of Na_2SO_4 through filtration, the filtrate was treated with activated charcoal. The activated charcoal was then filtered off and the filtrate was concentrated to dryness. The crude product was purified by flash column chromatography (FCC) on silica gel. Yields and physical and spectroscopic data of all amides are consistent with their structures.
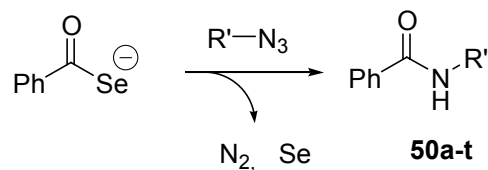
N-(4-Nitrophenyl)benzamide (50a).[193] The product was obtained after FCC (Hexane/EtOAc, 5:1) in 98% isolated yield by method A, 95% yield by method B, and 96% yield by method C. ^{1}H NMR (DMSO-d6, 200 MHz): δ 10.82 (s, -NH), 8.27 (d, 2H, J

= 7.4 Hz), 8.08 (d, 2H, J = 8.4 Hz), 7.99 (d, 2H, J = 8.4 Hz), 7.52-7.65 (m, 3H). [13]C

NMR (DMSO-d$_6$, 50 MHz): δ 167.1, 146.3, 143.3, 135.0, 132.9, 129.3, 128.7, 125.5,

120.6; IR (KBr, cm^{-1}): 3337, 1656, 1507, 1345; MS (ESI$^+$): m/z (intensity), 243.1, (MH$^+$,

100%), 284.1(MH$^+$+CH$_3$CN, 60%).

N-(2-Nitrophenyl)benzamide (50b). The product was obtained after FCC

(Hexane/EtOAc, 4:1) in 95% isolated yield by method A, and 93% by method B. [1]H

NMR (CDCl$_3$, 200 MHz): δ 11.38 (s, -NH), 9.04 (dd, 1H, J=8.4 Hz, J=1.6 Hz), 8.31 (dd,

1H, J=8.4 Hz, J=1.6 Hz), 8.02 (dd, 2H, J=8.0 Hz, J=1.6 Hz), 7.74 (td, 1H, J=8.0 Hz,

J=1.6 Hz), 7.52-7.64 (m, 3H), 7.25 (td, 1H, J=8.0 Hz, J=1.6 Hz). ^{13}C NMR (CDCl$_3$, 50

MHz): δ 165.9, 136.6, 136.3, 135.5, 134.2, 132.8, 129.2, 127.5, 126.0, 123.4, 122.3; IR

(KBr, cm^{-1}): 3363, 1685, 1502, 1342; MS (ESI$^+$): m/z (intensity), 243.1, (MH$^+$, 100%),

284.1(MH$^+$+CH$_3$CN, 60%).

N-(4-Cyanophenyl)benzamide (50c).[194] The product was obtained after FCC

(Hexane/EtOAc, 4:1) in 98% isolated yield by method A, 96% yield by method B, and

94% yield by method C. mp 166 – 168 °C; ^{1}H NMR (CDCl$_3$, 200 MHz): δ 8.13 (s, 1H, -

NH), 7.70-7.92 (m, 4H), 7.48-7.70 (m, 5H); ^{13}C NMR (CDCl$_3$, 50 MHz): δ 165.9, 142.1,

134.2, 133.5, 132.6, 129.1, 127.2, 120.0, 118.9, 107.5; IR (KBr, cm^{-1}): 3352, 2228, 1661;

MS (ESI$^+$): m/z (intensity), 223.1 (MH$^+$, 100%), 257.1 (MH$^+$+CH$_3$CN, 70%).

N-(4-Chlorophenyl)benzamide (50d). The product was obtained after FCC

(Hexane/EtOAc, 7:1) in 96% isolated yield by method A and 95% yield by method B. mp

190 – 191 °C; ^{1}H NMR (CDCl$_3$, 200 MHz): δ 7.89 (dd, 2H, J = 8.2 Hz, J = 1.8 Hz), 7.87 (s, 1H, -NH), 7.51-7.65 (m, 5H), 7.36 (d, 2H, J=8.2 Hz). ^{13}C NMR (CDCl$_3$, 50 MHz): δ 165.7, 136.6, 134.8, 132.1, 129.7, 129.2, 129.0, 127.1, 121.5; IR (KBr, cm^{-1}): 3337, 1638; MS (ESI$^+$): m/z (intensity), 232.1 (MH$^+$, 100%), 273.1 (MH$^+$+CH$_3$CN, 20%).

Methyl 4-Benzamidobenzoate (50e). The product was obtained after FCC (Hexane/EtOAc, 4:1) in 98% isolated yield by method A and 87% yield by method B. mp 162 – 164 °C; ^{1}H NMR (CDCl$_3$, 200 MHz): δ 8.06(d, 2H, J = 7.4 Hz), 7.90 (s, 1H, -NH), 7.89 (dd, 2H, J = 8.4 Hz, J = 1.8 Hz), 7.72 (d, 2H, J = 7.4 Hz), 7.47-7.59 (m, 3H), 3.93 (s, 3H); ^{13}C NMR (CDCl$_3$, 50 MHz): δ 166.7, 165.9, 142.3, 134.7, 132.3, 131.0, 129.0, 127.18, 119.3, 52.1. MS (ESI$^+$): m/z (intensity), 256.0 (MH$^+$, 100%), 297.0 (MH$^+$+CH$_3$CN, 5%).

4-Benzamidobenzoic acid (50f).[195] The product was obtained after FCC (Hexane-Hexane/EtOAc, 1:1) in 87% isolated yield by method A, 89% yield by method B and 91% yield by method C. mp 278 – 280 °C; ^{1}H NMR (DMSO-d$_6$, 200 MHz): δ 10.5 (s, -COOH), 7.95 (brs, 7H), 7.53-7.56 (m, 3H). ^{13}C NMR (DMSO-d$_6$, 50 MHz): δ 167.0, 166.0, 143.3, 134.7, 131.8, 130.2, 128.4, 127.8, 125.5, 119.5; IR (KBr, cm^{-1}): 3317, 1618; MS (ESI$^-$): m/z (intensity), 240.1 (M-H$^-$, 100%), 258.1 (M-H$^-$+H$_2$O, 10%).

N-(4-Acetylphenyl)benzamide (50g). The product was obtained after FCC (Hexane/EtOAc, 2:1) in 88% isolated yield by method A. mp 198-200 °C; ^{1}H NMR (DMSO-d$_6$, 200 MHz): δ 10.58 (s, 1H, -NH), 7.97-8.01 (m, 6H), 7.54-7.66 (m, 3H), 2.56

(s, 3H, -COCH$_3$). ^{13}C NMR (DMSO-d$_6$, 50 MHz): δ 198.0, 166.9, 144.1, 135.1, 132.8, 132.8, 130.1, 129.3, 128.5, 120.3, 27.2; MS (ESI$^+$): *m/z* (intensity), 240.0 (MH$^+$, 100%), 281.0 (MH$^+$+CH$_3$CN, 20%).

Diphenyl *N*-benzoylphosphoramidate (50h). The product was obtained after FCC (Hexane/EtOAc, 2:1) in 88% isolated yield by method B and 95% yield by method C. mp 124-126 $^{\circ}$C; ^{1}H NMR (CDCl$_3$, 200 MHz): δ 9.67 (brs, -NH), 7.98 (d, 2H, *J* = 8.6 Hz), 7.56 (t, 1H, *J* = 7.8 Hz), 7.39 (dd, 2H, *J* = 8.0 Hz, *J* = 7.6 Hz), 7.08-7.7.27 (m, 10H). ^{13}C NMR (CDCl$_3$, 50 MHz): δ 167.7, 150.2 (d, *J* = 6.8 Hz), 133.0, 132.4 (d, *J* = 11 Hz), 129.8, 128.6, 125.7, 120.7, 120.6. MS (ESI$^+$): *m/z* (intensity), 354.1 (M+H$^+$, 90%), 417.2 (M+Na$^+$+CH$_3$CN, 85%).

***N*-(4-Toluenesulfonyl)benzamide (50i).**[196] The product (270 mg) was obtained after FCC (Hexane/CH$_2$Cl$_2$/MeOH, 10:10:1) in 96% isolated yield by method B and 98% yield by method C. mp 115-116 $^{\circ}$C; ^{1}H NMR (CDCl$_3$, 200 MHz): δ 9.52 (brs, -NH), 8.05 (d, 2H, *J* = 8.4 Hz), 7.83 (d, 2H, *J* = 7.4 Hz), 7.32-7.58 (m, 5H), 2.43 (s, 3H). ^{13}C NMR (CDCl$_3$, 50 MHz): δ 164.4, 145.2, 135.4, 133.4, 131.1, 129.68, 128.8, 128.7, 127.9, 21.7. MS (ESI$^-$): *m/z* (intensity), 274.1 (M-H$^+$, 100%).

***N*-Benzoylbenzamide (50j).**[197] The product was obtained after FCC (Hexane/EtOAc, 1:1) in 51% isolated yield by method B and 81% yield by method C, respectively. mp 144-146 $^{\circ}$C; ^{1}H NMR (CDCl$_3$, 200 MHz): δ 9.26 (brs, -NH), δ 7.84 (dd, 4H, *J* = 8.0 Hz, *J* = 1.4 Hz), δ 7.40-7.60 (m, 6H). ^{13}C NMR (CDCl$_3$, 50 MHz): δ 166.7, 133.3, 133.0,

128.7, 127.9. MS (ESI$^+$): *m/z* (intensity), 226.1 (M+H$^+$, 100%), 289.1 (M+Na$^+$+CH$_3$CN, 85%).

N-(2,3,4,6-Tetra-*O*-acetyl-β-D-galactopyranosyl)benzamide (50k). The product was obtained after FCC (Hexane/EtOAc, 4:1) in 71% isolated yield by method C. mp 132-135 ^{o}C; ^{1}H NMR (CDCl$_3$, 200 MHz): δ 7.77(d, 2H, *J* = 6.6 Hz), 7.40-7.54 (m, 3H), 5.44-5.49 (m, 2H), 5.22-5.26 (m, 2H), 4.09-4.17 (m, 3H), 2.15 (s, 3H), 2.04 (s, 3H), 2.01 (s, 6H). ^{13}C NMR (CDCl$_3$, 50 MHz): δ 171.8, 170.5, 170.1, 169.9, 167.2, 133.0, 132.4, 128.8, 127.3, 79.3, 72.4, 70.9, 68.7, 67.4, 61.2, 20.9, 20.8, 20.7, 20.6. MS (ESI$^+$): *m/z* (intensity), 452.2 (M+H$^+$, 45%), 474.2 (M+Na$^+$, 100%), 515.2 (M+Na$^+$+CH$_3$CN, 25%).

N-Phenylbenzamide (50l). The product was obtained after FCC (Hexane/EtOAc, 9:1) in 25% isolated yield by method A and 40% yield by method B, respectively. mp 161-163 ^{o}C; ^{1}H NMR (CDCl$_3$, 200 MHz): δ 7.87-7.90 (m, 3H), 7.67 (d, 2H, J=8.8 Hz), 7.48-7.58 (m, 3H), 7.40 (t, 2H, J=8.4 Hz), 7.18 (t, 1H, J=7.4 Hz). ^{13}C NMR (CDCl$_3$, 50 MHz): δ 165.7, 138.2, 135.0, 131.8, 129.1, 128.6, 127.0, 124.7, 120.1. MS (ESI$^+$): *m/z* (intensity), 198.0 (MH$^+$, 100%), 239.1 (MH$^+$+CH$_3$CN, 30%).

N-(4-Methylphenyl)benzamide (50m). The product was obtained after FCC (Hexane/EtOAc, 9:1) in 7% isolated yield by method A. mp 153-155 ^{o}C; ^{1}H NMR (DMSO-d$_6$, 200 MHz): δ 10.17 (s, 1H, -NH), 7.96 (d, 2H, J=8.2 Hz), 7.66 (d, 2H, J=8.2 Hz), 7.56 (m, 3H), 7.14 (d, 2H, J=8.2 Hz), 2.32 (s, 3H, -CH$_3$). ^{13}C NMR (DMSO-d$_6$, 50

MHz): δ 165.6, 136.7, 135.1, 132.7, 131.1, 129.0, 128.2, 127.4, 120.5, 20.5. MS (ESI[+]):

m/z (intensity), 212.1 (MH[+], 100%), 253.1 (MH[+]+CH$_3$CN, 5%).

N-(4-Aminophenyl)benzamide (50n).[198] The product was obtained after FCC
(Hexane/EtOAc, 2:1) in 54% isolated yield by method B and 54% yield by method C. [1]H

NMR (CD$_3$OD, 200 MHz): δ 7.89 (dd, 2H, J = 8.0 Hz, J = 1.8 Hz), 7.42-7.52 (m, 3H),

7.37 (dd, 2H, J = 7.0 Hz, J = 2.0 Hz), 6.73 (dd, 2H, J = 8.0 Hz, J = 1.8 Hz). ^{13}C NMR

(CD$_3$OD, 50 MHz): δ 168.6, 145.9,136.3, 132.6, 130.4, 129.5, 128.4, 124.2, 116.6. MS

(ESI[+]): *m/z* (intensity), 213.1 (MH[+], 80%), 254.1 (MH[+]+CH$_3$CN, 100%).

N-(4-Methoxyphenyl)benzamide (50o).[199] The product was obtained after FCC
(Hexane/EtOAc, 4:1) in 7% isolated yield by method A, 65% yield by method B, and

63% yield by method C. mp 162-164 °C; ^{1}H NMR (acetone-d$_6$, 200 MHz): δ 9.40 (brs,

NH), 7.97 (dd, 2H, J = 7.8 Hz, J = 1.4 Hz), 7.72 (d, 2H, J = 8.6 Hz), 7.42-7.59 (m, 3H),

6.91 (dd, 2H, J = 6.8 Hz, J = 2.4 Hz), 3.78 (s, 3H, -OCH$_3$). ^{13}C NMR (acetone-d$_6$, 50

MHz): δ 165.7, 156.9, 136.3, 133.3, 131.9, 129.0, 125.0, 122.4, 114.4, 55.5. MS (ESI[+]):

m/z (intensity), 228.1 (MH[+], 100%), 269.1 (MH[+]+CH$_3$CN, 5%).

N-(4-Hydroxymethylphenyl)benzamide (50p). The product was obtained after FCC
(Hexane/EtOAc, 2:1) in 44% isolated yield by method A, 56% yield by method B, and

70% yield by method C. mp 149-151 °C; ^{1}H NMR (CD$_3$OD, 200 MHz): δ 7.94 (dd, 2H, J

= 8.4 Hz, J = 2.0 Hz), 7.67 (dd, 2H, J = 7.8 Hz, J = 1.8 Hz), 7.47-7.60 (m, 3H), 7.37 (d,

2H, J = 8.4 Hz), 4.61 (s, 2H, -CH$_2$OH). ^{13}C NMR (CD$_3$OD, 50 MHz): δ 168.9, 139.0,

136.3, 132.9, 129.6, 128.6, 128.5, 122.2, 64.9; MS (ESI$^+$): m/z (intensity), 228.1 (MH$^+$, 100%), 269.1 (MH$^+$+CH$_3$CN, 10%).

N-(4-acetyloxymethylphenyl)benzamide (50q). The product was obtained after FCC (Hexane/EtOAc, 2:1) in 77% isolated yield by method A, 68% yield by method B, and 70% yield by method C. mp 125-127 ^{o}C; ^{1}H NMR (CDCl$_3$, 200 MHz): δ 8.27 (brs, 1H, -NH), δ 7.86 (d, 2H, J =8.0 Hz), 7.67 (d, 2H, J = 8.4 Hz), 7.39-7.54 (m, 3H), 7.34 (d, 2H, J = 8.4 Hz), 5.08(s, 2H), 2.10 (s, 3H). ^{13}C NMR (CDCl$_3$, 50 MHz): δ 171.1, 166.1, 138.2, 134.9, 132.1, 131.9, 129.3, 128.8, 127.2, 120.5, 66.0, 21.1; MS (ESI$^+$): m/z (intensity), 270.1 (MH$^+$, 100%), 311.1 (MH$^+$+CH$_3$CN, 30%).

N-(3-Fluoro-4-hydroxymethylphenyl)benzamide (50r). The product was obtained after FCC (Hexane/EtOAc, 2:1) in 78% isolated yield (190 mg) by method B. mp 120 − 121 ^{o}C; ^{1}H NMR (CD$_3$OD, 200 MHz): δ 8.13 (dd, 2H, J = 8.0 Hz, J = 1.6 Hz), 7.87 (dd, 1H, J = 12.2 Hz, J = 1.8 Hz), 7.62-7.80 (m, 5H), 4.85 (s, 2H); ^{13}C NMR (CD$_3$OD, 50 MHz): δ 168.9, 161.8 (d, J = 242Hz), 136.1, 133.0, 132.4, 130.8, 129.9, 128.6, 125.4, 117.3 (d, J = 3.0 Hz), 108.8 (d, J = 27.0 Hz), 58.6 (d, J = 4.0 Hz); MS (ESI$^+$): m/z (intensity), 246.1 ([M+H]$^+$, 100%), 287.0 ([M+H]$^+$+CH$_3$CN, 40%).

**N-(2-Fluoro-4-hydroxymethylphenyl)benzamide (50s).** The product was obtained after FCC (Hexane/EtOAc, 2:1) in 44% isolated yield by method A, 56% yield by method B, and 70% yield by method C. mp 108-110 ^{o}C; ^{1}H NMR (CDCl$_3$, 200 MHz): δ 8.42 (t, 1H, J = 8.4 Hz), 8.04 (brs, -NH), 7.87 (dd, 2H, J = 8.4 Hz, J = 1.8 Hz), 7.44-7.56 (m, 3H),

7.13-7.20 (m, 2H), 4.66 (s, 2H). ^{13}C NMR (CDCl$_3$, 50 MHz): δ 165.4, 152.8 (d, J = 242.0

Hz), 137.8, 134.6, 132.2, 128.9, 127.1, 123.0, 122.9, 121.8, 113.4 (d, J = 20.0 Hz), 64.4;

MS (ESI$^+$): m/z (intensity), 246.1 ([M+H]$^+$, 100%), 287.0 ([M+H]$^+$+CH$_3$CN, 40%).

N-{6-[(tert-Butyldiphenylsilyl)oxy]hexyl}benzamide (50t). The product (286 mg) was

obtained after FCC (Hexane/EtOAc, 4:1) in 62% isolated yield. ^{1}H NMR (CDCl$_3$, 200

MHz): δ 7.75(dd, 2H, J =7.2 Hz, J =1.4 Hz), δ 7.61-7.71 (m, 3H), 7.24-7.50 (m, 10H),

6.2 (brs, -NH), 3.65 (t, 2H, J = 6.4 Hz), 3.41(dd, 2H, J =7.0 Hz, J =7.2 Hz), 1.51-1.61 (m,

4H), 1.35-1.47 (m, 4H), 1.04 (s, 9H),. ^{13}C NMR (CDCl$_3$, 50 MHz): δ 167.5, 135.2, 134.8,

134.0, 131.3, 129.5, 128.5, 127.5, 126.8, 63.7, 40.0, 32.4, 29.6, 26.8, 26.7, 25.5, 19.2. MS

(ESI$^+$): m/z (intensity), 482.3 (M+Na$^+$, 100%), 523.3 (M+Na$^+$+CH$_3$CN, 10%).
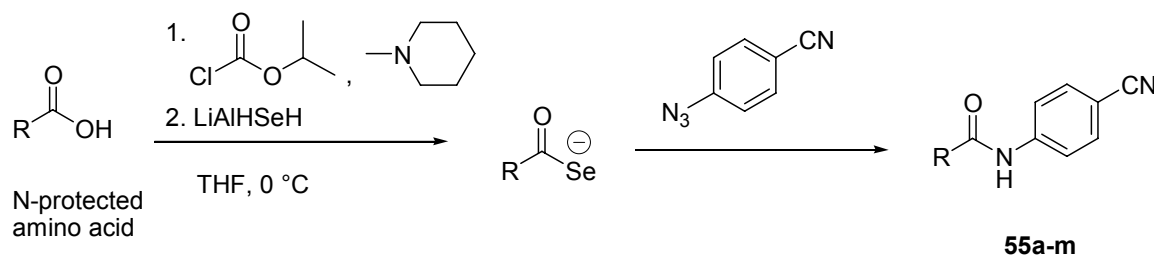
N$^\alpha$-Benzyloxycarbonyl-N´-(4-cyanophenyl)-L-phenylalaninamide (55a). The product

(340 mg) was obtained after FCC (CH$_2$Cl$_2$/MeOH, 10:1) in 85% isolated yield. ^{1}H NMR

(CDCl$_3$, 200 MHz): δ 8.80 (brs, 1H, -NH), 7.16-7.48 (m, 14H), 5.82 (d, -NH, J = 8.0

Hz), 5.07 (s, 2H), 4.66 (q, 1H, J = 8.0 Hz), 3.13 (dd, 2H, J = 6.6 Hz, J = 7.4 Hz). ^{13}C

NMR (CDCl$_3$, 50 MHz): δ 170.2, 156.7, 141.5, 136.0, 135.8, 133.2, 129.3, 129.0, 128.7,

128.5, 128.1, 127.9, 127.4, 119.8, 107.3, 67.6, 57.4, 38.4. MS (ESI$^+$): *m/z* (intensity), 400.2 (MH$^+$, 100%), 441.2 (MH$^+$+CH$_3$CN, 15%).

O^3-Benzyl-N^α-benzyloxycarbonyl-N'-(4-cyanophenyl)-L-serinamide (55b). The product (384 mg) was obtained after FCC (CH$_2$Cl$_2$/MeOH, 50:1) in 89% isolated yield. ^{1}H NMR (CDCl$_3$, 200 MHz): δ 8.85 (brs, 1H, -NH), 7.45-7.55 (m, 4H), 7.23-7.32 (m, 10H), 5.92 (d, 1H, *J* = 6.8 Hz), 5.11 (s, 2H), 4.47-4.60 (m, 3H), 3.92-3.97 (m, 1H), 3.62-3.70 (m, 1H). ^{13}C NMR (CDCl$_3$, 50 MHz): δ 16.8.7, 156.3, 141.4, 136.9, 135.7, 133.0, 128.5, 128.4, 128.2, 128.1, 127.9, 127.7, 119.6, 118.7, 107.1, 73.5, 69.3, 67.3, 55.0. MS (ESI$^+$): *m/z* (intensity), 430.2 (MH$^+$, 100%), 452.2 (M+Na$^+$, 20%).

N^α-Benzyloxycarbonyl-N'-(4-cyanophenyl)-L-glutaminamide (55c). The product (342 mg) was obtained after FCC (CH$_2$Cl$_2$/MeOH, 20:1) in 90% isolated yield. ^{1}H NMR (DMSO-d$_6$, 200 MHz): δ 10.55 (s, 1H), 7.70-7.85 (m, 4H), 7.36 (brs, 5H), 6.85 (s, 1H), 5.04 (s, 2H), 4.11-4.20 (m, 1H), 2.15-2.21 (m, 2H), 1.70-1.99 (m, 2H). ^{13}C NMR (DMSO-d$_6$, 50 MHz): δ 174.2, 172.4, 156.8, 143.9, 137.7, 134.0, 129.1, 128.9, 128.5, 120.1, 119.8, 105.9, 66.3, 56.1, 32.1, 28.0. MS (ESI$^+$): *m/z* (intensity), 381.2 (MH$^+$, 100%), 444.4 (M+Na$^+$+CH$_3$CN, 15%).

N^α-Benzyloxycarbonyl-N'-(4-cyanophenyl)-L-methioninamide (55d). The product (337 mg) was obtained after FCC (CH$_2$Cl$_2$/MeOH, 40:1) in 88% isolated yield. ^{1}H NMR (CDCl$_3$, 200 MHz): δ 9.02 (brs, 1H, -NH), 7.48-7.61 (m, 4H), 7.35 (brs, 5H), 5.78 (d, *J* = 8.0 Hz), 5.14 (s, 2H), 4.51-4.62 (m, 1H), 2.62 (t, 2H, *J* = 6.6 Hz), 1.98-2.26 (m, 5H). ^{13}C

NMR (CDCl$_3$, 50 MHz): δ 170.3, 156.9, 141.7, 135.8, 133.3, 128.8, 128.6, 128.1, 119.8, 118.8, 107.4, 67.7, 54.9, 30.9, 30.3, 15.4. MS (ESI$^+$): *m/z* (intensity), 384.1 (MH$^+$, 100%).

O^5-Benzyl-N^α-benzyloxycarbonyl-N'-(4-cyanophenyl)-*L*-glutamic amide (55e). The product (394 mg) was obtained after FCC (CH$_2$Cl$_2$/MeOH, 50:1) in 90% isolated yield. ^{1}H NMR (CDCl$_3$, 200 MHz): δ 9.30 (brs, 1H, -NH), 7.51-7.64 (m, 4H), 7.36 (brs, 5H), 5.61 (d, -NH, *J* = 6.6 Hz), 5.13 (s, 2H), 4.37-4.40 (m, 1H), 2.45-2.65 (m, 2H), 1.98-2.29 (m, 2H), 1.49 (s, 9H). ^{13}C NMR (CDCl$_3$, 50 MHz): δ 173.3, 170.7, 156.5, 142.0, 135.6, 133.2, 128.7, 128.5, 128.3, 119.7, 118.9, 107.2, 81.0, 66.9, 54.7, 30.7, 28.4, 27.5. MS (ESI$^+$): *m/z* (intensity), 438.2 (MH$^+$, 100%).

N^α-*t*-Butyloxycarbonyl-N'-(4-cyanophenyl)-*L*-prolinamide (55f). The product (285 mg) was obtained after FCC (CH$_2$Cl$_2$/MeOH, 50:1) in 89% isolated yield. ^{1}H NMR (CDCl$_3$, 200 MHz): δ 10.05 (brs, 1H, -NH), 7.38-7.52 (m, 4H), 4.50 (brs, -NH), 3.41-3.53 (m, 2H), 1.91-2.28 (m, 4H), 1.49 (s, 9H). ^{13}C NMR (CDCl$_3$, 50 MHz): δ 171.2, 156.3, 142.6, 133.0, 119.4, 119.0, 106.3, 81.2, 60.7, 47.4, 28.5, 28.3, 24.6. MS (ESI$^+$): *m/z* (intensity), 316.2 (MH$^+$, 40%), 334.2 (MH$^+$+H$_2$O, 100%).

N^α-*t*-Butyloxycarbonyl-N'-(4-cyanophenyl)-*L*-valinamide (55g). The product (282 mg) was obtained after FCC (CH$_2$Cl$_2$/MeOH, 50:1) in 89% isolated yield. ^{1}H NMR (CDCl$_3$, 200 MHz): δ 9.35 (brs, 1H, -NH), 7.39-7.52 (m, 4H), 5.40 (d, -NH), 4.09-4.16 (m, 1H), 2.06-2.16 (m, 1H), 1.43 (s, 9H), 1.01 (d, 6H, *J* = 7.0 Hz). ^{13}C NMR (CDCl$_3$, 50 MHz): δ

171.5, 156.8, 142.0, 133.0, 119.5, 118.9, 106.9, 80.9, 61.2, 30.8, 28.4, 19.6, 18.5. MS (ESI$^+$): m/z (intensity), 318.2 (MH$^+$, 100%).

N^α-(9-Fluorenyloxycarbonyl)-N'-(4-cyanophenyl)-L-glutaminamide (55h). The product (328 mg) was obtained after FCC (CH$_2$Cl$_2$/MeOH, 20:1) in 70% isolated yield. ^{1}H NMR (DMSO-d$_6$, 200 MHz): δ 10.54 (s, 1H, -NH), 7.72-7.91 (m, 8H), 7.30-7.46 (m, 4H), 6.83 (s, 1H, -NH), 4.09-4.32 (m, 4H), 2.17-2.21 (m, 2H), 1.83-1.99 (m, 2H). ^{13}C NMR (DMSO-d$_6$, 50 MHz): δ 173.4, 171.7, 156.1, 143.8, 143.1, 140.7, 133.3, 127.7, 127.1, 125.3, 120.1, 119.3, 119.1, 105.1, 65.8, 55.4, 46.6, 31.5, 27.3. MS (ESI$^+$): m/z (intensity), 469.2 (MH$^+$, 100%), 491.2 (M+Na$^+$, 50%).

N^α-(9-Fluorenyloxycarbonyl)-N'-(4-cyanophenyl)-L-tryptophanamide (55i). The product (458 mg) was obtained after FCC (Hexane/CH$_2$Cl$_2$/MeOH, 10:10:1) in 87% isolated yield. ^{1}H NMR (CDCl$_3$, 200 MHz): δ 8.38 (brs, 1H, -NH), 8.10 (s, 1H, NH), 7.78 (d, 2H, J =7.4 Hz), 7.28-7.61 (m, 11H), 7.17 (t, 2H, J = 8.0 Hz), 7.05 (t, 2H, J = 8.0 Hz), 6.95 (brs, 1H, NH), 4.68 (m, 1H), 4.34 (d, 2H, J = 6.8 Hz), 4.17 (t, 1H, J = 7.4 Hz), 3.26-3.31 (m, 2H). ^{13}C NMR (CDCl$_3$, 50 MHz): δ 170.4, 156.5, 143.5, 143.4, 141.3, 136.1, 133.0, 127.8, 127.1, 127.0, 124.9, 123.2, 122.5, 120.1, 120.0, 119.7, 118.7, 118.4, 111.4, 109.9, 107.1, 67.4, 56.4, 46.9, 28.2. MS (ESI$^+$): m/z (intensity), 527.2 (MH$^+$, 100%), 549.2 (M+Na$^+$, 20%).

N^α-t-Butyloxycarbonyl-L-leucyl-N'-(4-cyanophenyl)-L-tryptophanamide (55j). The product (450 mg) was obtained after FCC (CH$_2$Cl$_2$/MeOH, 20:1) in 87% isolated yield.

^{1}H NMR (CD$_3$OD, 200 MHz): δ 7.59(d, 2H, J =8.4 Hz), δ 7.43-7.50 (m, 3H), 7.21 (d, 1H, J = 8.0 Hz), 7.01 (s, 1H), 6.85-6.97 (m, 2H), 4.67 (m, 1H), 3.95 (t, 1H), 3.22-3.25 (m, 2H), 1.40-1.60 (m, 1H), 1.35 (t, 2H, J = 6.6 Hz), 1.25 (s, 9H), 0.80 (dd, 6H, J = 8.2 Hz). ^{13}C NMR (CD$_3$OD, 50 MHz): δ 175.7, 172.7, 158.2, 143.8, 138.0, 134.0, 128.7, 124.7, 122.5, 121.2, 119.9, 119.8, 119.3, 112.3, 110.2, 107.8, 80.9, 56.1, 55.1, 41.6, 28.6, 25.8, 23.3, 21.8. MS (ESI$^+$): m/z (intensity), 540.3(M+Na$^+$, 100%), 581.3 (M+Na$^+$+CH$_3$CN, 37%).

O^3-Acetyl-N^α-t-butyloxycarbonyl-D,L-seryl-$N´$-(4-cyanophenyl)-L-phenylalaninamide (55k). The product (454 mg) was obtained after FCC (CH$_2$Cl$_2$/MeOH, 20:1) in 92% isolated yield. ^{1}H NMR (CD$_3$OD, 200 MHz): δ 7.68 (d, 2H, J = 8.4 Hz), 7.55 (d, 2H, J = 8.4 Hz), 7.14 (brs, 5H), 4.67 (dd, 1H, J = 8.4 Hz, J = 8.4 Hz), 4.14-4.20 (m, 1H), 4.00-4.09 (m, 2H), 2.88-3.18 (m, 2H), 1.89 (s, 3H),), 1.36 (s, 9H). ^{13}C NMR (CD$_3$OD, 50 MHz): δ 172.2, 171.8, 157.6, 143.7, 137.9, 137.7, 134.1, 130.3, 129.5, 127.9, 121.2, 119.7, 107.8, 81.0, 64.7, 56.5, 55.1, 38.9, 28.6, 20.7. MS (ESI$^+$): m/z (intensity), 517.3 (M+Na$^+$, 100%), 558.2 (M+Na$^+$+CH$_3$CN, 40%).

N^α-t-Butyloxycarbonyl-L-asparaginyl-L-leucyl-$N´$-(4-cyanophenyl)-L-tryptophanamide (55l). The product (523 mg) was obtained after FCC (CH$_2$Cl$_2$/MeOH, 20:1) in 83% isolated yield. ^{1}H NMR (CD$_3$OD, 200 MHz): δ 7.78 (d, 2H, J =8.8 Hz), 7.52 (d, 3H, J =8.8 Hz), 7.34 (d, 1H, J = 8.8 Hz), 7.05 (s, 1H), 6.85-7.00 (m, 2H), 4.59-4.68(m, 1H), 4.30-4.37 (m, 1H), 4.05 (t, 1H, J = 7.2 Hz), 3.19-3.4 (m, 2H), 2.48-3.13(m, 2H), 1.47-1.60 (m, 3H), 1.33(s, 9H), 0.70 (dd, 6H, J = 8.8 Hz). ^{13}C NMR (CD$_3$OD, 50

MHz): δ 175.0, 174.9, 172.9, 157.5, 144.0, 138.0, 134.0, 128.7, 124.6, 122.4, 121.3, 119.8, 119.3, 112.3, 111.3, 107.8, 80.9, 56.8, 54.5, 52.3, 40.8, 37.8, 28.6, 28.2, 25.6, 23.9, 21.6. MS (ESI$^+$): m/z (intensity), 632.3 (MH$^+$, 10%), 654.3 (M+Na$^+$, 100%).

Stability Studies. Aliquots of freshly prepared benzeneselenocarboxylate in solvents were incubated at room temperature and at 55 °C under nitrogen atmosphere. The amount of benzeneselenocarboxylate was measured at different time intervals by reaction with 2 equiv of p-tosyl azide for 1 h. The reaction mixtures were separated on a Shimadzu 2010 LCMS system using a Chromolith SpeedROD RP-18e column (50×4.6mm) at 1 mL/min with a 10-min gradient of 10-90% acetonitrile containing 0.1% formic acid. The N-p-tosyl-benzamide was quantitated based on UV absorption at 220 nm, and its structure was confirmed by the mass spectrometer. The relative peak area of N-p-tosyl-benzamide represents the amount of benzeneselenocarboxylate remained in the solution at a given time point and was plotted against the time of incubation prior to the addition of p-tosyl azide. The data was fitted using the single, two-parameter exponential decay equation in Sigma Plot to obtain the first-order rate constant and calculate the $t_{1/2}$ value.

Determination of racemic amino acids

Hydrolysis of amides. 10 μL of the solutions of amide 10 (0.03 M), *N*-Cbz-*N′*-benzyl-L-phenylalaninamide (0.03 M), and *N*-Cbz-phenylalanine (0.03 M) were added into each 6 x 50 mm corning tube respectively. The samples were then dried using a Savant SpeedVac system at room temperature. The corning tubes containing samples were placed into a Waters hydrolysis vessel and 200 μL of 6N HCl (sequencing grade) was added. The vessel was evacuated and backfilled with nitrogen. After 3 cycles, the vessel was evacuated and sealed, and then baked at $110\pm2\ ^{\circ}\text{C}$ in a convection oven for 24 hours. The corning tubes were taken out from the vessel. Solvent was removed via a Savant SpeedVac system for 30 min and were ready for derivatization.

Derivatization of amino acids. The OPA/NBC reagent solutions were freshly prepared by dissolving 11 mg of *o*-phthaldialdehyde (OPA) and 20 mg of *N*-Boc-L-cysteine (NBC) in 1 mL of methanol, respectively. 50 μL of 0.1 M $Na_2B_4O_7$ (PH 9.6), 50 μL of milipore water, 20 μL of OPA solution and 20 μL of NBC solution were added into the above corning tubes containing hydrolyzed samples, respectively. The resulting solution was vortexed for 5 min and stored at $-20\ ^{\circ}\text{C}$ until HPLC analysis.

HPLC analysis. 20 μL of the derivatized sample solution was injected into an HP 1090 HPLC system. A Waters Symmetry C_{18} column (3.5 μm, 150 × 4.6mm) was used for separation. Aqueous acetonitrile containing 0.1% trifluoroacetic acid was used as mobile phase. With the flow rate at 1 mL/min, the gradient profile was followed as below: 50%

B for 5 min, 50-100% B in 25min, where A is water containing 0.1% trifluoroacetic acid and B is 80% aqueous acetonitrile containing 0.1% trifluoroacetic acid. A UV detector was set at 340 nm. The racemization of enantiomeric amino acid was evaluated by comparing the peak area ratio between L- and D- derivatives. It was observed that the amide 10 contains 1.7% D-isomer and N-CBZ-N´-benzyl-L-phenylalaninamide contain s 1.5% D-isomer.

Synthesis of amino acid-pNAs and amino acid-AMCs through Selenocarboxylate/azide amidation using sodium hydrogen selenide as a selenating agent.

$$4\,NaBH_4 \; + \; 2\,Se \; + \; 7\,H_2O \longrightarrow 2\,NaHSe \; + \; Na_2B_4O_7 \; + \; 14\,H_2$$

Preparation of an isopropanol solution of sodium hydrogenselenide (NaHSe). NaHSe was prepared essentially following literature procedure.[162] Briefly, to a suspension of selenium (40mg, 0.5 mmol) in deaerated isopropanol (5 mL) was added sodium borohydride (24 mg, 0.6 mmol) at one portion at room temperature. The mixture was stirred under nitrogen atmosphere to provide a colorless isopropanol solution of NaHSe, which was ready to be used.

$$NaBH_4 \; + \; Se \; + \; 3\,i\text{-PrOH} \longrightarrow NaHSe \; + \; B(O\text{-}i\text{-Pr})_3 + \; 3\,H_2$$
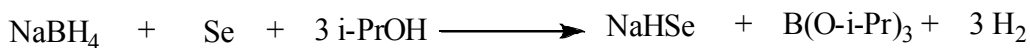
Preparation of an aqueous solution of sodium hydrogenselenide (NaHSe). NaHSe was prepared essentially following literature procedure.[162] Briefly, to a suspension of selenium (40mg, 0.5 mmol) in deaerated distilled water (5 mL) was added sodium borohydride (40 mg, 1.0 mmol) at one portion at 5 $^{\circ}$C. The mixture was vigorously stirred under nitrogen atmosphere to provide a colorless aqueous solution of NaHSe, which was ready to be used.

Method D starting from amino acid-OSu esters. In an ice-bath, to a freshly prepared isopropanolic or aqueous solution of NaHSe (0.5 mmol) was added a solution of N-protected amino acid-OSu (0.5 mmol) in THF via syringe. The resulting mixture was stirred at 0-5 $^{\circ}$C for 1h under nitrogen atmosphere to afford the corresponding N-protected amino selenocarboxylate solution. Then, a solution of the azide (0.42 mmol) in CH_2Cl_2 was added to the above amino selenocarboxylate via syringe. The reaction was then carried out at room temperature under nitrogen atmosphere for 2 h. The organic solvents were removed under reduced pressure, and the remaining was suspended in a saturated $NaHCO_3$ aqueous solution followed by extraction with CH_2Cl_2. The combined organic phase was washed with water and brine, and dried over anhydrous Na_2SO_4. After removal of Na_2SO_4 through filtration, the filtrate was treated with activated charcoal. The activated charcoal was then filtered off and the filtrate was concentrated to dryness. The crude product was purified by flash column chromatography (FCC) on silica gel. Yields and physical and spectroscopic data of all amides were consistent with their structures.

Method E starting from amino acids. To a solution of *N*-protected amino acid (0.5 mmol) and *N*-methylpiperidine (61 µL, 0.5 mmol) in THF (5 mL) was added a 1.0 M solution of isopropylchloroformate in toluene (0.5 mL, 0.5 mmol) at −15°C under nitrogen atmosphere. The resulting mixture was stirred for 20 minutes at −15 $^{\circ}$C - 0 °C. Then, the obtained mixed anhydride solution was added into the freshly prepared NaHSe (0.5 mmol) solution via cannula over a period of 5 min. The reaction mixture was stirred for additional 30 min below 5 °C under nitrogen atmosphere. Then, a solution of azide (0.42 mmol) in CH_2Cl_2 was added into the above selenocarboxylate solution via syringe. The reaction was then carried out at room temperature under nitrogen atmosphere for 2 h. The organic solvents were removed via reduced pressure, and the remaining was suspended in a saturated $NaHCO_3$ aqueous solution followed by extraction with CH_2Cl_2. The combined organic phase was washed water and brine, and dried over anhydrous Na_2SO_4. After removal of Na_2SO_4 through filtration, the filtrate was treated with activated charcoal. The activated charcoal was then filtered off and the filtrate was concentrated to dryness. The crude product was purified by flash column chromatography (FCC) on silica gel. Yields and physical and spectroscopic data of all amides were consistent with their structures.

Synthesis of amino acid-pNAs (56a-h) using method D
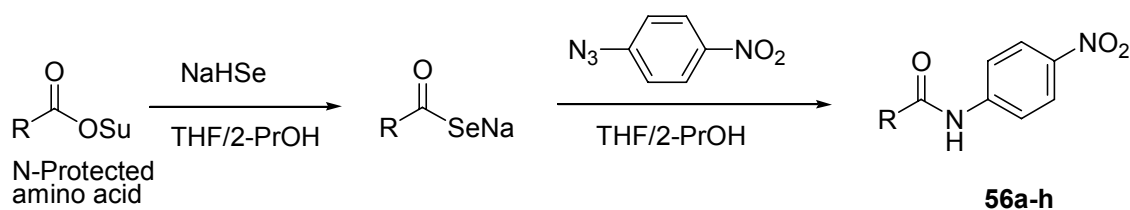
N^{α}-Benzyloxycarbonyl-L-glycyl-p-nitroanilide (56a). The product (135 mg) was obtained after FCC [CH_2Cl_2 - CH_2Cl_2/EtOAc (50:50)] in 98% isolated yield. ^{1}H NMR (DMSO-d_6, 200 MHz): δ 10.57 (brs, -NH), 8.22 (d, 2H, J = 9.2 Hz), 7.83 (d, 2H, J = 9.2 Hz), 7.61 (t, -NH, J = 5.8 Hz), 7.36 (brs, 5H), 5.05 (s, 2H), 3.87 (d, 2H, J = 5.8 Hz); ^{13}C NMR (DMSO-d_6, 50 MHz): δ 169.0, 156.6, 145.0, 142.3, 137.0, 128.3, 127.8, 127.7, 125.0, 118.8, 65.6, 44.3; MS (ESI$^-$): m/z (intensity), 328.0 ([M-H]$^-$, 70%), 442.0 ([M-H]$^-$ + TFA, 100%).

N^{α}-Benzyloxycarbonyl-L-tyrosyl-p-nitroanilide (56b). The product (164 mg) was obtained after FCC [CH_2Cl_2 - CH_2Cl_2/EtOAc (50:50)] in 90% isolated yield. ^{1}H NMR (DMSO-d_6, 200 MHz): δ 10.69 (s, 1H, -NH), 9.20 (s, 1H, -OH), 8.22 (d, 2H, J = 9.2 Hz), 7.84 (d, 2H, J = 9.2 Hz), 7.30 (brs, 5H), 7.11 (d, 2H, J = 8.0 Hz), 6.65 (d, 2H, J = 8.2 Hz), 4.98 (s, 2H), 4.32-4.39 (m, 1H), 2.69-2.97 (m, 2H). ^{13}C NMR (DMSO-d_6, 50 MHz): δ 171.8, 155.9, 155.8, 145.0, 142.4, 136.9, 130.1, 128.3, 127.7, 127.5, 127.4, 124.9, 119.0, 114.9, 65.4, 57.5, 36.5; MS (ESI$^-$): m/z (intensity), 434.2 ([M-H]$^-$, 20%), 548.2 ([M-H]$^-$ + TFA, 100%).

N^{α}-(9-Fluorenyloxycarbonyl)-L-threonyl-p-nitroanilide (56c). The product (176 mg) was obtained after FCC (CH_2Cl_2/MeOH, 20:1) in 91% isolated yield. ^{1}H NMR (DMSO-d_6, 200 MHz): δ 10.54 (s, -NH), 8.23 (d, 2H, J = 9.2 Hz), 7.83-7.87 (m, 4H), 7.75 (d, 2H, J = 7.2 Hz), 7.23-7.41 (m, 5H), 4.95 (d, 1H, J = 5.8 Hz), 4.05-4.35 (m, 5H), 1.12 (d, 3H, J = 6.2 Hz), 1.03 (d, -OH, J = 6.2 Hz); ^{13}C NMR (DMSO-d_6, 50 MHz): δ 170.3, 156.2,

144.9, 143.8, 142.3, 140.7, 127.6, 127.0, 125.2, 124.9, 120.0, 119.0, 66.6, 65.8, 61.6, 46.7, 20.1; MS (ESI⁻): *m/z* (intensity), 460.2 ([M-H]⁻, 20%), 574.3 ([M-H]⁻ + TFA, 100%).

N^α-(9-Fluorenyloxycarbonyl)-*L*-isoleucyl-*p*-nitroanilide (56d). The product (179 mg) was obtained after FCC (CH$_2$Cl$_2$/MeOH, 40:1) in 90% isolated yield. ^{1}H NMR (DMSO-d$_6$, 200 MHz): δ 10.71 (s, -NH), 8.22 (d, 2H, *J* = 8.8 Hz), 7.85-7.90 (m, 4H), 7.71-7.78 (m, 3H), 7.26-7.43 (m, 4H), 4.23-4.31 (m, 3H), 4.07 (t, 1H, *J* = 8.4 Hz), 1.80-1.88 (m, 1H), 1.40-1.56 (m, 1H), 1.16-1.26 (m, 1H), 0.81-0.89 (m, 6H); ^{13}C NMR (DMSO-d$_6$, 50 MHz): δ 171.8, 156.2, 144.8, 143.8, 142.3, 140.7, 127.6, 126.9, 125.2, 124.9, 120.0, 119.0, 65.7, 60.0, 46.7, 36.0, 24.5, 15.2, 10.6; MS (ESI⁻): *m/z* (intensity), 508.3 ([M-H]⁻ + 2 H$_2$O, 20%), 586.3 ([M-H]⁻ + TFA, 100%).

N^α-*t*-Butyloxycarbonyl-*L*-phenylalanyl-*p*-nitroanilide (56e). The product (147 mg) was obtained after FCC (CH$_2$Cl$_2$/MeOH, 50:1) in 91% isolated yield. ^{1}H NMR (CDCl$_3$, 200 MHz): δ 9.17 (brs, -NH), 8.04 (d, 2H, *J* = 9.2 Hz), 7.49 (d, 2H, *J* = 9.2 Hz), 7.18-7.30 (m, 5H), 5.46 (d, -NH, *J* = 7.8 Hz), 4.55-4.70 (m, 1H), 3.19 (dd, 1H, *J* = 6.2 Hz, *J* = 14 Hz), 3.04 (dd, 1H, *J* = 8.0 Hz, *J* = 14 Hz), 1.39 (s, 9H); ^{13}C NMR (CDCl$_3$, 50 MHz): δ 170.7, 156.3, 143.5, 143.4, 136.0, 129.1, 128.8, 127.2, 124.7, 119.1, 81.1, 27.0, 38.1, 28.2; MS (ESI⁻): *m/z* (intensity), 384.2 ([M-H]⁻, 25%), 498.2 ([M-H]⁻ + TFA, 100%).

N^α-(9-Fluorenyloxycarbonyl)-*L*-methionyl-*p*-nitroanilide (56f). The product (190 mg) was obtained after FCC (CH$_2$Cl$_2$/MeOH, 50:1) in 92% isolated yield. ^{1}H NMR

(CD$_3$COCD$_3$-d$_6$, 200 MHz): δ 9.90 (s, -NH), 8.17 (d, 2H, J = 8.8 Hz), 7.88 (d, 2H, J = 8.8 Hz), 8.11 (d, 2H, J = 7.2 Hz), 7.65-7.67 (m, 2H), 7.23-7.39 (m, 4H), 6.98 (d, -NH, J = 7.6 Hz), 4.33-4.48 (m, 3H), 4.21 (q, 1H, J = 8.8 Hz), 2.04-2.20 (m, 7H); ^{13}C NMR (CD$_3$COCD$_3$-d$_6$, 50 MHz): δ 172.0, 157.3, 145.7, 145.0, 144.1, 142.1, 128.5, 127.9, 126.1, 125.5, 120.8, 120.2, 67.3, 56.2, 48.1, 32.5, 29.8, 15.2; MS (ESI$^-$): m/z (intensity), 604.2 ([M-H]$^-$ + TFA, 100%).

N^α-(9-Fluorenyloxycarbonyl)-L-tryptophanyl-p-nitroanilide (56g). The product (216 mg) was obtained after FCC (CH$_2$Cl$_2$/MeOH, 50:1) in 94% isolated yield. ^{1}H NMR (DMSO-d$_6$, 200 MHz): δ 10.84 (s, -NH), 10.74 (s, -NH), 8.23 (d, 2H, J = 8.8 Hz), 7.85-7.89 (m, 5H), 7.68 (m, 3H), 7.24-7.38 (m, 6H), 6.95-7.10 (m, 2H), 4.51-4.54 (m, 1H), 4.21 (m, 3H), 3.02-3.27 (m, 2H); ^{13}C NMR (DMSO-d$_6$, 50 MHz): δ 172.4, 156.4, 145.5, 144.2, 142.8, 141.1, 136.5, 128.0, 127.6, 127.4, 125.6, 124.3, 121.3, 120.4, 120.0, 119.6, 118.9, 118.7, 111.7, 110.1, 66.2, 56.9, 47.0, 28.0; MS (ESI$^-$): m/z (intensity), 659.3 ([M-H]$^-$ + TFA, 100%).

N^α-(9-Fluorenyloxycarbonyl)-N^ε-trityl-L-histidyl-p-nitroanilide (56h). The product (328 mg) was obtained after FCC (CH$_2$Cl$_2$/MeOH, 20:1) in 70% isolated yield. ^{1}H NMR (CDCl$_3$, 200 MHz): δ 10.87 (brs, 1H, -NH), 8.11 (d, 2H, J = 8.8 Hz), 7.68-7.74 (m, 4H), 7.53-7.56 (m, 3H), 7.47 (s, 1H), 7.24-7.39 (m, 12H), 7.04-7.07 (m, 7H), 6.71 (s, 1H), 4.741-4.77 (m, 1H), 4.34 (d, 2H, J = 6.6 Hz), 4.17 (t, 1H, J = 6.6 Hz), 3.10 (d, 2H, J = 6.2 Hz); ^{13}C NMR (DMSO-d$_6$, 50 MHz): δ 170.5, 156.2, 144.1, 143.7, 143.6, 143.2,

142.0, 141.1, 138.4, 136.3, 129.5, 128.1, 128.0, 127.6, 126.9, 125.0, 124.7, 119.9, 119.7, 119.1, 75.4, 67.2, 55.6, 47.0, 31.0; MS (ESI$^+$): m/z (intensity), 243.1 (Ph$_3$C$^+$, 100%).

Synthesis of amino acid-pNAs (56i-l) using method E
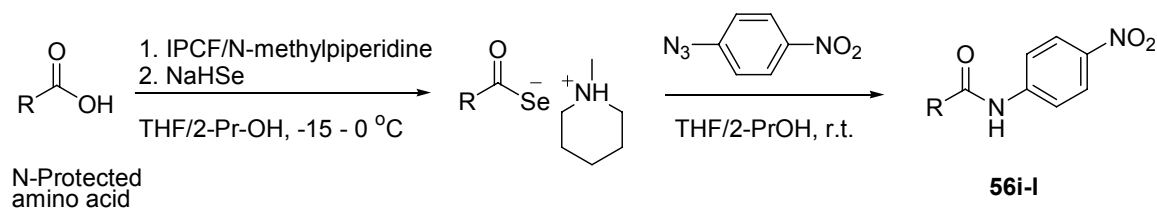
N^{α}-t-**Butyloxycarbonyl**-L-**arginyl**-p-**nitroanilide (56i).** The product (134 mg) was obtained after FCC (CH$_2$Cl$_2$/MeOH, 20:1) in 81% isolated yield. ^{1}H NMR (CD$_3$OD, 200 MHz): δ 8.28 (d, 2H, J =9.0 Hz), 7.95 (d, 2H, J =9.0 Hz), 4.32 (m, 1H), 1.76-1.96 (m, 4H), 1.49 (s, 9H), 1.37 (t, 2H, J =7.4 Hz); ^{13}C NMR (CD$_3$OD, 50 MHz): δ 169.6, 154.5, 141.7, 140.6, 121.5, 116.5, 76.8, 52.3, 37.9, 26.3, 24.5, 22.3; MS (ESI$^+$): m/z (intensity), 395.3 ([M+H]$^+$, 100%).

N^{α}-t-**Butyloxycarbonyl**-L-**glutaminyl**-p-**nitroanilide (56j).** The product (140 mg) was obtained after FCC (Hexane/CH$_2$Cl$_2$/MeOH, 10:10:1) in 91% isolated yield. ^{1}H NMR (DMSO-d$_6$, 200 MHz): δ 10.60 (s, -NH), 8.22 (d, 2H, J =9.2 Hz), 7.851 (d, 2H, J =9.2 Hz), 7.29 (s, -NH), 7.18(d, -NH, J =6.8 Hz), 6.79 (s, -NH), 4.05 (m, 1H), 2.11-2.22 (m, 2H), 1.77-1.88 (m, 2H), 1.36 (s, 9H); ^{13}C NMR (DMSO-d$_6$, 50 MHz): δ 173.4, 172.0,

155.4, 145.0, 142.2, 124.8, 118.9, 78.2, 55.1, 31.4, 28.1, 27.1; MS (ESI⁻): *m/z* (intensity), 365.1 ([M-H]⁻, 20%), 479.2 ([M-H]⁻ + TFA, 100%)

N^α-Benzyloxycarbonyl-*L*-seryl-*p*-nitroanilide (56k). The product (130 mg) was obtained after FCC (CH₂Cl₂/MeOH, 20:1) in 86% isolated yield. ¹H NMR (DMSO-d₆, 200 MHz): δ 10.65 (s, -NH), 8.22 (d, 2H, *J* = 9.2 Hz), 7.88 (d, 2H, *J* = 9.2 Hz), 7.44 (m, 6H), 5.05 (s, 2H), 4.25-4.35 (m, 1H), 3.60-3.70 (m, 2H); ¹³C NMR (DMSO-d₆, 50 MHz): δ 170.4,156.0, 145.1, 144.9, 142.4, 136.9, 128.3, 127.8, 124.9, 119.0, 65.7, 61.6, 58.0; MS (ESI⁻): *m/z* (intensity), 358.1 ([M-H]⁻, 30%), 472.2 ([M-H]⁻+TFA, 100%).

N^α-Benzyloxycarbonyl-*L*-seryl-*L*-phenylalanyl-*p*-nitroanilide (56l). The product (176 mg) was obtained after FCC (CH₂Cl₂/MeOH, 20:1) in 83% isolated yield. ¹H NMR (CDCl₃, 200 MHz): δ 9.08 (s, -NH), 8.05 (d, 2H, *J* = 9.2 Hz), 7.768 (d, 2H, *J* =8.8 Hz), 7.12 – 7.28 (m, 5H), 5.61 (d, -NH, *J* = 4.4 Hz), 4.87 (q, 1H, *J* = 6.2 Hz), 4.13 (t, 1H, *J* = 6.2 Hz), 3.64-3.92 (m, 2H), 3.19-3.4 (m, 2H), 1.33(s, 9H). ¹³C NMR (CDCl₃, 50 MHz): δ 171.3, 169.9, 156.3, 143.6, 143.5, 135.7, 129.1, 128.9, 127.4, 124.7, 119.5, 81.2, 62.4, 56.7, 55.0, 37.4, 28.2; MS (ESI⁻): *m/z* (intensity), 585.3 ([M-H]⁻ + TFA, 100%).

Synthesis of amino acid-AMCs (57a-f) using method D
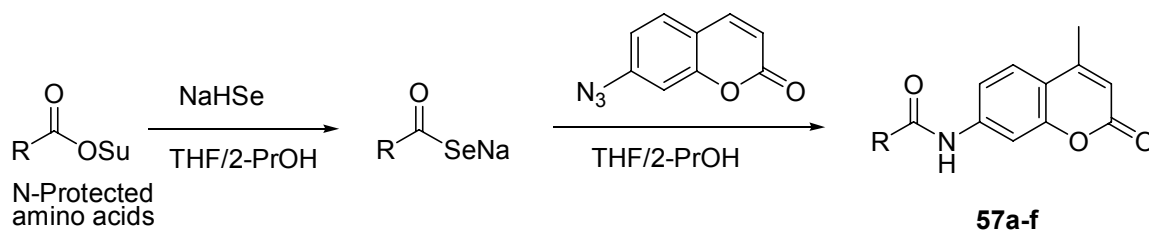
7-(N^{α}-Benzyloxycarbonyl-*L*-glycyl)amino-4-methylcoumarin (57a). The product (141 mg) was obtained after FCC (Hexane/EtOAc, 5:1) in 92% isolated yield. ^{1}H NMR (DMSO-d$_{6}$, 200 MHz): δ 10.44 (s, -NH), 7.73 (s, 1H), 7.66 (d, 1H, J = 8.4 Hz), 7.47 (d, 1H, J = 8.4 Hz), 7.36 (brs, 5H), 6.25 (s, 1H), 5.06 (s, 2H), 3.86 (s, 2H), 2.38 (s, 3H); ^{13}C NMR (DMSO-d$_{6}$, 50 MHz): δ 168.8, 160.0, 156.6, 153.7, 153.1, 142.2, 137.0, 128.3, 127.8, 127.7, 126.0, 115.1, 115.0, 112.3, 105.6, 65.6, 44.2, 17.9; MS (ESI^{-}): *m/z* (intensity), 364.9 ([M-H]$^{-}$, 100%), 479.1 ([M-H]$^{-}$ + CH$_{3}$CN, 100%).

7-(N^{α}-Benzyloxycarbonyl-*L*-tyrosyl)amino-4-methylcoumarin (57b). The product (170 mg) was obtained after FCC (Hexane/EtOAc, 4:1) in 86% isolated yield. ^{1}H NMR (DMSO-d$_{6}$, 200 MHz): δ 10.51 (s, 1H, -NH), 9.21 (s, 1H, -OH), 7.76 (s, 1H), 7.69 (d, 1H, J = 8.8 Hz), 7.47 (d, 1H, J = 8.8 Hz), 7.31 (brs, 5H), 7.12 (d, 2H, J = 8.0 Hz), 6.67 (d, 2H, J = 8.6 Hz), 6.24 (s, 1H), 4.98 (s, 2H), 4.37 (dd, 1H, J = 4.0 Hz, J = 8.0 Hz), 2.71-2.97 (m, 2H), 2.37 (s, 3H); ^{13}C NMR (DMSO-d$_{6}$, 50 MHz): δ 171.5, 160.0, 156.0, 153.6, 153.0, 142.1, 136.9, 130.2, 128.3, 127.7, 127.6, 125.8, 115.3, 115.1, 114.9, 112.3, 105.8, 65.4, 27.4, 36.7, 17.9. MS (ESI^{-}): *m/z* (intensity), 471.0 ([M-H]$^{-}$, 70%), 585.1 ([M-H]$^{-}$ + CH$_{3}$CN, 100%).

7-(N^{α}-*t*-Butyloxycarbonyl-*L*-phenylalanyl)amino-4-methylcoumarin (57c). The product (152 mg) was obtained after FCC (Hexane- Hexane/EtOAc, 1:1) in 86% isolated yield. ^{1}H NMR (CDCl$_{3}$, 200 MHz): δ 9.11 (brs, -NH), 7.65 (s, 1H), 7.37 (d, 1H, J = 8.4 Hz), 7.21 (brs, 5H), 7.07 (m, 1H), 6.08 (s, 1H), 5.40 (d, -NH, J = 7.6 Hz), 4.66 (m, 1H),

3.17 (dd, 1H, J = 6.2 Hz, J = 14 Hz), 3.01 (dd, 1H, J = 8.4 Hz, J = 14 Hz), 2.33 (s, 3H), 1.39 (s, 9H); ^{13}C NMR (CDCl$_3$, 50 MHz): δ 170.6, 160.9, 156.2, 153.9, 152.4, 141.0, 136.1, 129.1, 128.7, 127.0, 124.9, 115.8, 115.5, 113.1, 107.2, 80.8, 56.7, 38.3, 28.3, 18.3; MS (ESI$^-$): m/z (intensity), 421.2 ([M-H]$^-$, 30%), 535.2 ([M-H]$^-$+CH$_3$CN, 100%).

7-(N^{α}-(9-Fluorenyloxycarbonyl)-L-methionyl)amino-4-methylcoumarin (57d). The product (182 mg) was obtained after FCC (Hexane/EtOAc, 2:1) in 95% isolated yield. ^{1}H NMR (DMSO-d$_6$, 200 MHz): δ 10.5 (brs, -NH), 7.68-7.89 (m, 7H), 7.28-7.53 (m, 4H and -NH), 6.25 (s, 1H), 4.20-4.30 (m, 4H), 2.50-2.55 (m, 2H), 2.38 (s, 3H), 2.06 (s, 3H), 1.97-2.04 (m, 2H); ^{13}C NMR (DMSO-d$_6$, 50 MHz): δ 171.8, 160.4, 156.6, 154.1, 153.4, 144.3, 142.6, 141.2, 128.1, 127.5, 126.3, 125.7, 120.5, 115.8, 115.6, 112.8, 106.3, 66.2, 55.3, 47.1, 31.8, 30.2, 18.4, 15.1; MS (ESI$^-$): m/z (intensity), 641.3 ([M-H]$^-$+CH$_3$CN, 100%).

7-(N^{α}-(9-Fluorenyloxycarbonyl)-L-trptophanyl)amino-4-methylcoumarin (57e). The product (200 mg) was obtained after FCC (Hexane/CH$_2$Cl$_2$/MeOH, 10:10:1) in 98% isolated yield. ^{1}H NMR (DMSO-d$_6$, 200 MHz): δ 10.85 (brs, -NH), 10.58 (brs, -NH), 7.82-7.87 (m, 4H), 7.65-7.71 (m, 4H), 7.25-7.53 (m, 6H and -NH), 6.96-7.11 (m, 2H), 6.25 (s, 1H), 4.53 (m, 1H), 4.21 (brs, 3H), 3.10-3.27 (m, 2H), 2.38 (s, 3H); ^{13}C NMR (DMSO-d$_6$, 50 MHz): δ 171.7, 160.0, 155.9, 153.6, 152.9, 143.7, 142.2, 140.6, 136.1, 127.5, 127.2, 127.0, 125.7, 125.2, 123.9, 120.9, 120.0, 118.5, 118.2, 115.4, 115.1, 112.3, 111.3, 109.7, 105.9, 65.7, 56.4, 46.6, 27.7, 17.9; MS (ESI$^-$): m/z (intensity), 696.2 ([M-H]$^-$+CH$_3$CN, 100%).

7-(N^{α}-(9-Fluorenyloxycarbonyl)-N^{ε}-trityl-*L*-histidyl)amino-4-methylcoumarin (57f).

The product (268 mg) was obtained after FCC (Hexane/EtOAc, 1:1) in 82% isolated

yield. ^{1}H NMR (CDCl$_3$, 200 MHz): δ 10.57 (brs, 1H, -NH), 7.71 (d, 2H, J = 7.4 Hz),

7.67 (s, 1H), 7.56 (d, 2H, J = 6.2 Hz), 7.46 (s, 1H), 7.23-7.37 (m, 14H), 7.03-7.06 (m,

6H), 6.91 (d, 1H, J = 6.6 Hz), 6.68 (s, 1H), 6.12 (s,1H), 4.74 (q, 1H, J = 6.2 Hz), 4.33 (d,

2H, J = 6.6 Hz), 4.17 (t, 1H, J = 6.6 Hz), 3.10 (brs, 2H), 2.34 (s,3H). ^{13}C NMR (CDCl$_3$,

50 MHz): δ 170.2, 160.8, 156.3, 154.0, 152.0, 143.7, 143.6, 142.0, 141.5, 141.1, 138.3,

136.3, 129.5, 127.9, 127.5, 126.9, 125.0, 124.8, 119.8, 119.7, 115.6, 115.5, 113.0, 106.9,

75.3, 67.2, 55.7, 46.9, 30.9, 18.3. MS (ESI^{+}): *m/z* (intensity), 243.1 (Ph$_3$C^{+}, 100%).

II. Nitroarylmethyl Phosphoramide Mustards

Synthesis of 2,6-difluoro-4-nitrobenzoic acid (60c)
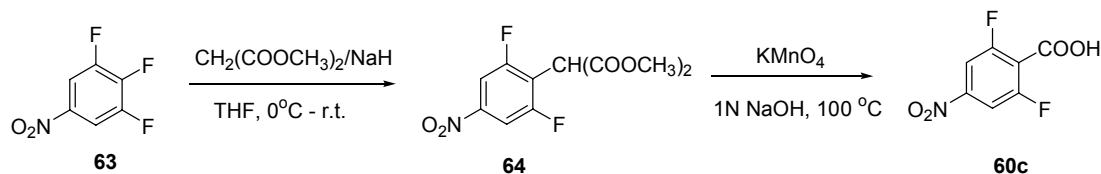
Preparation of 64. At 0 ^{o}C, to a solution of dimethyl malonate (2.3 mL, 20.0 mmol) in anhydrous THF (20 mL) was added 60% sodium hydride (0.8 g, 20.0 mmol). The resulting mixture was stirred at 0 – 5 ^{o}C for 1 h followed by addition of 3,4,5-trifluoro-nitrobenzene (**63**) (1.77g, 10.0 mmol). The reaction was then carried out at room temperature for 24 h and was quenched by addition of 5 ml 10% HCl. After evaporation of THF under reduced pressure, the remaining was redissolved in 100 ml of EtOAc. The organic phase was then washed with water and brine, and dried over Na_2SO_4. After removal of Na_2SO_4 via filtration, the filtrate was concentrated to dryness. The crude product was crystallized from hexane, affording the desired product **64** (2.1g) as a white solid in a yield of 71%. ^{1}H NMR (200 MHz, CDCl$_3$): δ 7.80 (d, 2H, J = 7.0 Hz), 5.00 (s, 1H), 3.77 (s, 3H); ^{13}C NMR (50 MHz, CDCl$_3$): 165.7, 160.7 (dd, J = 255.0 Hz, J = 8.0 Hz), 148.5 (t, J = 11.0 Hz), 117.5 (t, J = 19.0 Hz), 107.8 (dd, J = 28.0 Hz, J = 3,.0 Hz), 53.4, 41.0; MS (ESI$^-$): m/z (intensity), 288.0 ([M - H]$^-$, 100%).

Preparation of 60c. At 50 ^{o}C, to a solution of **64** (2.0g, 6.92 mmol) in 0.5N NaOH (56mL) was added potassium permanganate (5.47g, 34.60 mmol) portionwise over 1h.

After addition of all potassium permanganate, the resulting reaction mixture was stirred at reflux for additional 2 h. The mixture was then passed through a Celite pad when still hot. The brown Celite pad was rinsed with hot water (2 x 50 mL). The combined aqueous phase was acidified by conc. HCl to pH 1 followed by extraction with EtOAc (3 x 50 mL). The combined organic phase was then washed with water and brine, and dried over Na_2SO_4. After removal of Na_2SO_4 via filtration, the filtrate was concentrated to dryness. The crude product was purified by flash chromatograph (hexane to EtOAc) to afford the desired product (1.1g) as a white solid in a yield of 78%. ^{1}H NMR (200 MHz, Acetone-d_6): δ 9.24 (brs, -COOH), 8.04 (d, 2H, J = 7.4 Hz); ^{13}C NMR (50 MHz, Acetone-d_6): 160.6, 160.3 (dd, J = 255.0 Hz, J = 8.0 Hz), 150.4 (t, J = 12.0 Hz), 118.0 (t, J = 20.0 Hz), 108.9 (dd, J = 28.0 Hz, J = 4.0 Hz); MS (ESI$^-$): m/z (intensity), 405.1 ([2M − H]$^-$, 100%), 158.0 ([M - COOH]$^-$, 50%).

Synthesis of substituted 4-nitro-benzyl alcohols 64a-e

63a-e　　　　　　**64a-e**

a　R_1=F, R_2, R_3=H
b　R_1, R_3=H, R_2=F
c　R_1=H, R_2, R_3=F
d　R_1, R_3=H, R_2=Cl
e　R_1, R_3=H, R_2=CF$_3$
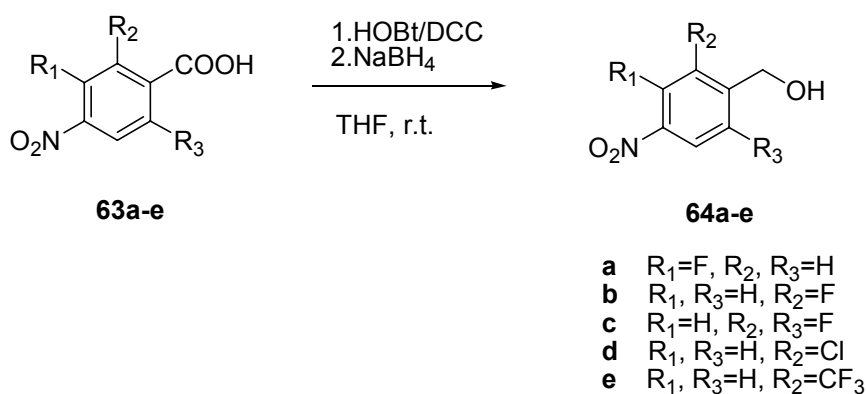
To a solution of acid (**63a-e**) (1.0 mmol) in THF (10 mL) was added HOBt (135 mg, 1.0 mmol) and DCC (227 mg, 1.1 mmol). The resulting mixture was stirred at room

temperature for 1 h. The white precipitates were filtered off and rinsed with THF (2 x 5 mL). The filtrate was added dropwise to a suspension of NaBH$_4$ (38 mg, 1.0 mmol) in THF (10 mL) over 30 min. The reaction was carried out at room temperature for additional 1.5 h and quenched by adding 10 ml 1.0 N HCl. After evaporation of THF under reduced pressure, the remaining aqueous solution was extracted EtOAc (3 x 20 mL). The combined EtOAc phase was washed with water and brine, and dried over Na$_2$SO$_4$. After removal of Na$_2$SO$_4$ via filtration, the filtrate was concentrated to dryness. The crude product was purified by flash column chromatography (hexane to 50% EtOAc/hexane) to afford the desired alcohol **64a-e**.

3-Fluoro-4-nitrobenzyl alcohol (64a). A yellow solid (161 mg, 94%); ^{1}H NMR (200 MHz, CDCl$_3$): δ 8.01 (t, 1H, J = 7.8 Hz), 7.29 (d, 1H, J = 11.8 Hz), 7.22 (d, 1H, J = 8.4 Hz), 4.77 (s, 2H), 2.00 (s, -OH); ^{13}C NMR (50 MHz, CDCl$_3$): 155.7 (d, J = 265.0 Hz), 150.3 (t, J = 8.0 Hz), 136.9 (t, J = 8.0 Hz), 126.2 (d, J = 2.0 Hz), 121.7 (d, J = 4.0 Hz), 115.8 (d, J = 21.0 Hz), 63.4.

2-Fluoro-4-nitrobenzyl alcohol (64b). A yellow solid (161 mg, 94%); ^{1}H NMR (200 MHz, CDCl$_3$): δ 8.06 (dd, 1H, J = 8.4 Hz, J = 1.8 Hz), 7.90 (dd, 1H, J = 9.6 Hz, J = 1.8 Hz), 7.70 (t, 1H, J = 7.8 Hz), 4.78 (s, 2H), 2.16 (s, -OH); ^{13}C NMR (50 MHz, CDCl$_3$): 159.3 (d, J = 250.0 Hz), 148.1 (d, J = 5.0 Hz), 135.5 (d, J = 15.0 Hz), 129.0 (d, J = 5.0 Hz), 119.4 (d, J = 4.0 Hz), 110.9 (d, J = 27.0 Hz), 58.4 (d, J = 4.0 Hz); IR (KBr): 3524, 1516, 1355, 1051 cm^{-1}.

2,6-Difluoro-4-nitrobenzyl alcohol (64c). A yellow solid (164 mg, 87%); ^{1}H NMR (200 MHz, CDCl$_3$): δ 8.02 (d, 2H, J = 6.8 Hz), 5.05 (s), 2.31 (s, -OH); ^{13}C NMR (50 MHz, CDCl$_3$): 161.7 (dd, J = 252.0 Hz, J = 9.0 Hz), 148.0 (t, J = 10.0 Hz), 123.7 (t, J = 20.0 Hz), 108.4 (dd, J = 30.0 Hz, J = 2.0 Hz), 53.4 (t, J = 4.0 Hz).

2-Chloro-4-nitrobenzyl alcohol (64d). A yellow solid (172 mg, 92%); ^{1}H NMR (200 MHz, CDCl$_3$): δ 8.14 (d, 1H, J = 2.2 Hz), 8.08 (dd, 1H, J = 8.0 Hz, J = 2.2 Hz), 7.72 (d, 1H, J = 8.0 Hz), 4.81 (s), 2.78 (s, -OH); ^{13}C NMR (50 MHz, CDCl$_3$): 147.9, 146.4, 133.1, 128.7, 124.8, 122.5, 62.4.

2-Trifluoromethyl-4-nitrobenzyl alcohol (64e). A yellow solid (201 mg, 91%); ^{1}H NMR (200 MHz, CDCl$_3$): δ 8.44 (s, 1H), 8.36 (d, 1H, J = 8.4 Hz), 8.01 (d, 1H, J = 8.4 Hz), 4.97 (s), 2.69 (s, -OH); ^{13}C NMR (50 MHz, CDCl$_3$): 146.9, 146.5, 129.1, 128.0 (d, J = 32.0 Hz), 126.7, 122.9 (q, J = 270.0 Hz), 121.2 (q, J = 6.0 Hz), 60.3 (d, J = 3.0 Hz).

Synthesis of substituted 4-nitro-benzyl phosphoramide mustards 30a-e
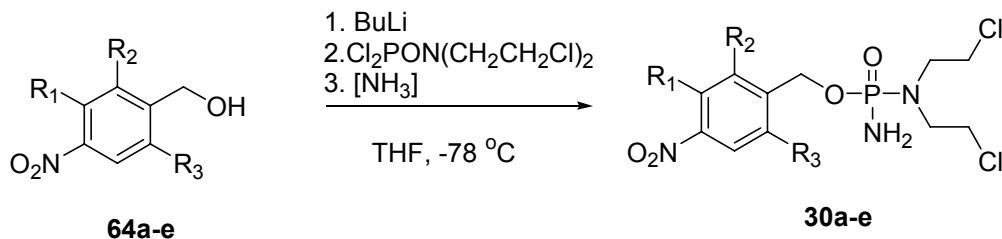
a R$_1$=F, R$_2$, R$_3$=H
b R$_1$, R$_3$=H, R$_2$=F
c R$_1$=H, R$_2$, R$_3$=F
d R$_1$, R$_3$=H, R$_2$=Cl
e R$_1$, R$_3$=H, R$_2$=CF$_3$

To a solution of alcohol **64a-e** (1.0 mmol) in anhydrous THF (5 mL) was added a solution of n-BuLi in cyclohexane (2.0 M, 0.55 mL) at −78 ºC. After 20 min, the above solution was transferred to a pre-cooled solution of bis(2-chloroethyl)phosphoramidic dichloride (285 mg, 1.1mmol) in THF (5 mL) at −78 ºC via cannula. The resulting mixture was stirred at −78 ºC for 5 h followed by bubbling with ammonia for 10 min. The reaction mixture was allowed to gradually warm up to room temperature over 2 h. After removal of THF via distillation under reduced pressure, the residue was suspended in saturated aqueous sodium bicarbonate (10 mL) followed by extraction with dichloromethane (3 x 25 mL). The combined organic phase was washed with water (25 mL) and saturated brine (25 mL), and dried over Na_2SO_4. After filtration off Na_2SO_4, the filtrate was concentrated to dryness under reduced pressure. The crude product was purified by flash column chromatography (dichloromethane to 5% methanol in dichloromethane) to afford the desired product **30a-e**.

3-Fluoro-4-nitrobenzyl phosphoramide mustard (30a). A yellow solid (206 mg, 55%); ^{1}H NMR (200 MHz, CDCl$_3$): δ 8.00 (t, 1H, J = 7.8 Hz), 7.27 (d, 1H, J = 12.4 Hz), 7.22 (d, 1H, J = 8.0 Hz), 5.03 (t, 2H, J = 7.2 Hz), 3.56-3.63 (m, 4H), 3.40-3.49 (m, 4H), 2.97 (s, -NH$_2$); ^{13}C NMR (50 MHz, CDCl$_3$): 155.6 (d, J = 265.0 Hz), 145.7 (d, J = 8.0 Hz), 136.9 (t, J = 8.0 Hz), 126.4 (d, J = 2.0 Hz), 122.6 (d, J = 4.0 Hz), 116.6 (d, J = 22.0 Hz), 65.0, 48.8 (d, J = 5.0 Hz), 42.5. HRMS (FAB$^+$) m/z calc'd for $C_{11}H_{15}Cl_2FN_3O_4P$, [M + H]$^+$, 374.0240, found 374.0229.

2-Fluoro-4-nitrobenzyl phosphoramide mustard (30b). A yellow solid (183 mg, 49%); ^{1}H NMR (200 MHz, CDCl$_3$): δ 7.96 (d, 1H, J = 8.4 Hz), 7.84 (d, 1H, J = 9.6 Hz), 7.63 (t, 1H, J = 7.8 Hz), 5.08 (d, 2H, J = 7.0 Hz), 3.46-3.61 (m, 4H), 3.34-3.46 (m, 4H); ^{13}C NMR (50 MHz, CDCl$_3$): 159.3 (d, J = 250.0 Hz), 148.2 (d, J = 9.0 Hz), 131.4 (dd, J = 14.0 Hz, J = 8.0 Hz), 129.8 (d, J = 5.0 Hz), 119.3 (d, J = 4.0 Hz), 111.0 (d, J = 26.0 Hz), 60.1 (t, J = 4.0 Hz), 48.8 (d, J = 5.0 Hz), 42.3. HRMS (FAB$^+$) m/z calc'd for C$_{11}$H$_{15}$Cl$_2$FN$_3$O$_4$P, [M + H]$^+$, 374.0240, found 374.0235.

2,6-Difluoro-4-nitrobenzyl phosphoramide mustard (30c). A yellow solid (157 mg, 40%); ^{1}H NMR (200 MHz, CDCl$_3$): δ 7.81 (d, 2H, J = 6.6 Hz), 5.13 (t, J = 6.8 Hz), 3.59-3.66 (m, 4H), 3.38-3.50 (m, 4H), 2.92 (s, -NH$_2$); ^{13}C NMR (50 MHz, CDCl$_3$): 160.4 (dd, J = 255.0 Hz, J = 8.0 Hz), 148.2 (t, J = 10.0 Hz), 118.7 (td, J = 18.0 Hz, J = 8.0 Hz), 107.0 (dd, J = 30.0 Hz, J = 2.0 Hz), 53.6 (d, J = 4.0 Hz), 48.2 (d, J = 5.0 Hz), 41.6. MS (ESI$^+$): m/z (intensity), 392.0 ([M + H]$^+$, 100%), 394.0 ([M + H]$^+$ + 2, 65%), 396.0 ([M + H]$^+$ + 4, 10%). HRMS (FAB$^+$) m/z calc'd for C$_{11}$H$_{14}$Cl$_2$F$_2$N$_3$O$_4$P, [M + H]$^+$, 392.0145, found 392.0142.

2-Chloro-4-nitrobenzyl phosphoramide mustard (30d). A yellow solid (250 mg, 64%). ^{1}H NMR (200 MHz, CDCl$_3$): δ 8.16 (d, 1H, J = 2.2 Hz), 8.08 (dd, 1H, J = 8.4 Hz, J = 2.2 Hz), 7.67 (d, 1H, J = 8.4 Hz), 5.12 (d, J = 7.0 Hz), 3.58-3.68 (m, 4H), 3.42-3.50 (m, 4H), 3.36 (brs, -NH2); ^{13}C NMR (50 MHz, CDCl$_3$): 147.6, 141.7 (d, J = 9.0 Hz), 132.9, 128.6, 124.3, 121.8, 63.4 (d, J = 3.0 Hz), 48.8 (d, J = 5.0 Hz), 42.3. HRMS (FAB$^+$) m/z calc'd for C$_{11}$H$_{15}$Cl$_3$N$_3$O$_4$P, [M + H]$^+$, as 389.9944, found 389.9943.

2-Trifluoromethyl-4-nitrobenzyl phosphoramide mustard (30e). A yellow solid (220 mg, 52%); ^{1}H NMR (200 MHz, CDCl$_3$): δ 8.49 (s, 1H), 8.40 (d, 1H, J = 8.4 Hz), 7.93 (d, 1H, J = 8.4 Hz), 5.27 (d, 1H, J = 6.6 Hz), 3.60-3.66 (m, 4H), 3.42-3.53 (m, 4H), 3.21 (brs, -NH$_2$); ^{13}C NMR (50 MHz, CDCl$_3$): 147.1, 142.3 (d, J = 10.0 Hz), 129.9, 128.6 (d, J = 32.0 Hz), 126.8, 122.7 (q, J = 273.0 Hz), 121.5 (q, J = 6.0 Hz), 60.3 (t, J = 3.0 Hz), 48.7 (d, J = 5.0 Hz), 42.3. HRMS (FAB$^+$) m/z calc'd for C$_{12}$H$_{15}$Cl$_2$F$_3$N$_3$O$_4$P, [M + H]$^+$, as 424.0208, found 424.0172.

III. Peptidylaminoarylmethyl Phosphoramide Mustards

Solid-phase synthesis of peptide. The peptide, Fm-glutaryl-Hyp-Ala-Ser-Chg-OH, was synthesized using Fmoc chemistry on 4-hydroxymethylphenoxy (WANG-type HMP) resin purchased from Advanced Chemtech. N^{α}-Fmoc protected L-amino acids and coupling reagents were purchased from Advanced Chemtech. Side-chain protection was Ser(t-Bu) and Lys(Cl-Z). First amino acid was attached to the resin via its C-terminal using HOBt/DMAP/DIC protocol. All N^{α}-Fmoc protected L-amino acids were used as 3-fold excess amount for each coupling in NMP. Following completion of the assembly on the resin support, the Fmoc protecting group was removed via the standard 20% piperidine/NMP protocol followed by washing with NMP 5 times and introduction of N-terminal capping group using acetic anhydride. Deprotection and cleavage of the peptide from the resin support were effected using 90% TFA/CH$_2$Cl$_2$. The benzyl ester and fluorenylmethyl ester (OFm) were not affected under these conditions. After removal of solvents under reduced pressure, the peptide was purified by preparative-HPLC on reversed phase C18 column. A linear gradient was used from 10% solvent A to 90% solvent B with a flow rate of 12 mL/min, where solvent A was 0.1% TFA/H$_2$O and solvent B was 0.1% TFA/CH$_3$CN. The UV detection wavelength was set at 220 nm. Homogeneous fractions containing the desired product were pooled and lyophilized to afford the peptide as a white powder. The purity and identity were confirmed by LC/MS.

Synthesis of fluorinated 4-azido-benzoic acids 69a-e

63a-c	
a	R_1 = F, R_2, R_3, R_4 = H
b	R_1, R_3, R_4 = H, R_2 = F
c	R_1, R_4 =H, R_2, R_3 = F

68a-e	
a	R_1 = F, R_2, R_3, R_4 = H
b	R_1, R_3, R_4 = H, R_2 = F
c	R_1, R_4 =H, R_2, R_3 = F
d	R_1, R_2, R_3, R_4 = F
e	R_1, R_2, R_3, R_4 = H

69a-e	
a	R_1 = F, R_2, R_3, R_4 = H
b	R_1, R_3, R_4 = H, R_2 = F
c	R_1, R_4 =H, R_2, R_3 = F
d	R_1, R_2, R_3, R_4 = F
e	R_1, R_2, R_3, R_4 = H
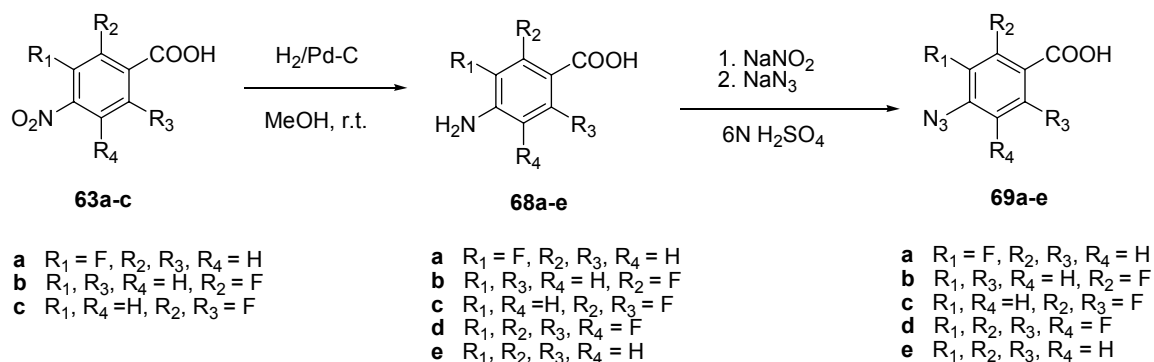
Synthesis of fluorinated 4-aminobenzoic acids (68a-c). To a solution of **63a-c** (1.0 mmol) in methanol (20 mL) was added 10% Pd-C (10 mg, 0.01 mmol). The resulting mixture was stirred at room temperature under a hydrogen balloon for 16 h and filtered through a Celite 545 pad. The filtrate was concentrated to dryness to afford the corresponding aminobenzoic acid **68a-c** that was used directly for the next step without purification.

Synthesis of fluorinate 4-azidobenzoic acids (69a-e). To an ice-cold suspension of **68a-e** (1.0 mmol) in 6 N H_2SO_4 (20 mL) was added dropwise an aqueous solution of sodium nitrite (83 mg, 1.2 mmol) over 10 min. The resulting mixture was stirred at 0 ^{o}C for additional 30 min. An aqueous solution of sodium azide (98 mg, 1.5 mmol) was added dropwise to the above mixture. The reaction was then carried out at room temperature for 1 h. The reaction mixture was extracted with EtOAc (3 x 30 mL). The combined EtOAc phase was washed with water and brine, and dried over Na_2SO_4. After removal of Na_2SO_4 via filtration, the filtrate was concentrated to dryness. The crude product was

purified by flash column chromatography (hexane to 50% EtOAc/hexane) to afford the desired azidobenzoic acid **69a-e**.

4-Azido-3-fluorobenzoic acid (69a). A white solid (163 mg, 90%); ^{1}H NMR (200 MHz, CD$_3$OD): δ 7.77 (d, 1H, J = 7.8 Hz), 7.69 (d, 1H, J = 11.4 Hz), 7.10 (dd, 1H, J = 7.8 Hz, J = 7.2 Hz); ^{13}C NMR (50 MHz, CD$_3$OD): 167.5, 154.9 (d, J = 250.0 Hz), 133.3 (d, J = 10.0 Hz), 129.1 (d, J = 6.0 Hz), 127.2 (d, J = 3.0 Hz), 121.3, 118.4 (d, J = 20.0 Hz); IR (KBr): 2146, 1691, 1432, 1298 cm^{-1}; MS (ESI$^-$): m/z (intensity), 180.1 ([M - H]$^-$, 100%).

4-Azido-2-fluorobenzoic acid (69b). A white solid (163 mg, 83%); ^{1}H NMR (200 MHz, CDCl$_3$): δ 7.78 (dd, 1H, J = 8.6 Hz, J = 8.4 Hz), 6.71 (d, 1H, dd, 1H, J = 8.4 Hz, J = 2.2 Hz), 6.62 (dd, 1H, J = 11.4 Hz, J = 2.2 Hz); ^{13}C NMR (50 MHz, CDCl$_3$): 164.0, 162.8 (d, J = 250.0 Hz), 146.2 (d, J = 10.0 Hz), 133.6, 114.2 (d, J = 3.0 Hz), 107.3 (d, J = 26.0 Hz. MS (ESI$^-$): m/z (intensity), 180.1 ([M - H]$^-$, 100%).

4-Azido-2,6-difluorobenzoic acid (69c). A white solid (163 mg, 83%); ^{1}H NMR (200 MHz, Acetone-d$_6$): δ 6.87 (d, 2H, J = 9.2 Hz); ^{13}C NMR (50 MHz, Acetone-d$_6$): 171.9, 162.1 (dd, J = 255.0 Hz, J = 8.4 Hz), 161.4, 146.0 (t, J = 12.9 Hz), 108.2 (t, J = 19.8 Hz); IR (KBr): 3432, 2119, 1738, 1636, 1312, 1280 cm^{-1}; MS (ESI$^-$): m/z (intensity), 154.0 ([M - COOH]$^-$, 100%).

4-Azido-2,3,5,6-tetrafluorobenzoic acid (69d). A yellow solid (188 mg, 80%); ^{1}H NMR (200 MHz, CDCl$_3$): δ 10.34 (brs, -COOH); ^{13}C NMR (50 MHz, CDCl$_3$): 164.3, 146.0

(dm, $J = 265.0$ Hz), 140.7 (dm, $J = 265.0$ Hz), 124.8 (t. $J = 13.0$), 106. (t, $J = 13.0$ Hz), 51.7; IR (film): 3388, 2123, 1652, 1489, 1241, 1002, 945 cm^{-1}. MS (ESI$^-$): m/z (intensity), 234.0 ([M -H]$^-$, 100%.

4-Azido-benzoic acid (69e). A white solid (163 mg, 98%); ^{1}H NMR (200 MHz, DMSO-d$_6$): δ 7.96 (d, 2H, $J = 8.4$ Hz), 7.17 (d, 2H, $J = 8.4$ Hz); ^{13}C NMR (50 MHz, DMSO-d$_6$): 167.5, 143.4, 131.9, 128.7, 119.7; MS (ESI$^-$): m/z (intensity), 162.0 ([M - H]$^-$, 100%).

Synthesis of fluorinated 4-azido-benzyl alcohols 67a-e

a R$_1$ = F, R$_2$, R$_3$, R$_4$ = H
b R$_1$, R$_3$, R$_4$ = H, R$_2$ = F
c R$_1$, R$_4$ =H, R$_2$, R$_3$ = F
d R$_1$, R$_2$, R$_3$, R$_4$ = F
e R$_1$, R$_2$, R$_3$, R$_4$ = H
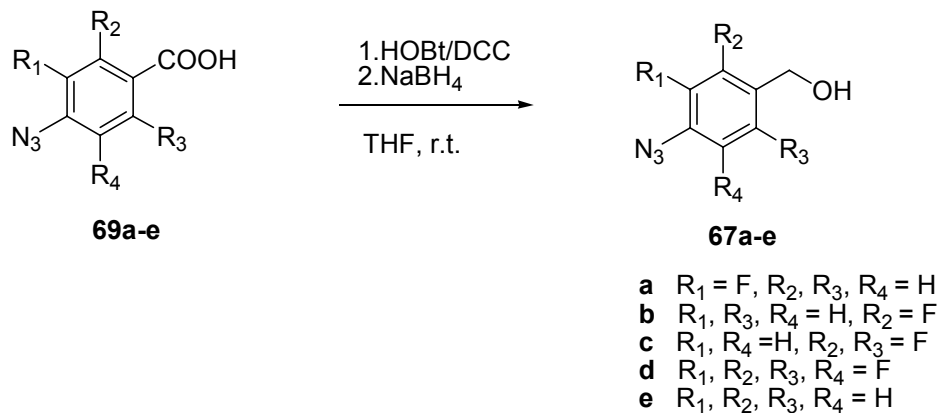
To a solution of **69a-e** (1.0 mmol) in THF (10 mL) was added HOBt (135 mg, 1.0 mmol) and DCC (227 mg, 1.1 mmol). The resulting mixture was stirred at room temperature for 1 h. The white precipitates were filtered off and rinsed with THF (2 x 5 mL). The filtrate was added dropwise to a suspension of NaBH$_4$ (38 mg, 1.0 mmol) in THF (10 mL) over 30 min. The reaction was carried out at room temperature for additional 1.5 h and quenched by adding 10 ml 1.0 N HCl. After evaporation of THF under reduced pressure,

the remaining aqueous solution was extracted EtOAc (3 x 20 mL). The combined EtOAc phase was washed with water and brine, and dried over Na_2SO_4. After removal of Na_2SO_4 via filtration, the filtrate was concentrated to dryness. The crude product was purified by flash column chromatography (hexane to 50% EtOAc/hexane) to afford the desired alcohol **67a-e**.

4-Azido-3-fluorobenzyl alcohol (67a). Yellow oil (117 mg, 70%); ^{1}H NMR (200 MHz, CDCl$_3$): δ 6.94 − 7.08 (m, 3H), 4.57 (s, 2H), 2.59 (brs, -OH); ^{13}C NMR (50 MHz, CDCl$_3$): 154.7 (d, J = 250.0 Hz), 139.2 (d, J = 6.0 Hz), 126.8 (d, J = 12.0 Hz), 122.9 (d, J = 4.0 Hz), 120.9, 115.0 (d, J = 20.0 Hz), 63.8 (d, J = 1.0 Hz); IR (film): 3334, 2134, 2096, 1508, 1315 cm^{-1}.

4-Azido-2-fluorobenzyl alcohol (67b). Yellow oil (124 mg, 74%); ^{1}H NMR (200 MHz, CDCl$_3$): δ 7.27 (t, 1H, J = 8.0 Hz), 6.73 (dd, 1H, J = 8.0 Hz, J = 2.2 Hz), 6.63 (dd, 1H, J = 10.6 Hz, J = 2.2 Hz), 4.58 (s, 2H), 3.63 (brs, -OH); ^{13}C NMR (50 MHz, CDCl$_3$): 160.7 (d, J = 250.0 Hz), 140.9 (d, J = 10.0 Hz), 130.2 (d, J = 6.0 Hz), 124.2 (d, J = 15.0 Hz), 114.5 (d, J = 3.0 Hz), 106.2 (d, J = 25.0 Hz), 58.1 (d, J = 4.0 Hz); IR (film): 3321, 2116, 1621, 1583, 1502, 1301, 1212 cm^{-1}.

4-Azido-2,6-difluorobenzyl alcohol (67c). A white solid (131 mg, 71%); ^{1}H NMR (200 MHz, CDCl$_3$): δ 6.56 (d, 2H, J = 7.6 Hz), 4.66 (s, 2H), 2.39 (brs, -OH); ^{13}C NMR (50 MHz, CDCl$_3$): 162.1 (dd, J = 250.0 Hz, J = 10.0 Hz), 142.5 (t, J = 13.0 Hz), 113.0 (t, J =

20.0 Hz), 102.6 (d, J = 30.0 Hz), 52.4 (t, J = 4.0 Hz); IR (film): 3330, 2116, 1641, 1587, 1441, 1237, 1060, 1026 cm^{-1}.

4-Azido-2,3,5,6-tetrafluorobenzyl alcohol (67d). A white solid (155 mg, 70%); ^{1}H NMR (200 MHz, CDCl$_3$): δ 4.71 (s, 2H), 2.85 (brs, -OH); ^{13}C NMR (50 MHz, CDCl$_3$): 144.6 (dm, J = 245.0 Hz), 139.7 (dm, J = 245.0 Hz), 119.2 (t. J = 20.0), 113.3 (t, J = 20.0 Hz), 51.7; IR (film): 3388, 2123, 1652, 1489, 1241, 1002, 945 cm^{-1}.

4-Azido-benzyl alcohol (67e). A yellow solid (115 mg, 77%); ^{1}H NMR (200 MHz, CDCl$_3$): δ 7.31 (d, J = 8.4 Hz), 7.00 (d, J = 8.4 Hz), 4.61 (s, 2H), 2.81 (brs, -OH); ^{13}C NMR (50 MHz, CDCl$_3$): 139.4, 137.7, 128.6, 119.2, 64.6; IR (film): 3332, 2107, 1506, 1287 cm^{-1}.

Synthesis of fluorinated 4-azido-benzyl phosphoramide mustards 44a-e

a R_1 = F, R_2, R_3, R_4 = H
b R_1, R_3, R_4 = H, R_2 = F
c R_1, R_4 =H, R_2, R_3 = F
d R_1, R_2, R_3, R_4 = F
e R_1, R_2, R_3, R_4 = H
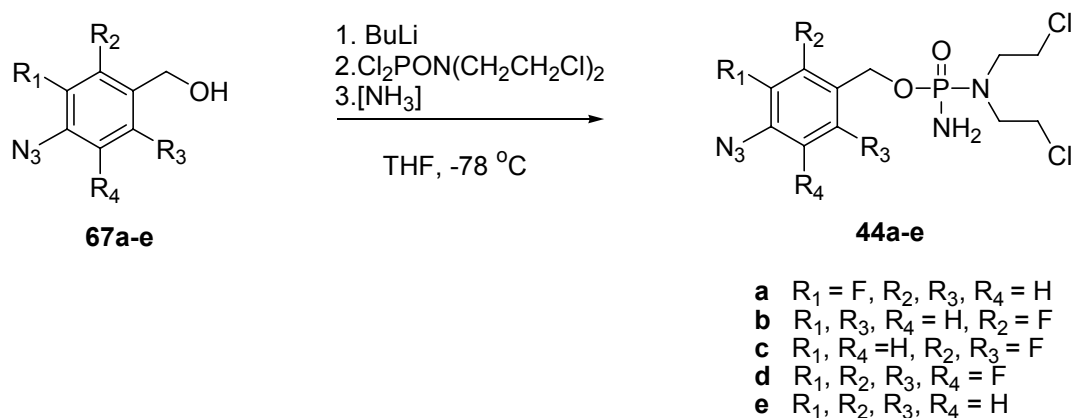
To a solution of alcohol **67a-e** (5.0 mmol) in anhydrous THF (25 mL) was added a solution of BuLi in cyclohexane (2.0 M, 2.75 mL) at −78 ºC. After 20 min, the above solution was transferred to a pre-cooled solution of bis(2-chloroethyl)phosphoramidic dichloride (1.43 g, 5.5 mmol) in THF (25 mL) at −78 ºC via cannula. The resulting mixture was stirred at −78 ºC for 5 h followed by bubbling with ammonia for 10 min. The reaction mixture was allowed to gradually warm up to room temperature over 2 h. After removal of THF via distillation under reduced pressure, the residue was suspended in saturated aqueous sodium bicarbonate (50 mL) followed by extraction with dichloromethane (3 x 50 mL). The combined organic phase was washed with water (50 mL) and saturated brine (50 mL), and dried over Na_2SO_4. After filtration off Na_2SO_4, the filtrate was concentrated to dryness under reduced pressure. The crude product was purified by flash column chromatography (dichloromethane to 5% methanol in dichloromethane) to afford the desired product **44a-e**.

4-Azido-3-fluorobenzyl phosphoramide mustard (44a): a yellow semi-solid (0.959 g, 52%); ^{1}H NMR (200 MHz, CDCl$_3$): δ 7.06 – 7.25 (m, 3H), 5.00 (dd, 2H, J = 7.8 Hz, J = 4.0 Hz), 3.66 - 3.73 (m, 4H), 3.43 - 3.55 (m, 4H); ^{13}C NMR (50 MHz, CDCl$_3$): 154.3 (d, J = 248.5 Hz), 134.7 (t, J = 7.5 Hz), 127.4 (d, J = 10.0 Hz), 123.7 (d, J = 3.4 Hz), 120.8, 115.7 (d, J = 19.7 Hz), 65.5 (d, J = 3.1 Hz), 48.9 (d, J = 4.6 Hz), 42.3; IR (film): 3424, 2134, 2099, 1643, 1509, 1218 cm^{-1}; MS (ESI$^+$): *m/z* (intensity), 370.10 ([M + H]$^+$, 100%), 372.10 ([M + H]$^+$ + 2, 65%), 374.10 ([M + H]$^+$ + 4, 10%), 411.1 ([M + H]$^+$ + CH$_3$CN, 30%), 413.1 ([M + H]$^+$ + 2 + CH$_3$CN, 20%, 415.1 ([M + H]$^+$ + 4 + CH$_3$CN, 3%).

4-Azido-2-fluorobenzyl phosphoramide mustard (44b): a yellow semi-solid (0.959 g, 52%); ^{1}H NMR (200 MHz, CDCl$_3$): δ 7.24 (t, 1H, J = 8.0 Hz), 6.63 (dd, 1H, J = 2.2 Hz, J = 8.0 Hz), 6.54 (dd, 1H, J = 2.2 Hz, J = 8.0 Hz), 4.79 (d, 2H, J = 7.2 Hz), 3.28 - 3.45 (m, 4H), 3.13 - 3.26 (m, 4H); ^{13}C NMR (50 MHz, CDCl$_3$): 161.2 (d, J = 248.9 Hz), 142.2 (d, J = 9.9 Hz), 131.5 (d, J = 5.4 Hz), 120.2 (dd, J = 15.0 Hz, J = 8.0 Hz), 114.8 (d, J = 3.4 Hz), 106.6 (d, J = 25.0 Hz), 60.7 (d, J = 4.1 Hz), 49.1 (d, J = 5.0 Hz), 42.4; IR (film): 3431, 2118, 1621, 1505, 1303, 1214, 1091, 1012, 980 cm^{-1}; MS (ESI$^+$): *m/z* (intensity), 370.1 ([M + H]$^+$, 100%), 372.1 ([M + H]$^+$ + 2, 65%), 374.1 ([M + H]$^+$ + 4, 10%), 411.1 ([M + H]$^+$ + CH$_3$CN, 20%), 413.1 ([M + H]$^+$ + 2 + CH$_3$CN, 13%, 415.1 ([M + H]$^+$ + 4 + CH$_3$CN, 2%).

4-Azido-2,6-difluorobenzyl phosphoramide mustard (44c): a light yellow solid (0.970 g, 50%); ^{1}H NMR (200 MHz, CD$_3$OD): δ 6.72 (d, 2H, J = 8.4 Hz), 4.95 (d, 2H, J = 7.0

Hz), 3.52 - 3.60 (m, 4H), 3.26 - 3.39 (m, 4H); ^{13}C NMR (50 MHz, CD$_3$OD): 163.6 (dd, J = 250.0 Hz, J = 9.5 Hz), 145.2 (t, J = 13.3 Hz), 110.5 (td, J = 20.0 Hz, J = 8.4 Hz), 103.9 (dd, J = 29.6 Hz, J = 2.0 Hz), 55.4 (dd, J = 8.0 Hz, J = 3.8 Hz), 50.6 (d, J = 4.6 Hz), 43.0; MS (ESI$^+$): m/z (intensity), 388.2 ([M + H]$^+$, 100%), 390.2 ([M + H]$^+$ + 2, 65%), 392.2 ([M + H]$^+$ + 4, 10%), 429.3 ([M + H]$^+$ + CH$_3$CN, 20%), 431.3 ([M + H]$^+$ + 2 + CH$_3$CN, 13%, 433.3 ([M + H]$^+$ + 4 + CH$_3$CN, 2%).

4-Azido-2,3,5,6-tetrafluorobenzyl phosphoramide mustard (44d): a dark green solid (1.02 g, 48%); ^{1}H NMR (200 MHz, CD$_3$OD): δ 5.03 (d, 2H, J = 7.8 Hz), 3.55 - 3.62 (m, 4H), 3.32 – 3.41 (m, 4H); ^{13}C NMR (50 MHz, CD$_3$OD): 145.4 (dm, J = 251.2 Hz), 140.4 (dm, J = 250.5 Hz), 121.0 (tt, J = 12.2 Hz, J = 3.1 Hz), 110.4 (td, J = 12.4 Hz, J = 8.4 Hz), 54.2, 49.1 (d, J = 5.0 Hz), 42.3; IR (film): 3241, 3113, 2964, 2159, 2124, 1654, 1496, 1238 cm^{-1}; MS (ESI$^+$): m/z (intensity), 424.0 ([M + H]$^+$, 100%), 426.0 ([M + H]$^+$ + 2, 65%), 428.0 ([M + H]$^+$ + 4, 10%), 465.1 ([M + H]$^+$ + CH$_3$CN, 20%), 467.1 ([M + H]$^+$ + 2 + CH$_3$CN, 13%, 469.1 ([M + H]$^+$ + 4 + CH$_3$CN, 2%).

4-Azido-benzyl phosphoramide mustard (44e): a yellow semi-solid (0.965 g, 55%); ^{1}H NMR (200 MHz, CD$_3$OD): δ 7.45 (d, 2H, J = 8.4 Hz), 7.09 (d, 2H, J = 8.4 Hz), 4.97 (d, 2H, J = 7.4 Hz), 3.61 - 3.69 (m, 4H), 3.33 - 3.48 (m, 4H); ^{13}C NMR (50 MHz, CD$_3$OD): 139.5, 133.3 (d, J = 8.0 Hz), 128.6, 118.2, 65.7 (d, J = 5.0 Hz), 48.8 (d, J = 5.0 Hz), 41.2; IR (film): 3415, 1655, 1437, 1407, 1315, 1022, 953 cm^{-1}; MS (ESI$^+$): m/z (intensity), 352.1 ([M + H]$^+$, 100%), 354.1 ([M + H]$^+$ + 2, 65%), 356.1 ([M + H]$^+$ + 4, 10%), 393.2

([M + H]$^+$ + CH$_3$CN, 20%), 395.2 ([M + H]$^+$ + 2 + CH$_3$CN, 13%, 397.2 ([M + H]$^+$ + 4 + CH$_3$CN, 2%).

Synthesis of TFA-*L*-glutamine (70)
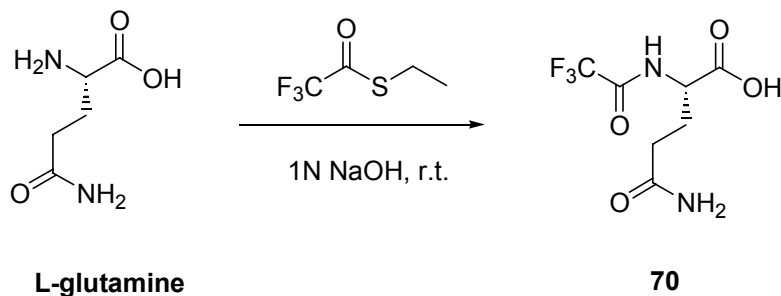
L-glutamine   70

To a solution of L-glutamine (14.6 g, 0.1 mol) in 1N NaOH (100 mL, 0.1 mol) was added S-ethyl thioacetate (17 mL, 0.13 mol). The reaction was carried out at room temperature for 24 h. The reaction solution was acidified with 12N HCl to pH ~ 2.0, saturated with NaCl, and then extracted with EtOAc. The combined EtOAc phase was washed with water, brine and dried over Na$_2$SO$_4$. After removal of Na$_2$SO$_4$ via filtration, the filtrate was concentrated to dryness to afford the desired product **70** (20.4 g) as white powder in a yield of 84%. ^{1}H NMR (200 MHz, CD$_3$OD): δ 4.47 (dd, 1H, J = 9.0 Hz, J = 4.8 Hz), 2.35-2.42 (m, 4H), 2.21-2.32 (m, 1H), 1.96-2.18 (m, 1H); ^{13}C NMR (50 MHz, CD$_3$OD): 175.6, 171.4, 157.2 (q, J = 37.0 Hz), 115.5 (q, J = 285.0 Hz), 51.8, 30.5, 25.6; MS (ESI$^-$): *m/z* (intensity), 241.1 ([M - H]$^-$, 100%).

Synthesis of fluorinated 4-(N^α-TFA-*L*-glutaminyl)amino-benzyl phosphoramide mustards 71a-e

a $R_1 = F$, R_2, R_3, $R_4 = H$
b R_1, R_3, $R_4 = H$, $R_2 = F$
c R_1, $R_4 = H$, R_2, $R_3 = F$
d R_1, R_2, R_3, $R_4 = F$
e R_1, R_2, R_3, $R_4 = H$
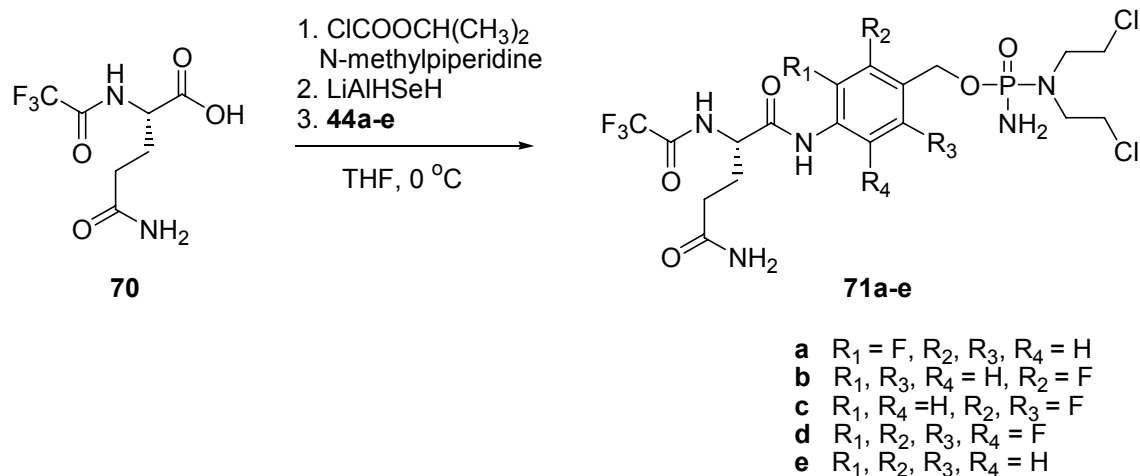
To a solution of TFA-glutamine (2.0 mmol) and *N*-methylpiperidine (0.244 mL, 2.0 mmol) in THF (10 mL) was added a solution of isopropylchloroformate in toluene (2.0 mL, 2.0 mmol) at - 15 °C. The resulting mixture was stirred for 30 minutes at - 15 to - 10 °C. Then, the obtained mixed anhydride solution was added into the freshly prepared solution of LiAlHSeH in THF via cannula over a period of 5 min. The reaction mixture was stirred for additional 30 min below 5 °C under nitrogen atmosphere. Then, a solution of azide **44a-e** (1.0 mmol) in THF (1 mL) was added into the above selenocarboxylate solution via syringe. The reaction was carried out at room temperature for 24 h. After evaporation of THF under reduced pressure, the residue was suspended in a saturated sodium bicarbonate aqueous solution (25 mL) followed by extraction with EtOAc (4 x 50 mL). The combined organic phase was washed with 1.0 M HCl (50 mL), water (50 mL) and saturated brine (50 mL), and dried over Na_2SO_4. After removal of

Na$_2$SO$_4$ through filtration, the filtrate was concentrated to dryness under reduced pressure. The crude product was purified by flash column chromatography (FCC) (dichloromethane to 10% methanol/dichloromethane) on silica gel to provide desired product **71a-e**.

4-(N^α-TFA-L-glutaminyl)amino-3-fluoro-benzyl phosphoramide mustard (71a): a yellow semi-solid (114 mg, 20%); ^{1}H NMR (200 MHz, CD$_3$OD): δ 7.83 (t, 1H, J = 8.0 Hz), 7.15 – 7.26 (m, 2H), 4.93 (d, 2H, J = 7.2 Hz), 4.61 (dd, 1H, J = 8.6 Hz, J = 5.2 Hz), 3.59 – 3.66 (m, 4H), 3.33 – 3.45 (m, 4H), 2.37 – 2.44 (m, 2H), 2.09 – 2.27 (m, 2H); MS (ESI$^+$): m/z (intensity), 348.2 ([M – OP(O)NH$_2$N(CH$_2$CH$_2$Cl)$_2$]$^+$, 100%), 366.3 ([M – OP(O)NH$_2$N(CH$_2$CH$_2$Cl)$_2$]$^+$ + H$_2$O, 55%), 407.3 ([M – OP(O)NH$_2$N(CH$_2$CH$_2$Cl)$_2$]$^+$ + H$_2$O + CH$_3$CN, 15%), 568.3 ([M + H]$^+$, 40%), 570.3 ([M + H]$^+$ + 2, 26%), 572.3 ([M + Na]$^+$ + 4, 4%), 590.3 ([M + Na]$^+$, 30%), 592.3 ([M + Na]$^+$ + 2, 20%), 594.23 ([M + Na]$^+$ + 4, 3%).

4-(N^α-TFA-L-glutaminyl)amino-2-fluoro-benzyl phosphoramide mustard (71b): a yellow semi-solid (312 mg, 55%); ^{1}H NMR (200 MHz, CD$_3$OD): δ 7.84 (dd, 1H, J = 1.8 Hz, J = 12.4 Hz), 7.66 (t, 1H, J = 8.2 Hz), 7.54 (dd, 1H, J = 2.2 Hz, J = 8.4 Hz), 5.21 (d, 2H, J = 6.8 Hz), 4.75 (dd, 1H, J = 8.0 Hz, J = 5.2 Hz), 3.82 – 3.89 (m, 4H), 3.58 – 3.68 (m, 4H), 2.57 – 2.67 (m, 2H), 2.22 – 2.48 (m, 2H); ^{13}C NMR (50 MHz, CD$_3$OD): 177.4, 170.8, 161.9 (d, J = 244.3 Hz), 159.0 (q, J = 36.8 Hz), 141.5 (d, J = 11.0 Hz), 131.7 (d, J = 5.3 Hz), 120.8 (dd, J = 15.0 Hz, J = 8.4 Hz), 117.3 (q, J = 284.9 Hz), 116.6 (d, J = 3.0 Hz), 108.1 (d, J = 26.6 Hz), 61.9, 53.4, 50.6 (d, J = 5.0 Hz), 43.1, 32.3, 28.2; IR (film):

3404, 2962, 1666, 1627, 1549, 1189, 1161, 998 cm^{-1}; MS (ESI$^+$): *m/z* (intensity), 348.2

([M − OP(O)NH$_2$N(CH$_2$CH$_2$Cl)$_2$]$^+$, 25%), 366.2 ([M − OP(O)NH$_2$N(CH$_2$CH$_2$Cl)$_2$]$^+$ +

H$_2$O, 100%), 407.3 ([M − OP(O)NH$_2$N(CH$_2$CH$_2$Cl)$_2$]$^+$ + H$_2$O + CH$_3$CN, 40%), 590.3

([M + Na]$^+$, 20%), 592.3 ([M + Na]$^+$ + 2, 13%), 594.3 ([M + Na]$^+$ + 4, 2%).

4-(N^α-TFA-*L*-glutaminyl)amino-2,6-difluoro-benzyl phosphoramide mustard (71c):
a yellow semi-solid (422 mg, 72%); ^{1}H NMR (200 MHz, CD$_3$OD): δ 7.31 (d, 1H, *J* = 9.6

Hz), 5.00 (d, 2H, *J* = 7.0Hz), 4.50 (dd, 1H, *J* = 8.6 Hz, *J* = 5.2 Hz), 3.53 − 3.64 (m, 4H),

3.33 − 3.44 (m, 4H), 2.30 − 2.41 (m, 2H), 2.04 − 2.25 (m, 2H); ^{13}C NMR (50 MHz,

CD$_3$OD): 177.3, 170.9, 163.0 (dd, *J* = 246.5 Hz, *J* = 9.9 Hz), 159.1 (q, *J* = 37.5 Hz),

142.4 (t, *J* = 14.0 Hz), 117.3 (q, *J* = 285.3 Hz), 109.2 (td, *J* = 19.8 Hz, *J* = 8.4 Hz), 103.7

(d, *J* = 29.6 Hz), 55.4, 50.6 (d, *J* = 4.9 Hz), 50.4, 42.9, 32.0, 28.0; IR (film): 3295, 3075,

2966, 1698, 1668, 1615, 1556, 1425, 1215, 1012 cm^{-1}; MS (ESI$^-$): *m/z* (intensity), 584.1

([M - H]$^-$, 100%), 586.1 ([M - H]$^-$ + 2, 65%), 588.1 ([M - H]$^-$ + 4, 10%), 698.1 ([M - H]$^-$

+ TFA, 40%), 700.1 ([M - H]$^-$ + 2 + TFA, 26%), 702.1 ([M - H]$^-$ + 4 + TFA, 4%).

**4-(N^α-TFA-*L*-glutaminyl)amino-2,3,5,6-tetrafluoro-benzyl phosphoramide mustard
(71d):** a yellow semi-solid (541 mg, 87%); ^{1}H NMR (200 MHz, CD$_3$OD): δ 5.13 (d, 2H,

J = 7.6Hz), 4.66 (dd, 1H, *J* = 8.0 Hz, *J* = 5.2 Hz), 3.60 − 3.68 (m, 4H), 3.37 − 3.47 (m,

4H), 2.40 − 2.47 (m, 2H), 2.07 − 2.37 (m, 2H); ^{13}C NMR (50 MHz, CD$_3$OD): 177.3,

171.3, 159.2 (q, *J* = 37.6 Hz), 147.6 (dm, *J* = 245.0 Hz), 143.8 (dm, *J* = 245.0 Hz), 118.5

(t, *J* = 14.8 Hz), 117.3 (q, *J* = 285.0 Hz), 114.9 (td, *J* = 17.7 Hz, *J* = 8.0 Hz), 55.5, 54.9,

50.6 (d, J = 4.9 Hz), 43.0, 32.0, 28.1; MS (ESI⁻): m/z (intensity), 620.1 ([M - H]⁻, 100%), 622.1 ([M - H]⁻ + 2, 65%), 624.1 ([M - H]⁻ + 2, 10%).

4-(N^α-TFA-L-glutaminyl)amino-benzyl phosphoramide mustard (71e): a yellow semi-solid (138 mg, 25%); ¹H NMR (200 MHz, CD₃OD): δ 7.62 (d, 2H, J = 8.4 Hz), 7.39 (d, 2H, J = 8.4 Hz), 4.97 (d, 2H, J = 7.2 Hz), 4.56 (dd, 1H, J = 8.0 Hz, J = 5.4 Hz), 3.61 – 3.68 (m, 4H), 3.32 – 3.41 (m, 4H), 2.38 – 2.45 (m, 2H), 2.09 – 2.27 (m, 2H); ¹³C NMR (50 MHz, CD₃OD): 175.5, 168.7, 157.2 (q, J = 37.5 Hz), 137.5, 132.5 (d, J = 7.5 Hz), 127.6, 119.5, 115.3 (q, J = 285.0 Hz), 65.9 (d, J = 5.3 Hz), 53.5, 48.8 (d, J = 5.0 Hz), 41.2, 30.3, 26.4; IR (film): 3261, 3063, 1715, 1608, 1545, 1213, 1185, 1159, 980 cm⁻¹; MS (ESI⁺): m/z (intensity), 572.1 ([M + Na]⁺, 100%), 574.1 ([M + Na]⁺ + 2, 65%), 576.1 ([M + Na]⁺ + 4, 10%).

Synthesis of fluorinated and non-fluorinated 4-L-glutamylamino-benzyl phosphoramide mustards 41a-e

a R_1 = F, R_2, R_3, R_4 = H
b R_1, R_3, R_4 = H, R_2 = F
c R_1, R_4 =H, R_2, R_3 = F
d R_1, R_2, R_3, R_4 = F
e R_1, R_2, R_3, R_4 = H

A solution of **71a-e** (1.0 mmol) and potassium carbonate (552 mg, 4.0 mmol) in 75% aqueous acetonitrile (20 mL) was stirred at room temperature for 48 h. The completion of

reaction was confirmed by LC/MS and TLC. The aqueous phase was saturated with sodium chloride followed by extraction with acetonitrile (3 x 10 mL). The combined acetonitrile phase was dried over Na_2SO_4 followed by filtration off Na_2SO_4. The filtrate was concentrated to dryness. The crude was purified by flash column chromatography (FCC) (dichloromethane to 25% methanol/dichloromethane containing 1% conc. NH_4OH) on silica gel to provide the desired product **41a-e**.

.

4-*L*-glutaminylamino-3-fluoro-benzyl phosphoramide mustard (41a). a yellow semi-solid (348 mg, 74%); ^{1}H NMR (200 MHz, CD_3OD): δ 8.03 (t, 1H, J = 8.0 Hz), 7.18 – 7.29 (m, 2H), 4.96 (d, 2H, J = 7.6 Hz), 4.17 (t, 1H, J = 8.0 Hz), 3.60 – 3.68 (m, 4H), 3.39 – 3.55 (m, 4H), 2.38 – 2.47 (m, 2H), 1.90 – 2.21 (m, 2H); MS (ESI[+]): *m/z* (intensity), 252.1 ([M – OP(O)NH_2N(CH_2CH_2Cl)$_2$][+], 100%), 472.2 ([M + H][+], 20%), 474.2 ([M + H][+] + 2, 13%), 476.2 ([M + Na][+] + 4, 2%), 494.2 ([M + Na][+], 50%), 496.2 ([M + Na][+] + 2, 33%), 498.2 ([M + Na][+] + 4, 5%). HRMS (FAB[+]) m/z calc'd for $C_{16}H_{25}Cl_2FN_5O_4P$, [M + H][+], 472.1084, found 472.1046.

4-*L*-glutaminylamino-2-fluoro-benzyl phosphoramide mustard (41b). a yellow semi-solid (358 mg, 76%); ^{1}H NMR (200 MHz, CD_3OD): δ 7.65 (dd, 1H, J = 12.4 Hz, J = 1.8 Hz), 7.46 (t, 1H, J = 8.4 Hz), 7.32 (dd, 1H, J = 8.4 Hz, J = 2.2 Hz), 5.00 (d, 2H, J = 7.4 Hz), 4.07 (t, 1H, J = 6.2 Hz), 3.59 – 3.66 (m, 4H), 3.36 – 3.46 (m, 4H), 2.46 – 2.53 (m, 2H), 2.09 – 2.25 (m, 2H); ^{13}C NMR (50 MHz, CD_3OD): 176.9, 168.6, 162.1 (d, J = 244.7 Hz), 141.0 (d, J = 11.0 Hz), 132.0 (d, J = 5.0 Hz), 121.3 (dd, J = 13.7 Hz, J = 7.6 Hz), 116.5 (d, J = 3.4 Hz), 108.1 (d, J = 26.6 Hz), 61.8, 54.8, 50.7 (d, J = 5.0 Hz), 43.0, 31.7,

28.2; IR (film): 3200, 3064, 1670, 1623, 1555, 1203, 1135, 982 cm^{-1}; MS (ESI$^+$): *m/z* (intensity), 252.1 ([M − OP(O)NH$_2$N(CH$_2$CH$_2$Cl)$_2$]$^+$, 100%), 494.3 ([M + Na]$^+$, 80%), 496.3 ([M + Na]$^+$ + 2, 52%), 498.3 ([M + Na]$^+$ + 4, 8%). HRMS (FAB$^+$) m/z calc'd for C$_{16}$H$_{25}$Cl$_2$FN$_5$O$_4$P, [M + H]$^+$, 472.1084, found 472.1034.

4-*L*-glutaminylamino-2,6-difluoro-benzyl phosphoramide mustard (41c). a yellow semi-solid (416 mg, 85%); ^{1}H NMR (200 MHz, CD$_3$OD): δ 7.36 (d, 1H, *J* = 9.4 Hz), 5.02 (d, 2H, *J* = 6.8 Hz), 4.61 (t, 1H, *J* = 8.6 Hz), 3.52 − 3.66 (m, 4H), 3.35 − 3.45 (m, 4H), 2.35 − 2.43 (m, 2H), 1.91 − 2.16 (m, 2H); ^{13}C NMR (50 MHz, CD$_3$OD): 177.6, 173.6, 163.1 (dd, *J* = 246.2 Hz, *J* = 10.3 Hz), 142.4 (t, *J* = 14.0 Hz), 109.4 (td, *J* = 19.8 Hz, *J* = 8.4 Hz), 103.7 (d, *J* = 30.4 Hz), 55.7, 55.5 (t, *J* = 3.4 Hz), 50.7 (d, *J* = 4.6 Hz), 43.0, 32.2, 30.6; IR (film): 3269, 3073, 1673, 1638, 1557, 1427, 1203, 1136, 1014 cm^{-1}; MS (ESI$^-$): *m/z* (intensity), 270.1 ([M − OP(O)NH$_2$N(CH$_2$CH$_2$Cl)$_2$]$^+$, 75%), 512.1 ([M + H]$^+$, 100%), 514.1 ([M + H]$^+$ + 2, 65%), 516.1 ([M + Na]$^+$ + 4, 10%). HRMS (FAB$^+$) m/z calc'd for C$_{16}$H$_{24}$Cl$_2$F$_2$N$_5$O$_4$P, [M + H]$^+$, 490.0989, found 490.0998.

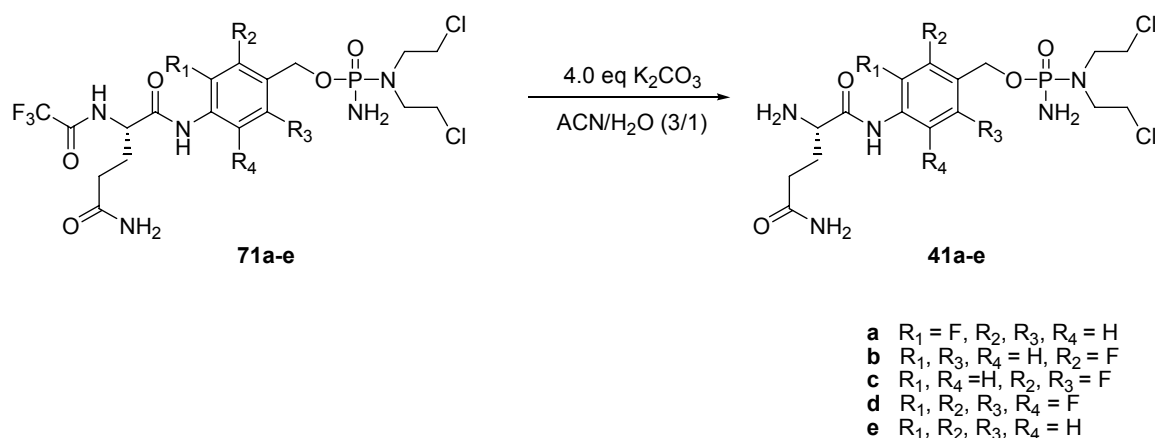**4-*L*-glutaminylamino-2,3,5,6-tetrafluoro-benzyl phosphoramide mustard (41d).** a yellow semi-solid (410 mg, 78%); ^{1}H NMR (200 MHz, CD$_3$OD): δ 5.14 (d, 2H, *J* = 8.2 Hz), 4.06 (dd, 1H, *J* = 7.0 Hz, *J* = 5.4 Hz), 3.60 − 3.68 (m, 4H), 3.35 − 3.47 (m, 4H), 2.47 − 2.54 (m, 2H), 1.90 − 2.28 (m, 2H); ^{13}C NMR (50 MHz, CD$_3$OD): 176.9, 169.6, 147.6 (dm, *J* = 245.1 Hz), 143.6 (dm, *J* = 247.4 Hz), 118.0 (t, *J* = 14.8 Hz), 115.3 (td, *J* = 17.7 Hz, *J* = 8.0 Hz), 55.5, 54.4, 50.6 (d, *J* = 5.0 Hz), 43.0, 31.5, 28.5; MS (ESI$^-$): *m/z*

(intensity), 526.1 ([M + H]$^+$, 100%), 528.1 ([M + H]$^+$ + 2, 65%), 530.1 ([M + Na]$^+$ + 4, 10%), 548.1 ([M + Na]$^+$, 40%), 550.1 ([M + Na]$^+$ + 2, 26%), 552.1 ([M + Na]$^+$ + 4, 4%). HRMS (FAB$^+$) m/z calc'd for $C_{16}H_{22}Cl_2F_4N_5O_4P$, [M + H]$^+$, 526.0801, found 526.0796.

4-*L*-glutaminylamino-benzyl phosphoramide mustard (41e). a yellow semi-solid (326 mg, 72%); ^{1}H NMR (200 MHz, CD$_3$OD): δ 7.66 (d, 2H, J = 8.4 Hz), 7.40 (d, 2H, J = 8.4 Hz), 4.97 (d, 2H, J = 7.6 Hz), 3.61 – 3.69 (m, 4H), 3.38 – 3.48 (m, 4H), 2.36 – 2.45 (m, 2H), 2.09 – 2.27 (m, 2H); IR (film): 3202, 3064, 1671, 1203, 1134cm^{-1}; MS (ESI$^+$): *m/z* (intensity), 476.1 ([M + Na]$^+$, 100%), 478.1 ([M + Na]$^+$ + 2, 65%), 480.1 ([M + Na]$^+$ + 4, 10%). HRMS (FAB$^+$) m/z calc'd for $C_{16}H_{26}Cl_2N_5O_4P$, [M + H]$^+$, 454.1178, found 454.1178.

Synthesis of fluorinated and non-fluorinated Glutaryl-Hyp-Ala-Ser-Chg-Gln-NH-benzyl phosphoramide mustards (40a-e)

72

1. HBTU/DIPEA, **41a-e**
2. 20 eq DEA

40a-e

a R_1 = F, R_2, R_3, R_4 = H
b R_1, R_3, R_4 = H, R_2 = F
c R_1, R_4 =H, R_2, R_3 = F
d R_1, R_2, R_3, R_4 = F
e R_1, R_2, R_3, R_4 = H
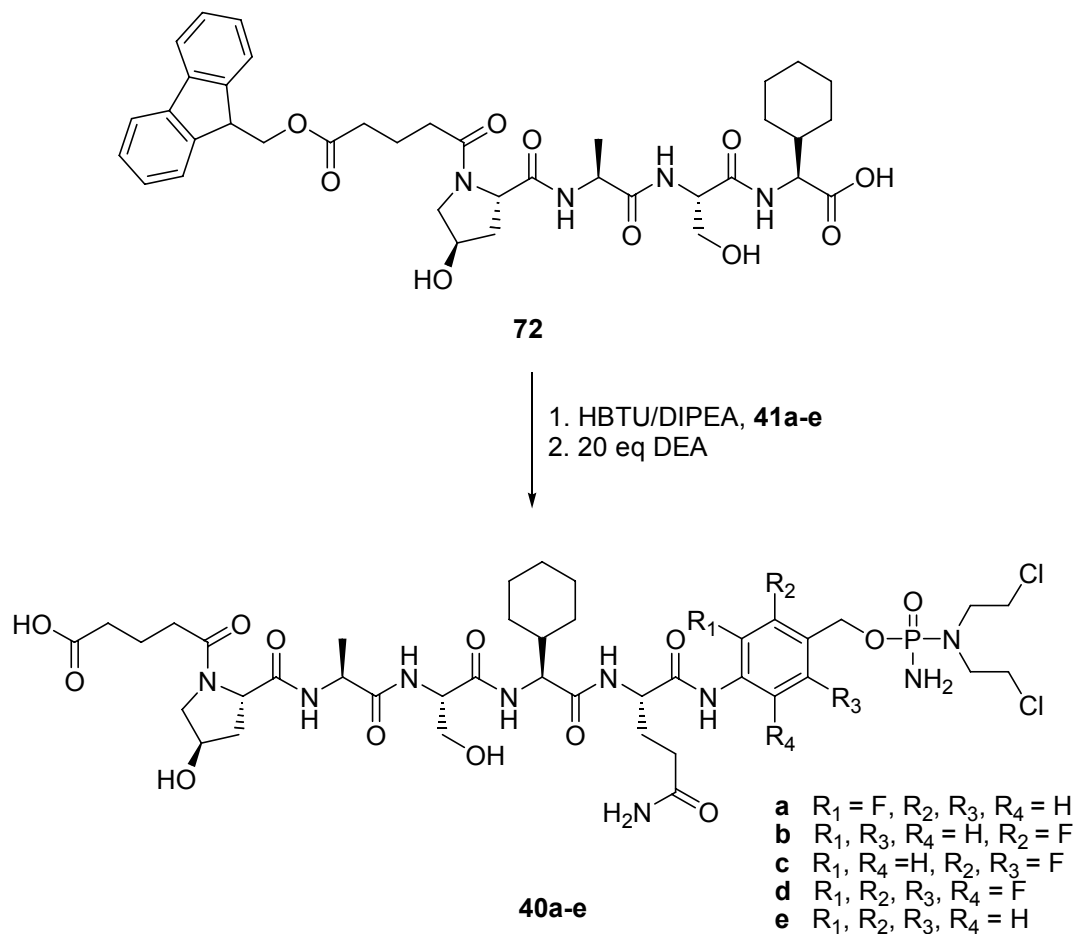
To a solution of Fm-glutaryl-Hyp-Ala-Ser-Chg-OH (72) (0.1 mmol) and HBTU (0.11 mmol) in NMP (2 mL) was added DIPEA (0.11 mmol). The resulting mixture was stirred at room temperature for 30 min followed by addition of a solution of **41a-e** (0.1 mmol) in NMP (0.5 mL). The reaction was carried out at room temperature for additional 2 h and quenched by adding ice-cold 5% aqueous sodium bicarbonate (10 mL). The resulting mixture was stirred at 0 – 5 $^{\circ}$C for 10 min and the resulting white precipitates were collected via centrifugation followed by successively washing with distilled water. The obtained solid was then dissolved in 50% MeOH/CH$_3$CN and treated with 10 equiv of

DEA for 1 h. After removal of solvents under reduced pressure, the remaining solid was suspended in diethyl ether and collected via centrifugation. The crude products were purified by preparative-HPLC on reversed phase C18 column. A linear gradient was used from 10% solvent A to 90% solvent B with a flow rate of 12 mL/min, where solvent A was 0.1% TFA/H_2O and solvent B was 0.1% TFA/CH_3CN. The UV detection wavelength was set at 245 nm. Homogeneous fraction containing the desired products were pooled and lyophilized to afford the desired products as white powder. The purities and identities were confirmed by LC/MS.

Glutaryl-Hyp-Ala-Ser-Chg-Gln-NH-3-fluorobenzyl phosphoramide mustard (40a). White powder (28 mg, 28%); HRMS (FAB$^+$) m/z calc'd for $C_{40}H_{61}Cl_2FN_9NaO_{13}P$, [M + Na]$^+$, 1018.3385, found 1018.3363.

Glutaryl-Hyp-Ala-Ser-Chg-Gln-NH-2-fluorobenzyl phosphoramide mustard (40b). White powder (40 mg, 38%); HRMS (FAB$^+$) m/z calc'd for $C_{40}H_{61}Cl_2FN_9NaO_{13}P$, [M + Na]$^+$, 1018.3385, found 1018.3357.

Glutaryl-Hyp-Ala-Ser-Chg-Gln-NH-2,6-difluorobenzyl phosphoramide mustard (74c). White powder (41 mg, 40%); HRMS (FAB$^+$) m/z calc'd for $C_{40}H_{60}Cl_2F_2N_9NaO_{13}P$, [M + Na]$^+$, 1036.3291, found 1036.3181.

Glutaryl-Hyp-Ala-Ser-Chg-Gln-NH-2,3,5,6-tetrafluorobenzyl phosphoramide mustard (40d). White powder (32 mg, 30%); HRMS (FAB$^+$) m/z calc'd for $C_{40}H_{58}Cl_2F_4N_9NaO_{13}P$, $[M + Na]^+$, 1072.3103, found 1072.2985.

Glutaryl-Hyp-Ala-Ser-Chg-Gln-NH-benzyl phosphoramide mustard (74e). White powder (30 mg, 30%); HRMS (FAB+) m/z calc'd for $C_{40}H_{62}Cl_2N_9NaO_{13}P$, $[M + Na]^+$, 1000.34790, found 1000.3477.

Stability study of 40a-e in buffers

The peptide conjugate **40a-e** (1 mg) was dissolved in 0.5 mL of 50 mM Na_2HPO4/NaH_2PO4 buffer (pH 7.4) containing 2% DMSO or 0.5 mL of 50 mM Tris-HCl/10 mM $CaCl_2$/0.1% Tween-20$^®$ buffer (pH 8.0) containing 2% DMSO, respectively. At different time intervals, aliquots (25 µL) were withdrawn and frozen prior to HPLC analysis (Waters Symmetry C_{18} column - 3.5 µm, 4.6 x 150 mm, gradient elution from 10-80% acetonitrile containing 0.1% TFA at a flow rate at 1 mL/min, detection wavelength at 220 nm and 245 nm). The half-life was determined based on the disappearance of the peptide conjugate **40a-e**.

Prostate-specific antigen (PSA) assay of 40a-e

PSA was purchased from CALIBIOCHEM. The stock solution of peptide conjugate **40a-e** (5 µL, 10 mM in DMSO) was added to PSA buffer (295 µL, 50 mM Tris-HCl/10

mM $CaCl_2$/0.1% Tween-20® buffer, pH 8.0), respectively. The prepared solution was warmed up to 37 °C and then 245 μL of solution was transferred to an eppendorf vial containing PSA (5 μL, 2.45 mg/mL), respectively. At different time intervals, aliquots (20 μL) were withdrawn, quenched with acetonitrile (5 μL) and frozen prior to HPLC analysis (Waters Symmetry C_{18} column - 3.5 μm, 4.6 x 150 mm, gradient elution from 10-80% acetonitrile containing 0.1% TFA at a flow rate at 1 mL/min, detection wavelength at 220 nm and 245 nm). The half-life was determined based on the disappearance of peptide conjugate **40a-e**.

Cell culture and antiproliferative assays of 40a-e

Nitroreductase-targeted 4-nitroarylmethyl phosphoramide mustards **30a-e**: V79 Chinese hamster lung fibroblasts were grown in monolayer culture in DMEM containing 10% fetal calf serum and 4 mM glutamine. Cells were maintained in a humidified atmosphere at 37 °C with 5% CO_2 and subcultured twice weekly by trypsinization. A bicistronic eukaryotic expression vector containing the coding regions for *E coli* nitroreductase together with puromycin acetyl transferase (conferring puromycin resistance) driven from a single CMV promoter was constructed by cloning into the XhoI site of the vector pIRES-P (EMBL:Z75185; 1) using conventional techniques. Insert orientation and identity were confirmed by diagnostic restriction digests and dideoxy sequencing using a Sequenase II kit (Amersham Pharmacia Biotech, St. Albans, Herts, U.K.). The V79 cells were transfected with the bicistronic vector, and the positive clones were selected in growth medium containing 10 μg/mL puromycin and maintained under selective

pressure. Cells expressing *E. coli* nitroreductase in exponential phase of growth were trypsinized, seeded in 96-well plates at a density of 1000 cells/well, and permitted to recover for 24 h. V79 cells transfected with vector only were used as the controls. Serial dilutions of the drug solution were performed in situ, and cells were then incubated with drug for 3 days at 37 $^\circ$C. The plates were fixed and stained with SRB before reading with optical absorption at 570 nm; results were expressed as a percentage of control growth. IC$_{50}$ values are the concentration required to reduce cell number to 50% of control and were obtained by interpolation. For the short drug exposure experiments, cells were exposed to each test drug for 1 h and culture media was then replaced with drug free, fresh medium for continued incubation. Cell viability assay was performed 3 days after drug addition. For the control experiment using 4-hydroperoxycyclophosphamide, sealed microtiter plates were used to prevent the volatile metabolite from contaminating neighboring wells.

SKOV3 human ovarian carcinoma cells grown in HEPES-buffered DMEM with 10% FCS were infected with an E1, E3-deleted replication-defective adenovirus vector vPS1233 expressing the wild type *E. coli* nitroreductase from the CMV promoter, using infection ratios of 10 or 100 plaque forming units (pfu) per cell. Cells were plated in 96-well plates (at 15 000 or 20 000 cells/well in different experiments) and incubated for 2 days to allow for nitroreductase expression. The used medium was exchanged with fresh medium containing a range of prodrug concentrations up to 1000 μM. After 18 h of incubation, the medium was replaced with fresh medium (without prodrugs). An MTT assay was performed 3 days after adding prodrug to assess cell viability.

SKOV NTR cells were generated by infecting SKOV3 cells with the retrovirus rv.RD18.LNC-nr[38] and selecting clones of transduced cells with 1 mg/mL G418. NTR expression was confirmed by Western blots. For prodrug sensitivity assays, SKOV NTR or parental SKOV3 cells were plated in 96-well plates at 20 000 cells per well and allowed to adhere for 24 h. The medium was exchanged for fresh medium containing a range of prodrug concentrations. After 18 h of exposure to prodrug, the medium was removed and replaced with fresh medium lacking prodrug, and cell survival was determined by MTT assay after an additional 2 days.

PSA-activated peptidylaminoarylmethyl phosphoramide mustards **40a-e**: LNCaP (PSA positive, ATCC) and DU145 (PSA negative, ATCC) human prostate carcinoma cells were grown as monolayer cultures in the culture medium (RPMI 1640 with L-glutamine and phenol red, supplemented with 10% FBS, 100 units/mL penicillin G and 100 units/mL streptomycin sulfate). Cells were cultured in a humidified atmosphere of 5% $CO2$ at 37 $^{\circ}$C. Media were routinely changed every 72 h. Cells were split at 80% confluence followed by trypsinization and subcultured at 1:4. Cells were plated in 96-well plates (7500 LNCaP cells/well and 500 DU145 cells/well) and grown for 48 h in the culture medium. The medium was then replaced by the serum-free medium (RPMI 1640 with L-glutamine and without phenol red, supplemented with 2% TCM, 100 units/mL penicillin G and 100 units/mL streptomycin sulfate). Subsequently, cells were incubated with various peptide-conjugate concentrations (100 μM – 0.01 μM) for 72 h where medium alone was used as a negative control. A MTT dye solution (5 mg/mL) was then

added to the wells. The cells were then incubated at 37 $^{\circ}$C for 4 h followed by addition of a solubilization solution (sodium laurate) and incubation at room temperature overnight in dark. The plates were read at a wavelength of 570 nm by a Dynatech MR5000 microtiter plate reader. Results were expressed at a percentage of control growth. IC_{50} values, the concentration required to reduce the cell number to 50% of the control, were obtained by interpolation.

REFERENCES

(1)   Denmeade, S. R.; Lin, Z. S.; Isaacs, J. T. Role of programmed (apoptic) cell death during the progression and therapy for prostate cancer. *Prostate* **1996***, 28*, 251-265.

(2)   Bostwick, D.; Montironi, R. Prostatic intraepithelial neoplasia and the origins of prostatic carcinoma. *Pathol. Res. Pract.* **1995***, 191*, 828-832.

(3)   Berges, R. R.; Vukanovic, J.; Epstein, J. L. Implication of cell kinetic changes during the progression of human prostatic cancer. *Clin. Cancer. Res.* **1995***, 1*, 473-480.

(4)   Jemal, A.; Siegel, R.; Ward, E.; Murray, T.; Xu, J.; Thun, M. J. Cancer statistics in 2007. *CA Cancer J. Clin.* **2007***, 57*, 43-66.

(5)   Coffey, D. S. Prostate cancer - an overview of an increasing dilemma. *Cancer Suppl.* **1993***, 71*, 880-886.

(6)   Huggins, C. B.; Hodges, C. V. Studies on prostate cancer: 1. the effects of castration, of estrogen and androgen injection on serum phosphatases in metastatic carcinoma of the prostate. *Cancer Res.* **1941***, 1*, 293-297.

(7)   Hellerstedt, B. A.; Pienta, K. J. The current state of hormonal therapy for prostate cancer. *CA Cancer J. Clin.* **2002***, 52*, 154–179.

(8)   Yagoda, A.; Petrylak, D. Cytotoxic chemotherapy for advanced hormone-resistant prostate cancer. *Cancer* **1993***, 71*, 1098-1109.

(9)   Dagher, R.; Li, N.; Abraham, S. Approval summary: docetaxel in combination with prednisone for the treatment of androgen-independent hormone-refractory prostate cancer. *Clin. Cancer. Res* **2004***, 10*, 8147-8151.

(10)   Vieweg, J. Immunotherapy for advanced prostate cancer. *Rev. Urol.* **2007***, 9*, 29-38.

(11)   Weber, J. S. Tumor regression and autoimmunity in cytotoxic T lymphocyte-associated antigen 4 blockade-treated patients. *Ann. Surg. Oncol.* **2005***, 12*, 957-959.

(12)   Vieweg, J.; Jackson, A. An antigenic target for renal cell carcinoma immunotherapy. *Expert Opin. Biol. Ther.* **2004***, 4*, 1791-1801.

(13) Rodriguez, R.; Schuur, E. R.; Lim, H. Y.; Henderson, G. A.; Simons, J. W.; Henderson, D. R. Prostate attenuated replication competent adenovirus (ARCA) CN706: a selective cytotoxic for prostate-specific antigen-positive prostate cancer cells. *Cancer Res.* **1999***, 57,* 2559-2563.

(14) DeWeese, T. L.; van der Poel, H.; Li, S. A phase I trial of CV706, a replication-competent, PSA selective oncolytic adenovirus, for the treatment of locally recurrent prostate cancer following radiation therapy. *Cancer Res.* **2001***, 61,* 7464-7472.

(15) Denmeade, S. R.; Isaacs, J. T. Enzymatic activation of prodrugs by prostate-specific antigen: targeted therapy for metastatic prostate cancer. *Cancer J. Sci. Am.* **1998***, 4(suppl. 1),* 515-521.

(16) Ast, G. Drug-targeting strategies for prostate cancer. *Curr. Pharm. Des.* **2003***, 9,* 455-466.

(17) Janssen, S.; Rosen, D. M.; Ricklis, R. M.; Dionne, C. A.; Lilja, H.; Christensen, S. B.; Isaacs, J. T.; Denmeade, S. R. Pharmacokinetics, biodistribution, and antitumor efficacy of a human glandular kallikrein 2 (hk2)-activated thapsigargin prodrug. *Prostate* **2006***, 66,* 358-368.

(18) Warren, P.; Li, L.; Song, W.; Holle, E.; Wei, Y.; Wagner, T.; Yu, X. In vitro targeted killing of prostate tumor cells by a synthetic amoebapore helix 3 peptide modified with two γ-linked glutamate residues at the COOH terminus. *Cancer Res.* **2001***, 61,* 6783-6787.

(19) Hara, M.; Inoue, T.; Koyanagi, Y.; Fukuyama, T.; Iki, H. Immunochemical characteristics of human specific component "gamma-Sm". *Nippon Hoigaku Zasshi* **1969***, 23,* 333.

(20) Wang, M. C.; Valenzuela, L. A.; Murphy, G. P.; Chu, T. M. Purification of a human prostate specific antigen. *Invest. Urol.* **1979***, 17,* 159-163.

(21) Lilja, H. Kallikrein-like serine protease in prostatic fluid cleaves the predominant seminal vesicle protein. *J. Clin. Invest.* **1985***, 76,* 1899-1903.

(22) Christensson, A.; Laurell, C. B.; Lilja, H. Enzymatic activity of prostate-specific antigen and its reactions with extracellular serine protease inhibitors. *Eur. J. Biochem.* **1990***, 194,* 755-763.

(23)   Lilja, H.; Oldbring, J.; Rannevik, G.; Laurell, C. B. Seminal vesicle-secreted protein and their reactions during gelation and liquefaction of human semen. *J. Clin. Invest.* **1987***, 80*, 281-285.

(24)   Yoshida, E.; Ohmura, S.; Sugiki, M.; Maruyama, M.; Mihara, H. Prostate-specific antigen activates single-chain urokinase-type plasminogen activator. *Int. J. Cancer* **1995***, 63*, 863-865.

(25)   Killian, C. S.; Corral, D. A.; Kawinski, E.; Constantine, R. I. Mitogenic response of osteoblast cells to prostate-specific antigen suggests an activation of latent TGF-beta and a proteolytic modulation of cell adhesion receptors. *Biochem. Biophys. Res. Commun.* **1993***, 192*, 940-947.

(26)   Cohen, P.; Graves, H. C.; Peehl, D. M.; Kamarei, M.; Giudice, L. C.; Rosenfeld, R. G. Prostate-specific antigen (PSA) is an insulin-like growth factor binding protein-3 protease found in seminal plasma. *J. Clin. Endocrinol. Metab.* **1992***, 75*, 1046-1053.

(27)   Fortier, A. H.; Nelson, B. J.; Grella, D. K.; Holaday, J. W. Antiangiogenic activity of prostate-specific antigen. *J. Natl. Cancer Inst.* **1999***, 91*, 1635-1640.

(28)   Heidtmann, H. H.; Nettelbeck, D. M.; Mingels, A.; Jager, R.; Welker, H. G.; Kontermann, R. E. Generation of angiostatin-like fragments from plasminogen by prostate-specific antigen. *Br. J. Cancer* **1999***, 81*, 1269-1273.

(29)   Hassan, M. I.; Kumar, V.; Singh, T. P.; Yadav, S. Structural model of human PSA: a target for prostate cancer therapy. *Chem. Biol. Drug Des.* **2007***, 70*, 261–267.

(30)   Denmeade, S. R.; Sokoll, L. J.; Chan, D. W.; Knan, S. R.; Isaacs, J. T. Concentration of enzymatically active prostate-specific antigen (PSA) in the extracellular fluid of primary human prostate cancers and human prostate cancer xenograft models. *Prostate* **2001***, 48*, 1-6.

(31)   Castelian, W. J. Cancer (prostate-specific antigen). *Anal. Chem.* **1995**, 399-403.

(32)   McCormack, R. T.; Rittenhouse, H. G.; Finlay, J. A.; Sokolof, R. L.; Wang, T. J.; Wolfert, R. L.; Lilja, H.; Oesterling, J. E. Molecular forms of prostate-specific antigen and the human kallikrein gene family: a new era. *Urol.* **1995***, 45*, 729-744.

(33)   Catalona, W. J.; Smith, D. S.; Ratliff, T. L.; Dodds, K. M.; Coplen, D. E.; Yuan, J. J.; Petros, J. A.; Andriole, G. L. Measurement of prostate-specific antigen in

serum as a screening test for prostate cancer. *N. Engl. J. Med.* **1991***, 324*, 1156-1161.

(34) Lilja, H.; Christensson, A.; Dahlen, U.; Matikainen, M.; Nilsson, O.; Pettersson, K.; Lovgren, T. Prostate-specific antigen in serum occurs predominantly in complex with alpha1-antichymotrypsin. *Clin. Chem.* **1991***, 37*, 1618-1625.

(35) Otto, A.; Bar, J.; Birkenmeier, G. Prostate-specific antigen forms complexes with human alpha2-macroglobulin and binds to the alpha2-macrogloblin receptor/LDL receptor related protein. *J. Urol.* **1998***, 159*, 297-303.

(36) Lilja, H.; Abrahamsson, P. A.; Lundwall, A. Semenogelin, the predominant protein in human semen. Primary structure and identification of closely related proteins in the male accessory sex glands and on the spermatozoa. *J. Biol. Chem.* **1989***, 264*, 1894-1900.

(37) Coombs, G. S.; Chakravarty, P. K.; Katzenellenbogen, J. A.; Weber, M. J. Substrate specificity of prostate-specific antigen (PSA). *Chem. Biol.* **1998***, 5*, 475-488.

(38) Akiyama, K.; Nakamura, T.; Iwanaga, S.; Hara, M. The chymotrypsin-like activity of human prostate-specific antigen, seminoprotein. *FEBS Lett.* **1987***, 225*, 168-172.

(39) Yang, C. F.; Porter, E. S.; Boths, J.; Kanyi, D.; Hsieh, M.; Cooperman, B. S. Design of synthetic hexapeptide substrates for prostate-specific antigen using single-position minilibraries. *J. Peptide Res.* **1999***, 54*, 444-448.

(40) Denmeade, S. R.; Lou, W.; Lovgren, T.; Malm, J.; Lilja, H. Specific and efficient peptide substrates for assaying the proteolytic activity of prostate-specific antigen. *Cancer Res.* **1997***, 57*, 4924-4930.

(41) Garsky, V. M.; Lumma, P.; Feng, D.-M.; Wai, J.; Ramjit, H. G.; Sardana, M. K.; Oliff, A.; Jones, R. E.; DeFeo-Jones, D.; Freidinger, R. The synthesis of a prodrug of doxorubicin designed to provide reduced systemic toxicity and greater target efficacy. *J. Med. Chem.* **2001***, 44*, 4216-4224.

(42) Malm, J.; Hellman, J.; Magnusson, H.; Laurell, C. B.; Lilja, H. Isolation and characterization of the major gel proteins in human semen, semenogen I and semenogen II. *Eur. J. Biochem.* **1996***, 238*, 48-53.

(43) DeFeo-Jones, D.; Garsky, V. M.; Wong, B. K.; Feng, D.-M.; Bolyar, T.; Haskell, K.; Kiefer, D. M.; Leander, K.; McAvoy, E.; Lumma, P.; Wai, J.; Senderak, E. T.;

Motzel, S. L.; Keenan, K.; Van Zwieten, M.; Lin, J. H.; Freidinger, R.; Huff, J.; Oliff, A.; Jones, R. E. A peptide-doxorubicin 'prodrug' activated by prostate-specific antigen selectively kills prostate tumor cells positive for prostate-specific antigen *in vivo*. *Nature Med.* **2000**, *6*, 1248-1252.

(44)   Denmeade, S. R.; Jakobsen, C. M.; Janssen, S.; Khan, S. R.; Garrett, E. S.; Lilja, H.; Christensson, S. B.; Isaacs, J. T. Prostate-specific antigen-activated thapsigargin prodrug as targeted therapy for prostate cancer. *J. Natl. Cancer Inst.* **2003**, *95*, 990-1000.

(45)   Jakobsen, C. M.; Denmeade, S. R.; Isaacs, J. T.; Grady, A.; Olsen, C. E.; Christensen, S. B. Design, synthesis, and pharmacological evaluation of thapsigargin analogues for targeting apoptosis to prostatic cancer cells. *J. Med. Chem.* **2001**, *44*, 4696-4703.

(46)   Brady, S. F.; Pawluczyk, J. M.; Lumma, P.; Wai, J.; Jones, R. E.; DeFeo-Jones, D.; Wong, B. K.; Miller-Stein, C.; Lin, J. H.; Oliff, A. Design and synthesis of a pro-drug of vinblastine targeted at treatment of prostate cancer with enhanced efficacy and reduced systemic toxicity. *J. Med. Chem.* **2002**, *45*, 4706-4715.

(47)   DeFeo-Jones, D.; Brady, S. F.; Feng, D.-M.; Wong, B. K.; Bolyar, T.; Haskell, K.; Kiefer, D. M.; Leander, K.; McAvoy, E.; Lumma, P.; Pawluczyk, J. M.; Wai, J.; Motzel, S. L.; Keenan, K.; Van Zwieten, M. A prostate-specific antigen (PSA)-activated vinblastine prodrug selectively kills PSA-secreting cells *in vivo*. *Mol. Cancer Ther.* **2002**, *1*, 451-459.

(48)   Mhaka, A.; Denmeade, S. R.; Yao, W.; Isaacs, J. T.; Khan, S. R. A 5-fluorodeoxyuridine prodrug as targeted therapy for prostate cancer. *Bioorg. Med. Chem. Lett.* **2002**, *12*, 2459-2461.

(49)   Tang, X.; Xian, M.; Trikha, M.; Honn, K. V.; Wang, P. G. Synthesis of peptide-diazeniumdiolate conjugates: towards enzyme activated antitumor agents. *Tetrahedron Lett.* **2001**, *42*, 2625-2629.

(50)   Jones, G. B.; Mitchell, M. O.; Weinberg, J. S.; D'Amico, A. V.; Bubley, G. J. Towards enzyme activated antiprostatic agents. *Bioorg. Med. Chem. Lett.* **2000**, *10*, 1987-1989.

(51)   Williams, S. A.; Merchant, R. F.; Garrett-Mayer, E.; Isaacs, J. T.; Buckley, J. T.; Denmeade, S. R. A prostate-specific antigen-activated channel-forming toxin as therapy for prostatic disease. *J. Natl. Cancer Inst.* **2007**, *99*, 376-385.

(52) Kumar, S. K.; Williams, S. A.; Isaacs, J. T.; Denmeade, S. R.; Khan, S. R. Modulating paclitaxel bioavailability for targeting prostate cancer. *Bioorg. Med. Chem.* **2007**, *15*, 4973-4984.

(53) Newling, D. W. W. The use of adriamycin and its derivatives in the treatment of prostatic cancer. *Cancer Chemother. Pharmacol.* **1992**, *30 (Suppl.)*, 90-94.

(54) Sella, A.; Kilboum, R.; Amato, R.; Bui, C.; Zukiwski, A. A.; Ellerhorst, J.; Logothetis, C. J. Phase II study of ketoconazole combined with weekly doxorubicin in patients with androgen-independent prostate cancer. *J. Clin. Oncol.* **1994**, *12*, 683-688.

(55) Denmeade, S. R.; Nagy, A.; Schally, A.; Isaacs, J. T. Enzymatic activation of a doxorubicin prodrug by prostate-specific antigen. *Proc. Am. Assoc. Cancer Res.* **1998**, *39*, 3765.

(56) Deprez-deCampeneere, D.; Baurain, R.; Trouet, A. Accumulation and metabolism of new anthracycline derivatives in the heart after iv injection into mice. *Cancer Chemother. Pharmacol.* **1982**, *8*, 193-197.

(57) DeJone, J.; Kleine, I.; Bast, A.; van der Vijgh, W. Analysis and pharmacokinetics of *N*-L-leucyldoxorubicin and metabolites in tissues of tumor-bearing BALB/c mice. *Cancer Chemother. Pharmacol.* **1992**, *31*, 156-160.

(58) DeJone, J.; Geijssen, J.; Munniksma, C. N.; Vermorken, J. B.; van der Vijgh, W. Plasma pharmacokinetics and pharmacodynamics of a new prodrug N-L-leucyldoxorubicin and its metabolites in phase I clinical trial. *J. Clin. Oncol.* **1992**, *10*, 1897-1906.

(59) Wong, B. K.; DeFeo-Jones, D.; Jones, R. E.; Garsky, V. M.; Feng, D.-M.; Oliff, A. PSA-specific and non-PSA-specific conversion of a PSA-targeted peptide conjugate of doxorubicin to its active metabolites. *Drug Metab. Dispos.* **2001**, *29*, 313-318.

(60) DiPaola, R. S.; Rinehart, J.; Nemunaitis, J.; Ebbinghaus, S.; Rubin, E.; Capanna, T. Characterization of a novel prostate-specific antigen-activated peptide-doxorubicin conjugate in patients with prostate cancer. *J. Clin. Oncol.* **2002**, *20*, 1874-1879.

(61) Kratz, F.; Beyer, U. Serum proteins as drug carriers of anticancer agents. *Drug Deliv.* **1998**, *5*, 1-19.

(62)   Kratz, F.; Mansour, A.; Soltau, J.; Warnecke, A.; Fichtner, I.; Unger, C.; Drevs, J. Development of albumin-binding doxorubicin prodrugs that are cleaved by prostate-specific antigen. *Arch. Pharm. Chem. Life Sci.* **2007***, 338*, 462-472.

(63)   Graeser, R.; Chung, D.; Esser, N.; Moor, S.; Schächtele, C.; Unger, C.; Kratz, F. Synthesis and biological evaluation of an albumin-binding prodrug of doxorubicin that is cleaved by prostate-specific antigen (PSA) in a PSA-positive orthotopic prostate carcinoma model (LNCaP). *Int. J. Cancer* **2007***, 122*, 1145-1154.

(64)   Pedersen, A.; Jacobsen, J. Reactivity of the thiol group in human and bovine albumin at pH 3-9, as measured by exchange with 2,2'-dithiopyridine. *Eur. J. Biochem.* **1980***, 106*, 291-295.

(65)   Kratz, F.; Mansour, A.; Soltau, J.; Warnecke, A.; Fichtner, I.; Unger, C.; Drevs, J. Development of albumin-binding doxorubicin prodrugs that are cleaved by prostate-specific antigen. *Arch. Pharm. Chem. Life Sci.* **2005***, 338*, 462-472.

(66)   Beyermann, M.; Bienert, M.; Niedrich, H.; Carpino, L. A.; Sadat-Aalee, D. Rapid continuous peptide synthesis via Fmoc amino acid chloride coupling and 4-(aminomethyl)piperidine deblocking. *J. Org. Chem.* **1990***, 55*, 721-728.

(67)   Stewart, D. E.; Sarkar, A.; Wampler, J. E. Occurrence and role of *cis* peptide bonds in protein structures. *J. Mol. Biol.* **1990***, 214*, 253-260.

(68)   Stein, C. A. Mechanisms of action of taxanes in prostate cancer. *Semin. Oncol.* **1999***, 26 (5 Suppl 17)*, 3-7.

(69)   Santi, D. V.; McHenry, C. S.; Raines, R. T.; Ivanetich, K. M. Kinetics and thermodynamics of the interaction of 5-fluoro-2'-deoxyuridylate with thymidylate synthase. *Biochemistry* **1987***, 26*, 8606-8613.

(70)   Wei, Y.; Pei, D. Activation of antibacterial prodrugs by peptide deformylase. *Bioorg. Med. Chem. Lett.* **2000***, 10*, 1073-1076.

(71)   Thastrup, O.; Cullen, P. J.; DrØbak, B. K.; Hanley, M. R.; Dawson, A. P. Thapsigargin, a tumor promoter, discharges intracellular Ca^{2+} stores by specific inhibition of the endoplasmic reticulum Ca^{2+}-ATPase. *Proc. Natl. Acad. Sci. USA.* **1990***, 87*, 2466-2470.

(72)   Randriamampita, C.; Tsien, R. Y. Emptying of intracellular Ca^{2+} stores releases a novel small messenger that stimulates Ca^{2+} influx. *Nature* **1993***, 364*, 809-814.

(73)   Wink, D. A.; Vodovotz, Y.; Laval, J.; Laval, F.; Dewhirst, M. W.; Mitchell, J. B. The multifaceted roles of nitric oxide in cancer. *Carcinogenesis* **1998***, 19*, 711-721.

(74)   Fitzhugh, A. L.; Keefer, L. K. Diazeniumdiolates: pro- and antioxidant applications of the "NONOates". *Free. Radic. Biol. Med.* **2000***, 28*, 1463-1469.

(75)   Saavedra, J. E.; Shami, P. J.; Wang, L. Y.; Davies, K. M.; Booth, M. N.; Citro, M. L.; Keefer, L. K. Esterase-sensitive nitric oxide donors of the diazeniumdiolate family: in vitro antileukemic activity. *J. Med. Chem.* **2000***, 43*, 261-269.

(76)   Abrami, L.; Fivaz, M.; van der Goot, F. G. Adventures of a pore-forming toxin at the target cell surface. *Trends Microbiol.* **2000***, 8*, 168-172.

(77)   Rossjohn, J.; Feil, S. C.; McKinstry, W. J.; Tsernoglou, D.; van der Goot, F. G.; Buckley, J. T. Aerolysin - a paradigm for membranes insertion of beta-sheet protein toxins? *J. Struct. Biol.* **1998***, 121*, 92-100.

(78)   Denny, W. A. Nitroreductase-based GDEPT. *Curr. Pharm. Des.* **2002***, 8*, 1349-1361.

(79)   Liu, B.; Hu, L. 5'-(2-Nitrophenylalkanoyl)-2'-deoxy-5-fluorouridines as potential prodrugs of FUDR for reductive activation. *Bioorg. Med. Chem.* **2003***, 11*, 3889-3899.

(80)   Li, Z.; Han, J.; Jiang, Y.; Browne, P.; Knox, R. J.; Hu, L. Nitrobenzocyclophosphamides as potential prodrugs for bioreductive activation: synthesis, stability, enzymatic reduction, and antiproliferative activity in cell culture. *Bioorg. Med. Chem.* **2003***, 11*, 4171-4178.

(81)   Hu, L.; Yu, C.; Jiang, Y.; Han, J.; Li, Z.; Browne, P.; Race, P. R.; Knox, R. J.; Searle, P. F.; Hyde, E. I. Nitroaryl phosphoramides as novel prodrugs for *E. coli* nitroreductase activation in enzyme prodrug therapy. *J. Med. Chem.* **2003***, 46*, 4818-4821.

(82)   Hu, L.; Liu, B.; Hacking, D. R. 5'-[2-(2-Nitrophenyl)-2-methylpropionyl]-2'-deoxy-5-fluorouridine as a potential bioreductive activated prodrug of FUDR: synthesis, stability, and reductive activation. *Bioorg. Med. Chem. Lett.* **2000***, 10*, 797-800.

(83)   Jiang, Y.; Han, J.; Yu, C.; Vass, S. O.; Searle, P. F.; Browne, P.; Knox, R. J.; Hu, L. Design, synthesis, and biological evaluation of cyclic and acyclic nitrobenzyl

phosphoramide mustards for E. coli nitroreductase activation. *J. Med. Chem.* **2006***, 49*, 4333-4343.

(84) Searle, P. F.; Chen, M.-J.; Hu, L.; Race, P. R.; Lovering, A. L.; Grove, J. I.; Guise, C.; Jaberipour, M.; James, N. D.; Mautner, V.; Young, L. S.; Kerr, D. J.; Mountain, A.; White, S. A.; Hyde, E. I. Nitroreductase: a prodrug-activating enzyme for gene therapy. *Clin. Exp. Pharmacol. Physiol.* **2004***, 31*, 811-816.

(85) Bridgewater, J. A.; Springer, C. J.; Knox, R. J.; Minton, N. P.; Michael, N. P.; Collins, M. K. Expression of the bacterial nitroreductase enzyme in mammalian cells renders them selectively sensitive to killing by the prodrug CB1954. *Eur. J. Cancer* **1995***, 31A*.

(86) Knox, R. J.; Friedlos, F.; Sherwood, R. F.; Melton, R. G.; Anlezark, G. M. The bioactivation of 5-(aziridin-1-yl)-2,4-dinitrobenzamide (CB1954). II. A comparison of an *Escherichia coli* nitroreductase and Walker DT diaphorase. *Biochem. Pharmacol.* **1992***, 44*, 2297-2301.

(87) Knox, R. J.; Boland, M. P.; Friedlos, F.; Coles, B.; Southan, C. The nitroreductase enzyme in Walker cells that activates 5-(aziridin-1-yl)-2,4-dinitrobenzamide (CB1954) to 5-(aziridin-1-yl)-4-hydroxylamino-2-nitrobenzamide is a form of NAD(P)H dehydrogenase (quinone) (EC 1.6.99.2). *Biochem. Pharmacol.* **1988***, 37*, 4671-4677.

(88) Knox, R. J.; Friedlos, F.; Marchbank, T.; Roberts, J. J. Bioactivation of CB1954: reaction of the active 4-hydroxylamino derivative with thioesters to form the ultimate DNA-DNA interstrand crosslinking species. *Biochem. Pharmacol.* **1991***, 42*, 1691-1697.

(89) Anlezark, G. M.; Melton, R. G.; Sherwood, R. F.; Wilson, W. R.; Denny, W. A. Bioactivation of dinitrobenzamide mustards by an *E. coli* B nitroreductase. *Biochem. Pharmacol.* **1995***, 50*, 609-618.

(90) Palmer, B. D.; van Zijl, P.; Denny, W. A.; Wilson, W. R. Reductive chemistry of the novel hypoxia-selective cytotoxin 5-[*N,N*-bis(2-chloroethyl)amino]-2,4-dinitrobenzamide. *J. Med. Chem.* **1995***, 38*, 1229-1241.

(91) Friedlos, F.; Denny, W. A.; Palmer, B. D.; Springer, C. J. Mustard prodrugs for activation by *Escherichia coli* nitroreductase in gene-directed enzyme prodrug therapy. *J. Med. Chem.* **1997***, 40*, 1270-1275.

(92) Mauger, A. B.; Burke, P. J.; Somani, H. H.; Friedlos, F.; Knox, R. J. Self-immolative prodrugs: candidates for antibody-directed enzyme prodrug therapy in conjugation with a nitroreductase enzyme. *J. Med. Chem.* **1994***, 37*, 3452-3458.

(93) Hay, M. P.; Atwell, G. J.; Wilson, W. R.; Pullen, S. M.; Denny, W. A. Structure-activity relationships for 4-nitrobenzyl carbamates of 5-aminobenzene indoline minor groove alkylating agents as prodrugs for GDEPT in conjugation with *E. coli* nitroreductase. *J. Med. Chem.* **2003**, *46*, 2456-2466.

(94) Hay, M. P.; Wilson, W. R.; Denny, W. A. A novel enediyne prodrug for antibody-directed enzyme prodrug therapy (ADEPT) using *E. coli* B nitroreductase. *Bioorg. Med. Chem. Lett.* **1995**, *5*, 2829-2834.

(95) Tercel, M.; Denny, W. A.; Wilson, W. R. A novel nitro-substituted seco-CI: application as a reductively activated ADEPT prodrug. *Bioorg. Med. Chem. Lett.* **1996**, *6*, 2741-2744.

(96) Wakselman, M.; Guibé-Jampel, E. An alkali-labile substituted benzyloxycarbonyl amino-protecting group. *J. Chem. Soc. Chem. Comm.* **1973**, 593-594.

(97) Papot, S.; Tranoy, I.; Tillequin, F.; Florent, J. C.; Gesson, J. P. Design of selectively activated anticancer prodrugs: elimination and cyclization strategies. *Curr. Med. Chem. - Anti-Cancer Agents* **2002**, *2*, 155-185.

(98) Colvin, O. M. An overview of cyclophosphamide development and clinical applications. *Curr. Pharm. Des.* **1999**, *5*, 555-560.

(99) Zon, G. Cyclophosphamide analogues. *Prog. Med. Chem.* **1982**, *19*, 205-246.

(100) Borch, R. F.; Millard, J. A. The mechanism of activation of 4-hydroxycyclophosphamide. *J. Med. Chem.* **1987**, *30*, 427-431.

(101) Stec, W. J. Cyclophosphamide and its congers. *J. Organophosphorous Chem.* **1982**, *13*, 145-174.

(102) Cox, P. J. Cyclophosphamide cystitis, identification of acrolein as the causative agent. *Biochem. Pharmacol.* **1979**, *28*, 2045-2049.

(103) Searle, P. F.; Weedon, S. J.; McNeish, I. A.; Gilligan, M. G.; Ford, M. Sensitisation of human ovarian cancer cells to killing by the prodrugs CB1954 following retroviral or adenoviral transfer of the *E. coli* nitroreductase gene. *Adv. Exp. Med. Biol.* **1998**, *451*, 107-113.

(104) McNeish, I. A.; Green, N. K.; Gilligan, M. G.; Ford, M. J.; Mautner, V. Virus directed enzyme prodrug therapy for ovarian and pancreatic cancer using retrovirally delivered *E. coli* nitroreductase and CB1954. *Gene Ther.* **1998**, *5*, 1061-1069.

(105) Westphal, E.-M.; Ge1, J.; Catchpole, J. R.; Ford, M.; Kenney, S. C. The nitroreductase/CB1954 combination in Epstein-Barr virus-positive B-cell lines: induction of bystander killing in vitro and in vivo. *Cancer Gene Ther.* **2000**, *7*, 97-106.

(106) Chung-Faye, G.; Palmer, D.; Anderson, D.; Clark, J.; Downes, M.; Baddeley, J.; Hussain, S.; Murray, P. I.; Searle, P.; Seymour, L.; Harris, P. A.; Ferry, D.; Kerr, D. J. Virus-directed, enzyme prodrug therapy with nitroimidazole reductase: a phase I and pharmacokinetic study of its prodrug, CB1954. *Clin. Cancer Res.* **2001**, *7*, 2662-2668.

(107) Palmer, D. H.; Mautner, V.; Mirza, D.; Oliff, S.; Gerritsen, W.; Sijp, J. R. M. V. D.; Hubscher, S.; Reynolds, G.; Bonney, S.; Rajaratnam, R.; Hull, D.; Horne, M.; Ellis, J.; Mountain, A.; Hill, S.; Harris, P. A.; Searle, P. F.; Young, L. S.; James, N. D.; Kerr, D. J. Virus-directed enzyme prodrug therapy: intratumoral administration of a replication-deficient adenovirus encoding nitroreductase to patients with resectable liver cancer. *J. Clin. Oncol.* **2004**, *22*, 1546-1552.

(108) Lipinski, C. A.; Lombardo, F.; Dominy, B. W.; Feeney, P. J. Experimental and computational approaches to estimate solubility and permeability in drug discovery and development settings. *Adv. Drug Deliv. Rev.* **1997**, *23*, 3-25.

(109) Denmeade, S. R.; Lou, W.; Lovgren, J.; Malm, J.; Lilja, H. Specific and efficient peptide substrates for assaying the proteolytic activity of prostate-specific antigen. *Cancer Res.* **1997**, *57*, 4924-4930.

(110) Garsky, V. M.; Lumma, P. K.; Feng, D. M.; Wai, J. The synthesis of a prodrug of doxorubicin designed to provide reduced systemic toxicity and greater target efficacy. *J. Med. Chem.* **2001**, *44*, 4216-4224.

(111) Montabetti, C. A. G. N.; Falque, V. Amide bond formation and peptide coupling. *Tetrahedron* **2005**, *61*, 10827-10852.

(112) Boyer, J. H. The acid-catalyzed reaction of alkyl azides upon carbonyl compounds. *J. Am. Chem. Soc.* **1955**, *77*, 951-954.

(113) Boyer, J. H.; Canter, F. C.; Hamer, J.; Putney, R. K. Acid-catalyzed reactions of aliphatic azides. *J. Am. Chem. Soc.* **1956**, *78*, 325-327.

(114) Boyer, J. H.; Morgan, L. R., Jr. Acid catalyzed reactions between carbonyl compounds and organic azides. II. aromatic aldehydes. *J. Org. Chem.* **1959**, *24*, 561-562.

(115) Aubé, J.; Milligan, G. L. Intramolecular Schmidt reaction of alkyl azides. *J. Am. Chem. Soc.* **1991***, 113*, 8965 - 8966.

(116) Milligan, G. L.; Mossman, C. J.; Aubé, J. Intramolecular Schmidt reactions of alkyl azide with ketones: scope and stereochemical studies. *J. Am. Chem. Soc.* **1995***, 117*, 10449-10459.

(117) Wrobleski, A.; Aubé, J. Intramolecular reactions of benzylic azides with ketones: competition between Schmidt and Mannich pathways. *J. Org. Chem.* **2001***, 66*, 886-889.

(118) Gracias, V.; Frank, K. E.; Milligan, G. L.; Aubé, J. Ring expansion by in situ tethering of hydroxy azides to ketones: the Boyer reaction. *Tetrahedron* **1997***, 53*, 16241-16252.

(119) Desai, P.; Schildknegt, K.; Agrios, K. A.; Mossman, C.; Milligan, G. L.; Aubé, J. Reactions of alkyl azides and ketones as mediated by Lewis acids: Schmidt and Mannich reactions using azide precursors. *J. Am. Chem. Soc.* **2002***, 122*, 7226-7232.

(120) Katz, C. E.; Aubé, J. Unusual tethering effects in the Schmidt reaction of hydroxyalkyl azides with ketones: cation- and steric stabilization of a pseudoaxial phenyl group. *J. Am. Chem. Soc.* **2003***, 125*, 13948-13949.

(121) Sahasrabudhe, K.; Gracias, V.; Furness, K.; Smith, B. T.; Katz, C. E.; Reddy, D. S.; Aubé, J. Asymmetric Schmidt reaction of hydroxyalkyl azides with ketones. *J. Am. Chem. Soc.* **2003***, 125*, 7914-7922.

(122) Staudinger, H.; Meyer, J. Über neue organische phosphorverbindungen III. phosphinmethylenderivate und phosphinimine. *Helv. Chim. Acta* **1919***, 2*, 635-646.

(123) Garcia, J.; Urpf, F.; Vilarrasa, J. New synthetic "tricks". Triphenylphosphine-mediated amide formation from carboxylic acids and azides. *Tetrahedron Lett.* **1984***, 25*, 4841-4844.

(124) Bosch, I.; Urpi, F.; Vilarrasa, J. Epimerisation-free peptide formation from carboxylic acid anhydrides and azido derivatives. *J. Chem. Soc., Chem. Commun.* **1995**, 91-92.

(125) Boullanger, P.; Maunier, V.; Lafont, D. Synthesis of amphiphilic glycosylamides from glycosyl azides without transient reduction to glycosylamines. *Carbohydr. Res.* **2000***, 324*, 97-106.

(126) Damkaci, F.; DeShong, P. Steroselective synthesis of α- and β-glycosylamide derivatives from glycopyranosyl azides via isoxazoline intermediates. *J. Am. Chem. Soc.* **2003**, *125*, 4408-4409.

(127) Saxon, E.; Armstrong, J. I.; Bertozzi, C. R. A " traceless" Staudinger ligation for the chemoselective synthesis of amide bonds. *Org. Lett.* **2000**, *2*, 2141-2143.

(128) Nilsson, B. L.; Kiessling, L. L.; Raines, R. T. Staudinger ligation: a peptide from a thioester and azide. *Org. Lett.* **2000**, *2*, 1939-1941.

(129) Saxon, E.; Bertozzi, C. R. Cell surface engineering by a modified Staudinger reaction. *Science* **2000**, *287*, 2007-2010.

(130) Saxon, E.; Luchansky, S. J.; Hang, H. C.; Yu, C.; Lee, S. C.; Bertozzi, C. R. Investigating cellular metabolism of synthetic azidosugars with the Staudinger ligation. *J. Am. Chem. Soc.* **2002**, *124*, 14893-14902.

(131) Vocadlo, D. J.; Hang, H. C.; Kim, E.-J.; Hanover, J. A.; Bertozzi, C. R. A chemical approach for identifying O-GlcNAc modified proteins in cells. *Proc. Natl. Acad. Sci. U.S.A.* **2003**, *100*, 9116-9121.

(132) Prescher, J. A.; Dube, D. H.; Bertozzi, C. R. Chemical remodelling of cell surfaces in living animals. *Nature* **2004**, *430*.

(133) He, Y.; Hinklin, R. J.; Chang, J.; Kiessling, L. L. Stereoselective N-glycosylation by Staudinger ligation. *Org. Lett.* **2004**, *6*, 4479-4482.

(134) Dube, D. H.; Prescher, J. A.; Quang, N. C.; Bertozzi, C. R. Probing much-type O-linked glycosylation in living animals. *Proc. Natl. Acad. Sci. U.S.A.* **2006**, *103*, 4819-4824.

(135) Soellner, M. B.; Nilsson, B. L.; Raines, R. T. Staudinger ligation of α-azido acids retains stereochemistry. *J. Org. Chem.* **2002**, *67*, 4993-4996.

(136) Nilsson, B. L.; Hondal, R. J.; Soellner, M. B.; Raines, R. T. Protein assembly by orthogonal chemical ligation methods. *J. Am. Chem. Soc.* **2003**, *125*, 5268-5269.

(137) Soellner, M. B.; Dickson, K. A.; Nilsson, B. L.; Raines, R. T. Site-specific protein immobilization by Staudinger ligation. *J. Am. Chem. Soc.* **2003**, *125*, 11790-11791.

(138) Merkx, R.; Rijkers, D. T. S.; Kemmink, J.; Liskamp, R. M. J. Chemoselective coupling of peptide fragments using the Staudinger ligation. *Tetrahedron Lett.* **2003***, 44*, 4515-4518.

(139) David, O.; Meester, W. J.; Bieräugel, H.; Schoemaker, H. E.; Hiemstra, H.; van Maarseven, J. H. Intramolecular Staudinger ligation: a powerful ring-closure method to form medium-sized lactams. *Angew. Chem. Int. Ed.* **2003***, 42*, 4373-4375.

(140) Lin, L. F.; Hoyt, M. H.; Halbeek, V. H.; Bergman, G. R.; Bertozzi, C. R. Mechanistic investigation of the Staudinger ligation. *J. Am. Chem. Soc.* **2005***, 127*, 2686-2695.

(141) Inazu, T.; Kobayashi, K. A new simple method for the synthesis of N^{α}-Fmoc-N^{β}-glycosylated-L-asparagine derivatives. *Synlett* **1993***, 869-870.*

(142) Mizuno, M.; Haneda, K.; Iguchi, R.; Muramoto, I.; Kawakami, T.; Aimoto, S.; Yamamoto, K.; Inazu, T. Synthesis of a glycopeptide containing oligosaccharides: chemoenzymatic synthesis of Eel calcitonin analogues having natural N-linked oligosaccharides. *J. Am. Chem. Soc.* **1999***, 121*, 284-290.

(143) Mizuno, M.; Muramoto, I.; Kobayashi, K.; Yaginuma, H.; Inazu, T. A simple method for the synthesis of N-glycosylated-asparagine and -glutamine derivatives. *Synthesis* **1999***, 162-165.

(144) Hakimelahi, G. H.; Just, G. A simple synthesis of 2,2-disubstituted tetrahydrothiophenes. *Tetrahedron Lett.* **1980***, 21*, 2119-2122.

(145) Rosen, T.; Lico, I. M.; Chu, D. T. W. A convenient and highly chemoselective method for the reductive acetylation of azides. *J. Org. Chem.* **1988***, 53*, 1580-1582.

(146) Kolawski, R. V.; Shangguan, N.; Sauers, R. R.; Williams, L. J. Mechanism of thio acid/azide amidation. *J. Am. Chem. Soc.* **2006***, 128*, 5695-5702.

(147) Fazio, F.; Wong, C.-H. $RuCl_3$-promoted amide formation from azides and thioacids. *Tetrahedron Lett.* **2003***, 44*, 9083-9085.

(148) Zhu, X. M.; Pachamuthu, K.; Schmidt, R. R. Synthesis of novel S-neoglycopeptides from glycosylthiomethyl derivatives. *Org. Lett.* **2004***, 6*, 1083-1085.

(149) Merkx, R.; Brouwer, J. A.; Rijkers, D. T. S.; Liskamp, R. M. J. Highly efficient coupling of α-substituted aminoethane sulfonyl azides with thio acids, toward a new chemical ligation reaction. *Org. Lett.* **2005***, 7*, 1125-1128.

(150) Barlett, K. N.; Kolawski, R. V.; Katukojvala, S.; Williams, L. J. Thio acid/azide amidation: an improved route to N-acyl sulfonamides. *Org. Lett.* **2006***, 8*, 823-826.

(151) Kolawski, R. V.; Shangguan, N.; Williams, L. J. Thioamides via thiatriazolines. *Tetrahedron Lett.* **2006***, 47*, 1163-1166.

(152) Pearson, R. G.; Sobel, H. R.; Songstad, J. Nucleophilic reactivity constants toward methyl iodide and trans-dichlorodi(pyridine)platinum(II). *J. Am. Chem. Soc.* **1968***, 90*, 319-326.

(153) Knapp, S.; Darout, E. New reactions of selenocarboxylates. *Org. Lett.* **2005***, 7*, 203-206.

(154) Niyomura, O.; Tani, K.; Kato, S. A facile synthesis of potassium selenocarboxylates and their oxidation with XeF₂ to diacyl diselenides: an X-ray structural analysis of di(4-methoxybenzoyl) diselenide. *Heteroatom Chem.* **1999***, 10*, 373-379.

(155) Kawahara, Y.; Kato, S.; Kanda, T.; Murai, T.; Ishihara, H. A facile preparation of rubidium and caesium selenocarboxylates. *J. Chem. Soc., Chem. Commun.* **1993**, 277-278.

(156) Kawahara, Y.; Kato, S.; Kanda, T.; Murai, T. Rubidium and cesium selenocarboxylates: synthesis and characterization. *Bull. Chem. Soc. Jpn.* **1994***, 67*, 1881-1885.

(157) Kojima, Y.; Ibi, K.; Kanda, T.; Murai, T.; Kato, S. A facile preparation of lithium selenocarboxylates. *Bull. Chem. Soc. Jpn.* **1993***, 66*, 990-992.

(158) Ishihara, H.; Hirabayashi, Y. The synthesis of potassium selenocarboxylates and their derivatives. *Chem. Lett.* **1976***, 5*, 203-204.

(159) Kageyama, H.; Takagi, K.; Murai, T.; Kato, S. Isolation of crystalline potassium alkanecarboselenoates. *Z. Naturforsch* **1989***, 44b*, 1519-1523.

(160) Ishilhara, H.; Muto, S.; Kato, S. A convenient preparation of piperidinium selenocarboxylates. *Synthesis* **1986**, 128-130.

(161) Fitzmaurice, J. C.; Williams, D. J.; Wood, P. T.; Woollins, J. D. Conversion of carboxylic acids to selenocarboxylic acids. *J. Chem. Soc., Chem. Commun.* **1988**, 741-743.

(162) Ishihara, H.; Koketsu, M.; Fukuta, Y.; Nada, F. Reaction of lithium aluminum hydride with elemental selenium: Its application as a selenating reagent into organic molecules. *J. Am. Chem. Soc.* **2001**, *123*, 8408 -8409.

(163) Wu, X.; Hu, L. Amide bond formation from selenocarboxylates and aromatic azides. *Tetrahedron Lett.* **2005**, *46*, 8401-8405.

(164) Surabhi, P.; Wu, X.; Hu, L. Improved solubility and stability of trialkylammonium selenocarboxylate in organic solvents for efficient amidation with azides. *Tetrahedron Lett.* **2006**, *47*, 4609-4613.

(165) Chernobrovkin, M. G.; Anan'eva, I. A.; Shapovalova, E. N.; Shpigun, O. A. Determination of amino acid enantiomers in pharmaceuticals by reverse-phase high-performance liquid chromatography. *J. Anal.Chem.* **2004**, *59*, 64-72.

(166) Benoiton, N. L.; Lee, Y. C.; Steinaur, R.; Chen, F. M. Studies on sensitivity to racemization of activated residues in coupling of N-benzoyloxycarbonyldipeptides. *Int. J. Peptide Protein Res.* **1992**, *40*, 559-566.

(167) Klayman, D. L.; Griffine, T. S. Reaction of selenium with sodium borohydride in protic solvents. A facile method for the introduction of selenium into organic molecules. *J. Am. Chem. Soc.* **1973**, *95*, 197-199.

(168) Laeter, J. R. d.; Böhlke, J. K.; Bièvre, P. D.; Hidaka, H.; Peiser, H. S.; Rosman, K. J. R.; Taylor, P. D. P. Atomic weights of the elements. *Pure Appl. Chem.* **2003**, *75*, 683-799.

(169) Hemker, H. C. *Handbook of synthetic substrates for the coagulation and fibrinolytic system*; Martinus Nijhoff Publisher: Boston, 1983.

(170) Erlanger, B. F.; Kokowsky, N.; Cohen, W. The preparation and properties of two new chromogenic substrates of trypsin. *Arch. Biochem. Biophys.* **1961**, *95*, 271-278.

(171) Okada, Y.; Tsuda, Y.; Hirata, A.; Nagamatsu, Y.; Okamoto, U. Synthesis of chromogenic substrates specific for human spleen fibrinolytic proteinase (SFP) and human leukocyte elastase (LE). *Chem. Pharm. Bull.* **1982**, *30*, 4060-4066.

(172) Teno, N.; Wanaka, K.; Okada, Y.; Tsuda, Y.; Okamoto, U.; Hyikata, A.; Okunomiya, A.; Naito, T.; Okamoto, S. Development of active center-directed inhibitors against plasmin. *Chem. Pharm. Bull.* **1991**, *39*, 2340-2346.

(173) Noda, K.; Oda, M.; Sato, M.; Yoshida, N. A facile method for preparation of t-butyloxycarbonylamino acid p-nitroanilides. *Int. J. Peptide Protein Res.* **1990**, *36.*

(174) Pozdnev, V. F. Activation of carboxylic acids by pyrocarbonates. Synthesis of arylamides of N-protected amino acids and small peptides using dialkyl pyrocarbonates as condensing reagents. *Int. J. Peptide Protein Res.* **1994**, *44*, 36-48.

(175) Nedev, H.; Naharisoa, H.; Haertle, T. A convenient method for synthesis of Fmoc-amino acid p-nitroanilides based on isobutyl chloroformate as condensation agent. *Tetrahedron Lett.* **1993**, *34*, 4201-4204.

(176) Schutkowski, M.; Mrestani-Klaus, C.; Neubert, K. Synthesis of dipeptide 4-nitroanilides containing non-proteinogenic amino acids. *Int. J. Peptide Protein Res.* **1995**, *45*, 257-265.

(177) Oyamada, H.; Saito, T.; Inaba, S.; Ueki, M. Reinvestigation of the phosphazo method and synthesis of N-(t-Butoxycarbonyl)-L-arginine p-pitroanilide and a chromogenic enzyme substrate for the factor Xa. *Bull. Chem. Soc. Jpn.* **1991**, *64*, 1422-1424.

(178) Schramm, G.; Wissmann, H. Peptidsynthesen mit hilfe von polyphosphorsäureestern. *Chem. Ber.* **1958**, *91*, 1073-1082.

(179) Erlanger, B. F.; Kokowsky, N. Phosphorus pentoxide as a reagent in peptide synthesis. *J. Org. Chem.* **1961**, *26*, 2534-2536.

(180) Rijkers, D. T. S.; Adams, H. P. H. M.; Hemker, H. C.; Tesser, G. I. A convenient synthesis of amino acid p-nitroanilides; synthons in the synthesis of protease substrates. *Tetrahedron* **1995**, *51*, 11235-11250.

(181) Reiter, L. A. Peptidic p-nitroanilide substrates of interleukin-1β-converting enzyme. *Int. J. Peptide Protein Res.* **1994**, *43*, 87-96.

(182) Nishi, N.; Tokura, S.; Noguchi, J. The synthesis of benzoyl-L-arginine-p-nitroanilide. *Bull. Chem. Soc. Jpn.* **1970**, *43*, 2900-2907.

(183) Höfle, G.; Steglich, W.; Vorbrüggen, H. 4-Dialkylaminopyridines as highly active acylation catalysts. *Angew. Chem. Int. Ed.* **1978**, *17*, 569-583.

(184)   Shioiri, T.; Murata, M.; Hamada, Y. New methods and reagents in organic synthesis. 69. a new synthesis of α-amino acid and peptide amides of aromatic aminoes using a modified Curtius reaction with diphenyl phosphorazidate. *Chem. Pharm. Bull.* **1987***, 35*, 2698-2704.

(185)   Wu, X.; Hu, L. Efficient amidation from carboxylic acids and azides via selenatriazoline: application to the coupling of amino acids and peptides with azides. *J. Org. Chem.* **2007***, 72*, 765-774.

(186)   Tietze, L. F.; Neumann, M.; Möllers, T.; Fischer, R.; Glüsenkamp, K. H.; Rajewsky, M. F.; Jähde, E. Proton-mediated liberation of aldophosphamide from a nontoxic prodrug: a strategy for tumor-selective activation of cytocidal drugs. *Cancer Res.* **1989***, 49*, 4179-4184.

(187)   Mulcahy, R. T.; Gipp, J. J.; Schmidt, J. P.; Joswig, C.; Borch, R. F. Nitrobenzyl phosphorodiamidates as potential hypoxia-selective alkylating agents. *J. Med. Chem.* **1994***, 37*, 1610-1615.

(188)   Firestone, A.; Mulcahy, R. T.; Borch, R. F. Nitroheterocycle reduction as a paradigm for intramolecular catalysis of drug delivery to hypoxic cells. *J. Med. Chem.* **1991***, 34*, 2933-2935.

(189)   Hernick, M.; Flader, C.; Borch, R. F. Design, synthesis, and biological evaluation of indolequinone phosphoramidate prodrugs targeted to DT-diaphorase. *J. Med. Chem.* **2002***, 45*, 3540-3548.

(190)   McGeary, R. P. Facile and chemoselective reduction of carboxylic acids to alcohols using BOP reagent and sodium borohydride. *Tetrahedron Lett.* **1998***, 39*, 3319-3322.

(191)   Friedlos, F.; Court, S.; Ford, M.; Denny, W. A.; Springer, C. Gene-directed enzyme prodrug therapy: quantitative bystander cytotoxicity and DNA damage induced by CB1954 in cells expressing bacterial nitroreductase. *Gene Ther.* **1998**, 105-112.

(192)   Wünsch, E.; Drees, F.; Jentsch, J. Zur synthese des glucagons VII. *Chem. Ber.* **1965***, 98*, 803-811.

(193)   Lee, C. K.; Yu, J. S.; Ji, Y. R. Determination of aromaticity indices of thiophene and furan by nuclear magnetic resonance spectroscopic analysis of their anilides. *J. Heterocyclic. Chem.* **2002***, 39*, 1219-1227.

(194) Largerona, M.; Vuilhorgneb, M.; Potiera, I. L.; Auzeila, N.; Bacquéb, E.; Parisa, J. M.; Fleury, M. B. Electrochemical reduction of pristinamycin IA and related streptogramins in aqueous acidic medium. *Tetrahedron* **1994***, 50*, 6307-6332.

(195) Lee, C. K.; Ahn, Y. M. Reactions of amides with potassium permanganate in neutral aqueous solution. *J. Org. Chem.* **1989***, 54*, 3744-3747.

(196) Singh, D. U.; Singh, P. R.; Samant, S. D. Fe-exchanged montmorillonite K10 - the first heterogeneous catalyst for acylation of sulfonamides with carboxylic acid anhydrides. *Tetrahedron Lett* **2004***, 45*, 4805-4807.

(197) Ette, M. C.; Reutzel, S. M. Hydrogen bond directed cocrystallization and molecular recognition properties of acyclic imides. *J. Am. Chem. Soc.* **1991***, 113*, 2586-2598.

(198) Mohmeyer, N.; Schmidt, H.-W. A new class of low-molecular-weight amphiphilic gelators. *Chem. Eur. J.* **2005***, 11*, 863 - 872.

(199) van den Nieuwendijk, A. M. C. H.; Pietra, D.; Heitman, L.; Göblyös, A.; IJzerman, A. P. Synthesis and biological evaluation of 2,3,5-substituted [1,2,4]thiadiazoles as allosteric modulators of adenosine receptors. *J. Med. Chem.* **2004***, 47*, 663-672.

CURRICULUM VITA

XINGHUA WU

EDUCATION

2002 – 2008   **Ph.D.** in **Medicinal Chemistry**
                Rutgers, The State University of New Jersey, New Brunswick, NJ

2001 – 2004   **M.S.** in **Quality Assurance/Regulatory Affairs**
                Temple University, Philadelphia, PA

1987 – 1992   **B.S.** in **Medicinal Chemistry**
                West China University of Medical Science, Chengdu, China

PUBLICATIONS

1. **Xinghua Wu** and Longqin Hu. Efficient amidation from carboxylic acids and azides via selenatriazoline: Application to the coupling of amino acids and peptides with azides. *J. Org. Chem.* **2007**, *72* (3), 765-774.

2. Prathima Surabhi, **Xinghua Wu**, and Longqin Hu. Improved solubility and stability of trialkylammonium selenocarboxylate in organic solvents for efficient amidation with azides. *Tetrahedron Lett.* **2006**, *47* (27), 4609-4613.

3. **Xinghua Wu** and Longqin Hu. Amide bond formation from selenocarboxylates and aromatic azides. *Tetrahedron Lett.* **2005**, *46* (28), 8401-8405.

4. **Xinghua Wu**, Hongfei Yue, and Gang Pu. Structural studies on idarubicin (4-demethoxydaunorubicin) I. Assignments of the ^{1}H and ^{13}C-NMR spectra in DMSO. *Chinese Journal of Antibiotics*. **2001**, *26* (2), 98-99.

5. **Xinghua Wu**, and Hongfei Yue. Synthesis of 5-chloro-3- (2-thenoyl)-2-oxindole-1-carboxamide. *The Journal of Huaxi Pharmaceutical Science*. **2001**, *16* (1), 8-10.

6. **Xinghua Wu**, and Hongfei Yue. An effective and facile method of isolating 6,11-O-dimehtyl-erythromycin A from Clarithromycin. *Chinese Journal of Antibiotics*. **2000**, *25* (6), 107-110.

PRESENTATIONS

1. Xinghua Wu and Longqin Hu, Application of selenocarboxylate/azide amidation to amino acids and peptides. *233rd ACS National Meeting*. **2007**, Chicago.

2. Xinghua Wu and Longqin Hu.6- (4'-N,N-dimethylamino) pyrid-2'-yl-7-amino-4-methylcoumarin (DAMC) as a novel fluorophore. *233rd ACS National Meeting*. **2007**, Chicago.

3. Xueqin Song and Xinghua Wu. Semi-synthesis of new Erythromycin derivatives. Chinese Antibiotic Society National Meeting.1996, Haikou, China.